Gamma-ray instruments
and
GRB observations at high energy

Frédéric Piron

Laboratoire Univers et Particules de Montpellier (CNRS / IN2P3)

IVth School of Astroparticle Physics (May 27th - June 1st, 2013)
OHP, Saint Michel l'Observatoire

Lecture content

General presentation of space-based and ground-based gamma-ray astronomy from an observation perspective, with a focus on Gamma-Ray Burst studies with current and future instruments

1. Observational techniques for GRB detection and localization

2. Current and future high-energy space missions

3. Prospects for GRB observation at very high energies with ground-based gamma-ray experiments

1. Observational techniques for GRB detection and localization

GRB prompt emission in a nutshell

- **Broad range in variability time scales**
  - From ms to 10^3 s, presence of quiescent times
  - No canonical evolution in the time history
- **Spectral diversity and complexity** (“Band model crisis”)
  - Thermal and non-thermal components,
    Cf. F. Daigne's lecture

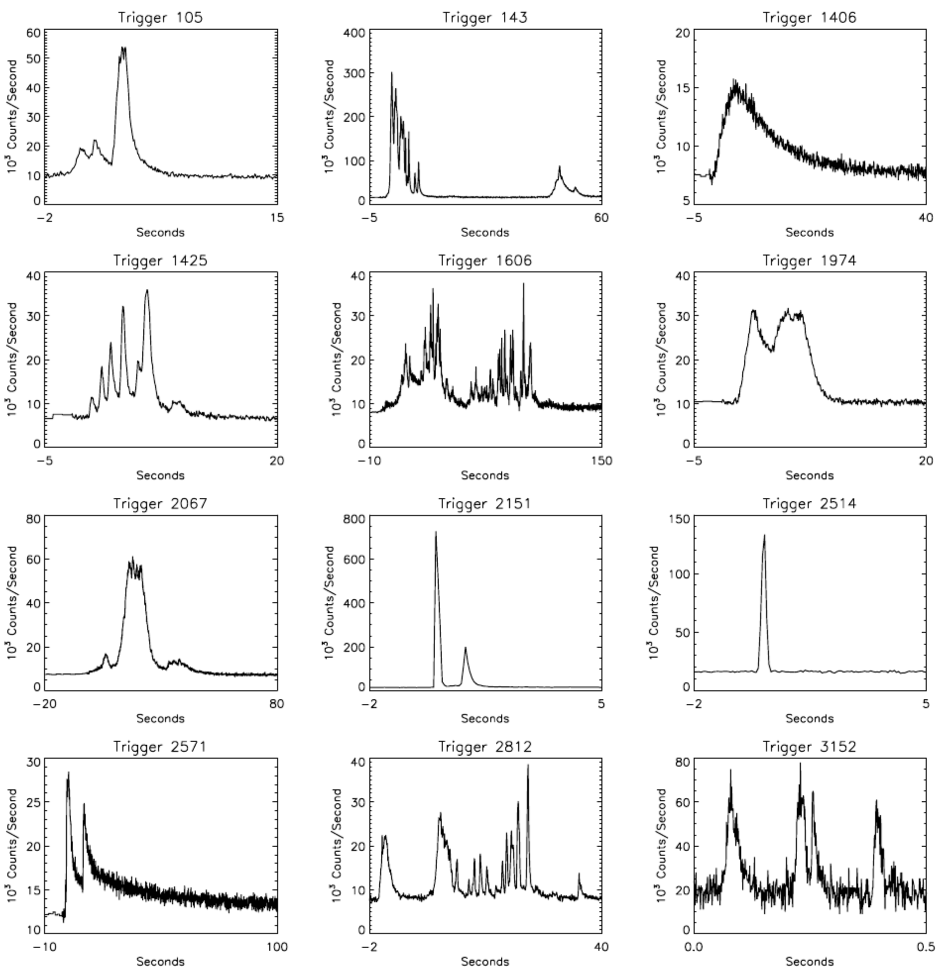

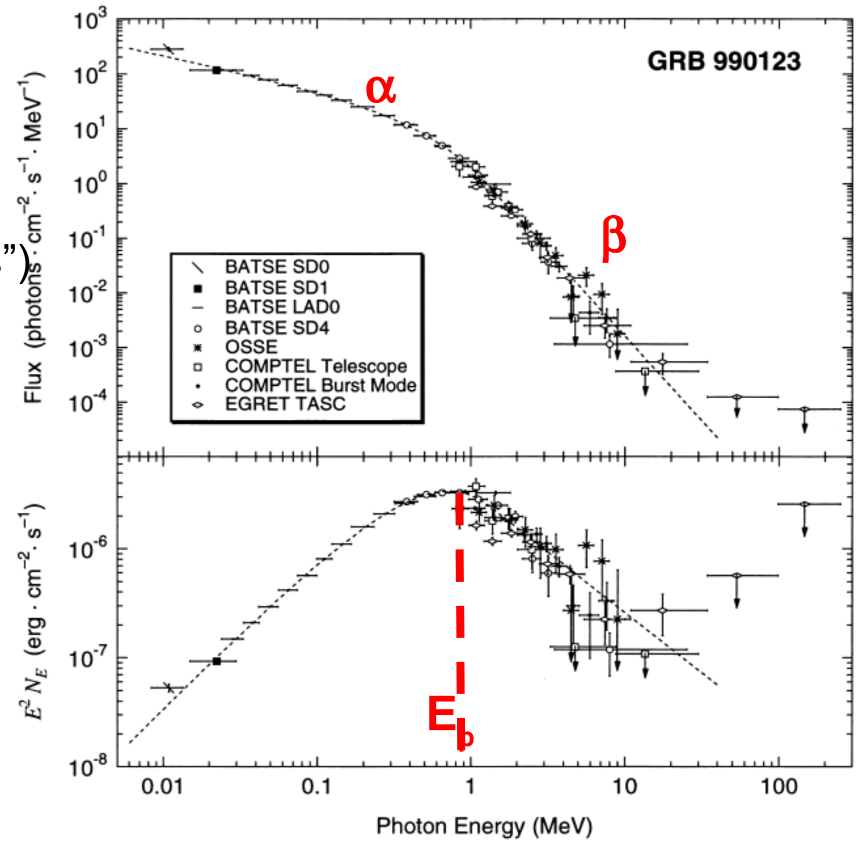

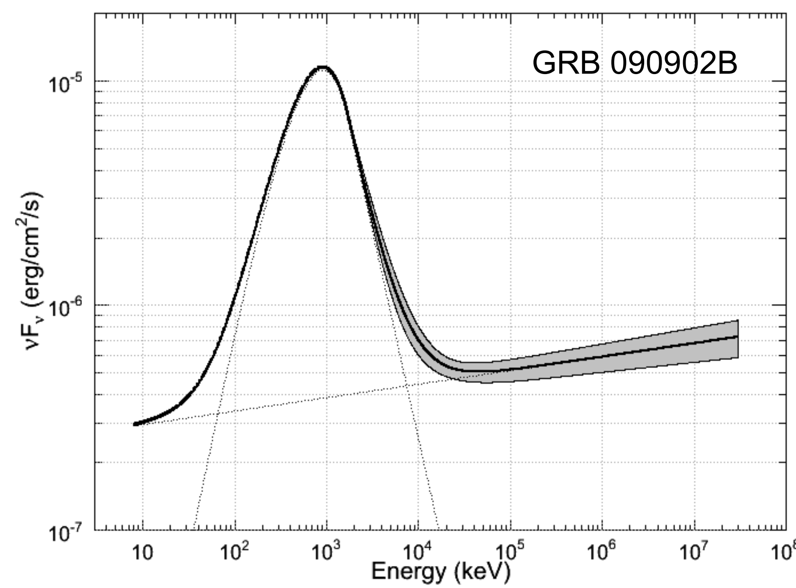

The gamma-ray domain

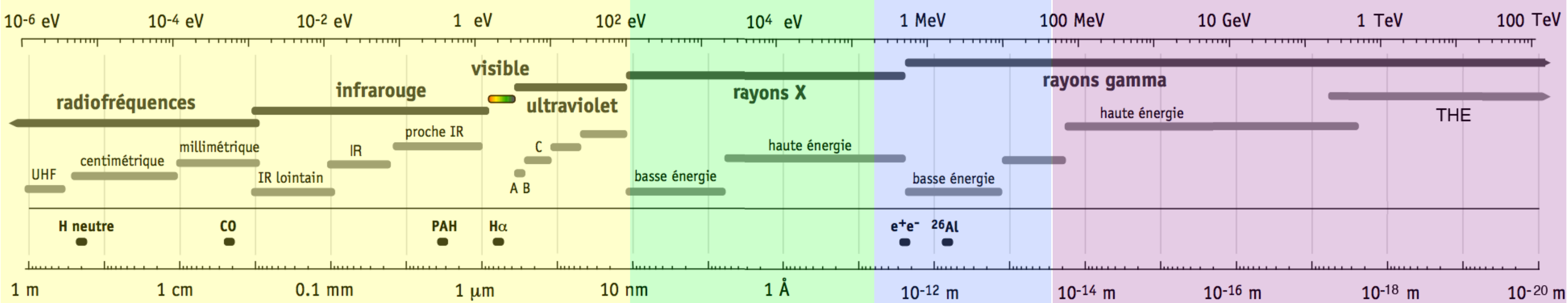

Radio, sub-mm, IR, visible, UV	Soft and hard X rays	Nuclear γ rays	HE and VHE γ rays

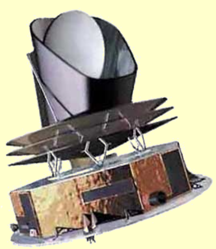
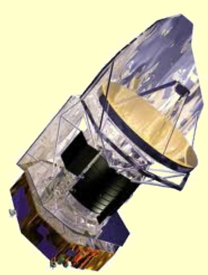
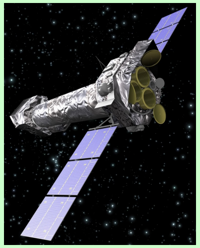
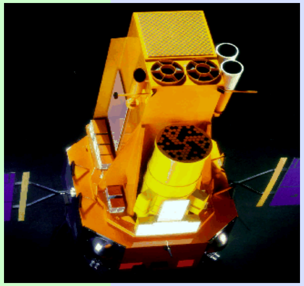



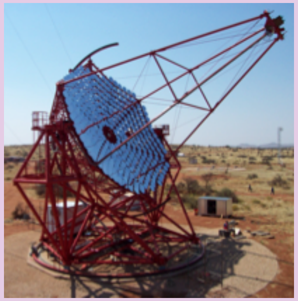

Reflection mirrors (including grazing incidence)	Space-based γ's	Ground-based γ's

Interaction processes (1/2)

3 main interaction processes of gamma rays with matter

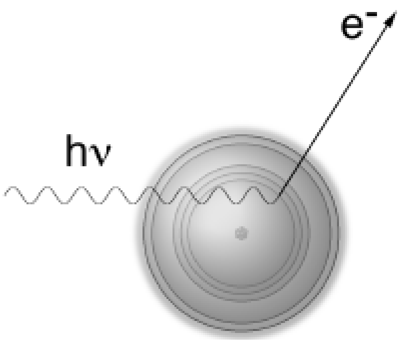

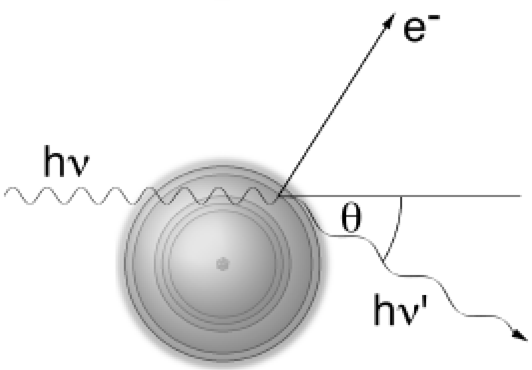

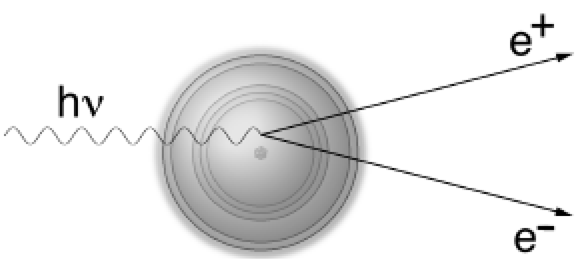

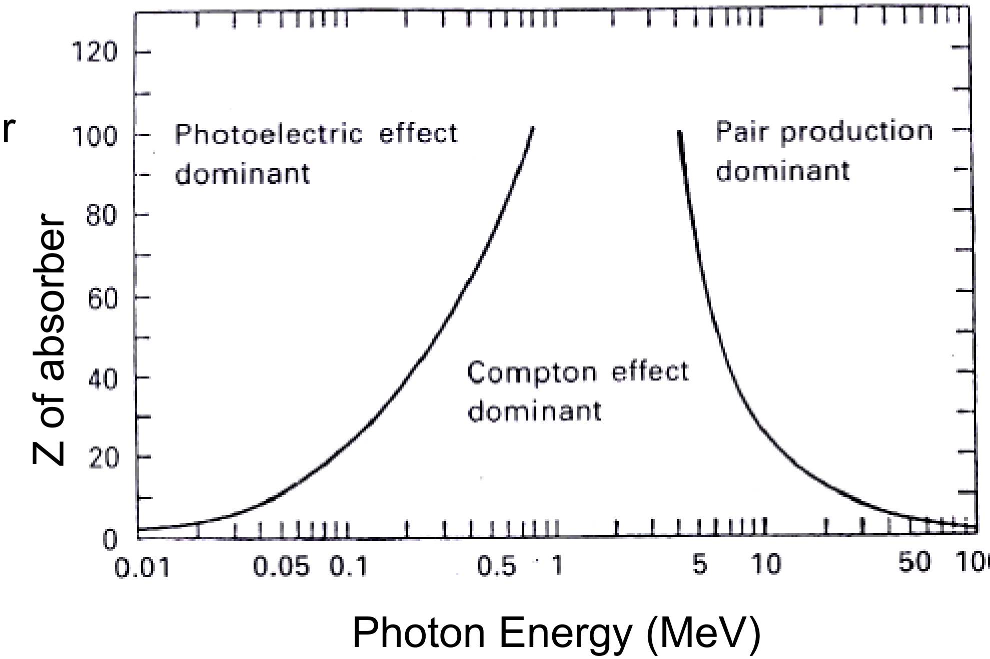

- **Photo-electric effect:** absorption of a photon of energy E_0 with ejection of a bound electron: $E = E_0 - E_{BINDING}$
- **Compton scattering:** the energy E_1 ($E_1 < E_0$) of the scattered photon is related to its energy and to the scattering angle θ: $1/E_1 - 1/E_0 = (1-\cos\theta)/m_e c^2$
- **Pair creation:** a photon of energy $E_0 > 2m_e c^2$ creates in the intense electric field of a nucleus an electron-positron pair such as $E_1 + E_2 = E_0 - 2m_e c^2$

Interaction processes (2/2)

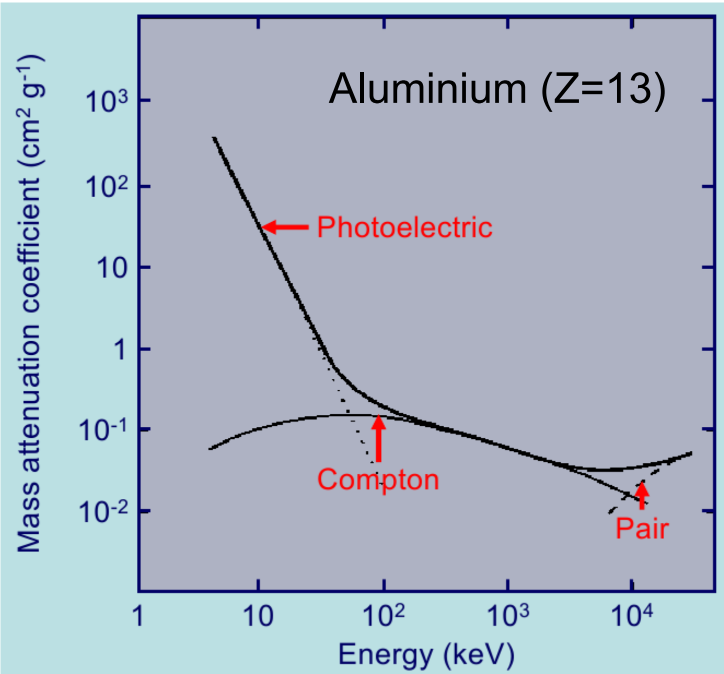

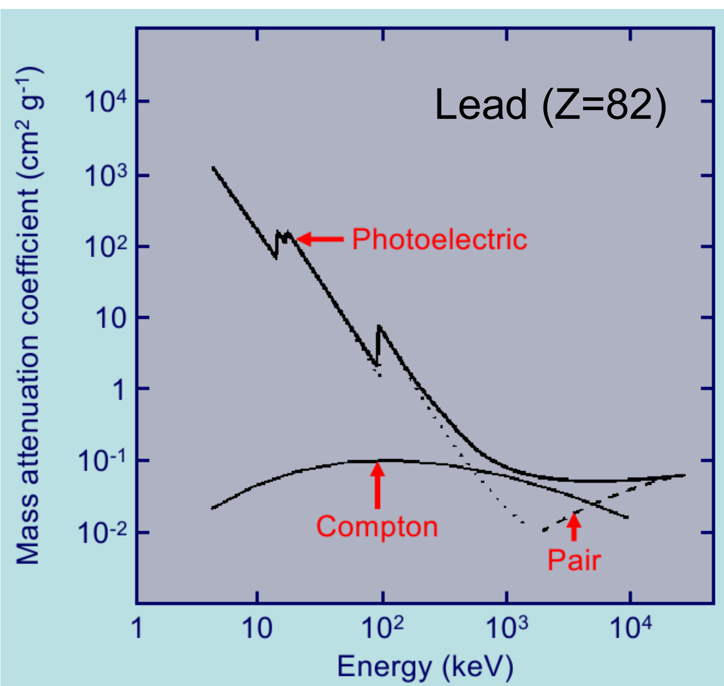

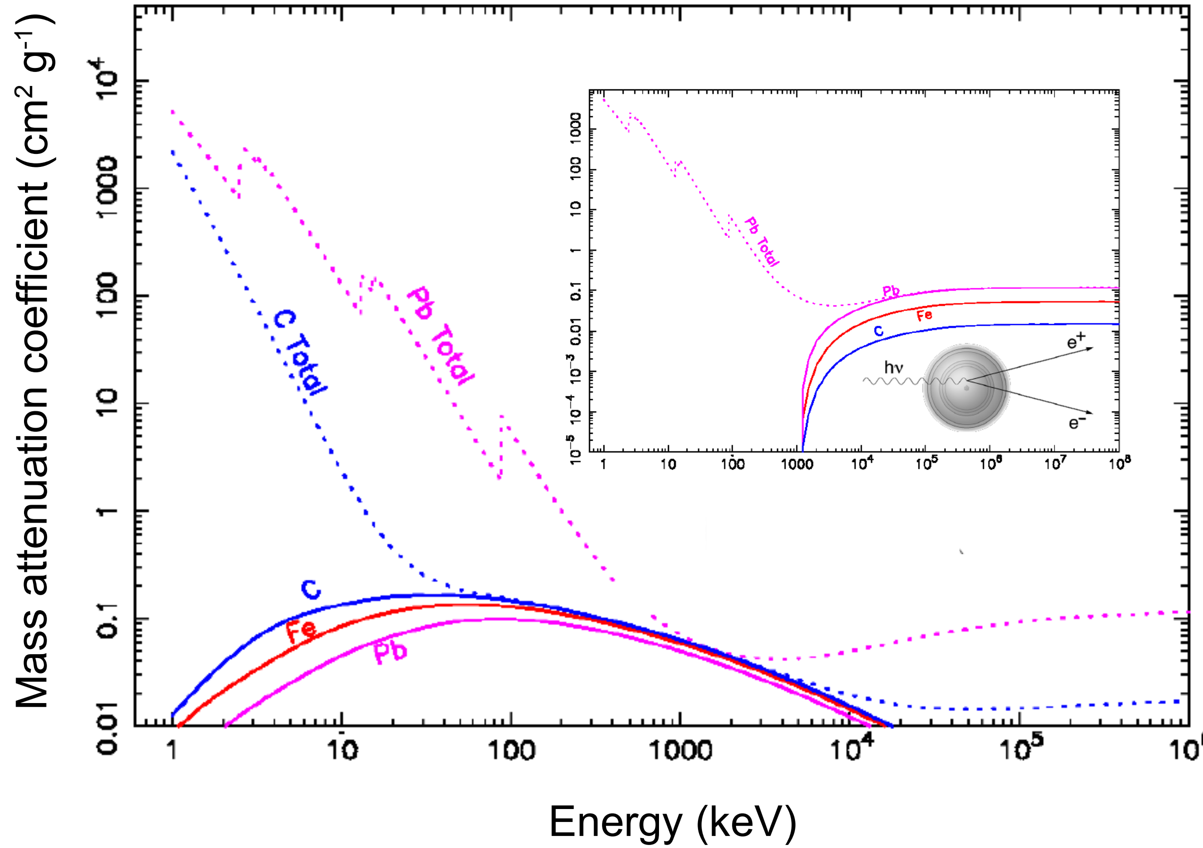

- Photo effect ~ $Z^{4\text{-}5}$, $E^{-3.5}$
- Compton ~ Z, E^{-1}
- Pair creation ~ Z, increases with E

- **High-Z materials**
  - Large stopping power (more absorbant than diffusive)
  - Lower critical energy: E_{crit} ~ 800 MeV / (Z+1.2)

Detection principles

- **Electrons ejected or created by the incident γ rays** lose energy by ionization in the detection material
  - Secondary electrons also ionize the material
  - Amplification effect
- Gamma-ray space detectors take advantage of ionization processes
  - **Commonly used detection materials: gas, semi-conductors, scintillation materials**

- **Semi-conductors**
  - **CdTe, CdZnTe, Si, Ge**
  - Fragile, can't be made (0.1-several mm) as big as scintillators
  - Pixelized readout, one channel per pixel
  - Energy resolution ~10x better than scintillators...
  - ...but need complex infrastructure (cooling)

- **Crystal scintillators**
  - Cheaper than semi-conductors, offer high-Z materials
  - Organic ("plastics")
    - light generated by fluorescence of molecules
    - usually fast, but low light yield
  - **Inorganic: NaI(Tl), CsI(Na or Tl), BGO**
    - light generated by electron transitions within the crystalline structure
    - usually good light yield, but slow

NaI (top) vs. Ge (bottom)

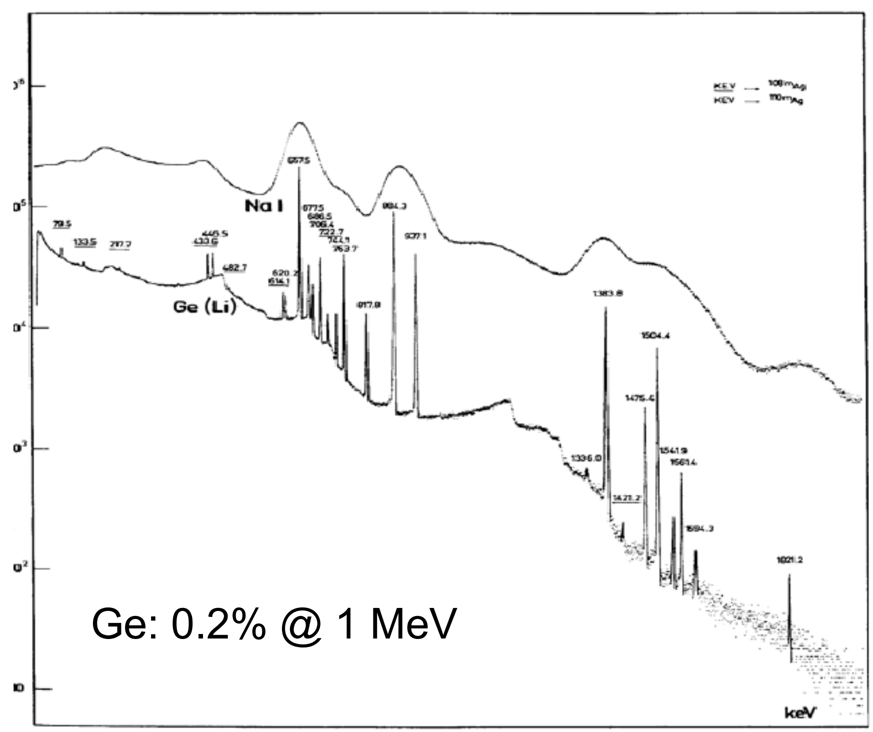

Properties of some inorganic scintillators

	light yield ph/keV	scint. yield [%NaI]	$\Delta E/E$ at 662	decay time [ns]	after-glow	λ_{peak} [nm]	n refr.	hygro	ρ [g/cm^3]
NaI(Tl)*	38	100	7.5 %	250	5 %	415	1.85	yes	3.67
CsI(Na)*	41	85	9 %	630	5 %	420	1.84	yes	4.51
CsI(Tl)*	54	45	9 %	1005	5 %	550	1.79	low	4.51
CaF_2(Eu)*	19	50		940		435	1.47	no	3.18
BaF_2* fc	1.9	3	~10%	.6-.8	-	225	1.54	low	4.88
sc	10	16		630	-	310	1.50		4.88
BGO	8-10	20	13%	300	0.1 %	480	2.15	no	7.13
$CdWO_4$*	12-15	30-50		14000		475	~2.3	no	7.9
PWO †	~ 0.1	0.3-1.3		10,20, 500(3)	(3)	420 500	2.16	no	8.28

Vela spacecrafts (1967-1972)

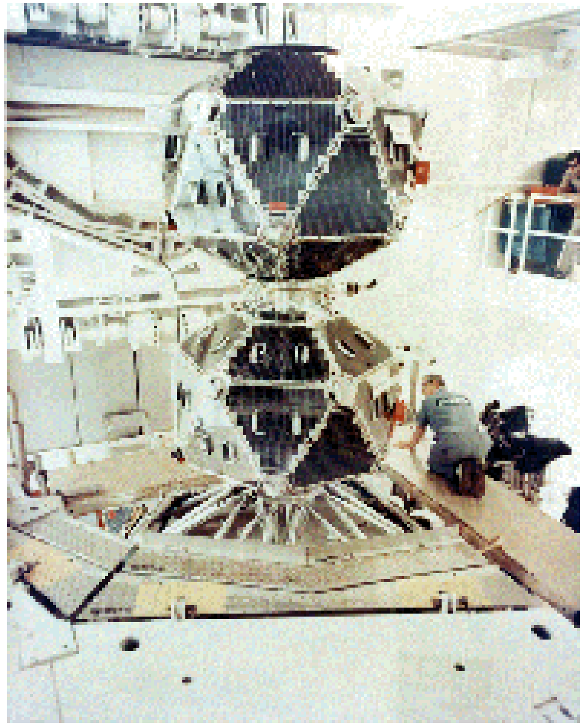

- **Pairs of satellites in Vela 5a/b and Vela 6a/b** on opposite sides of the Earth (120 000 km orbit radius)
  - **Six 10 cm^3 CsI scintillation counters (0.2-1.5 MeV)**
- Timing of events with accuracy ~0.2 s, sometimes as good as 0.05 s
- **Direction could be constrained**
  - From relative delays b/w trigger times of the different s/c units
  - **~10 deg accuracy**

- **The first gamma-ray burst: GRB 670702**

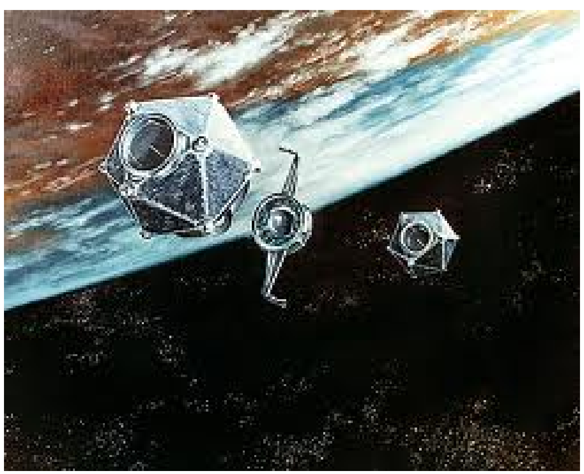

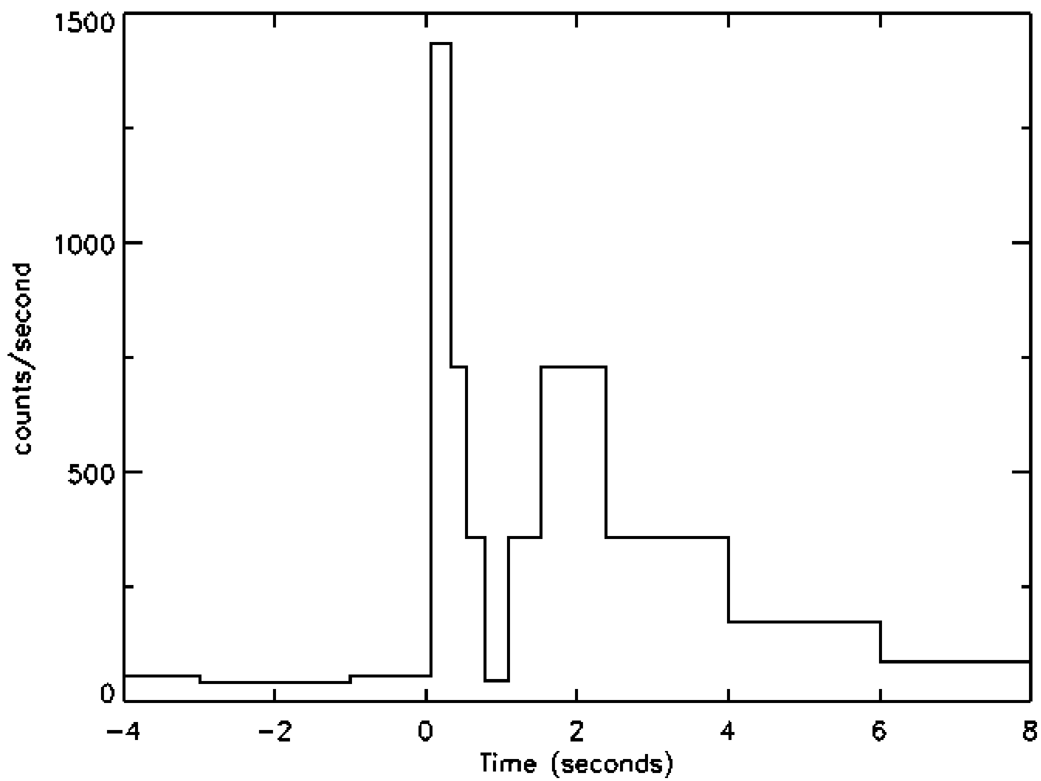

The Inter-Planetary Network

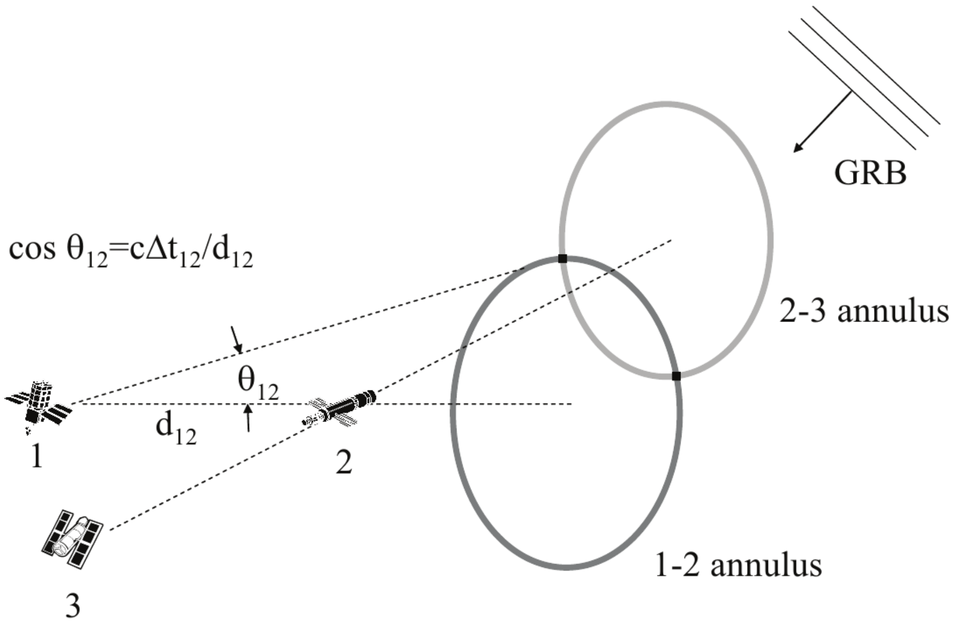

- **Triangulation technique**
  - Each pair of s/c provides an annulus
  - 3 s/c → two annuli intersecting in two boxes
  - 4 s/c → one unique error box
- **Accurate but slow**
- **Current IPN: 9 s/c equipped with γ-ray detectors (325 GRBs / yr)**
- **Effectively acts as a full time, all sky monitor**
  - 4 s/c have no planet blocking

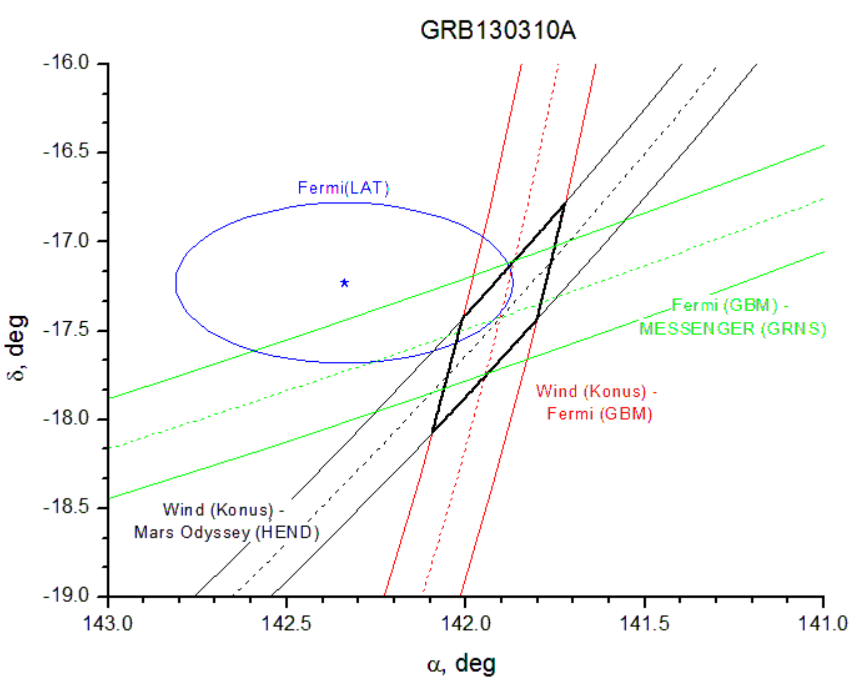

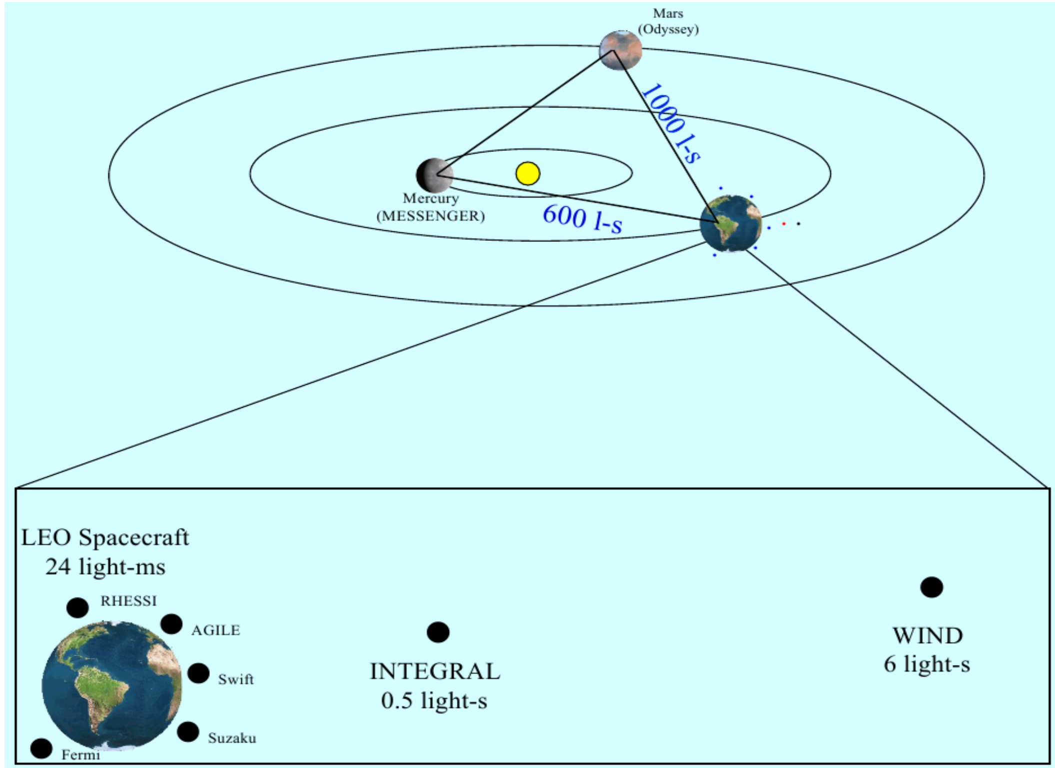

GRB localization with scintillators

BATSE aboard *CGRO* (1991-2000)

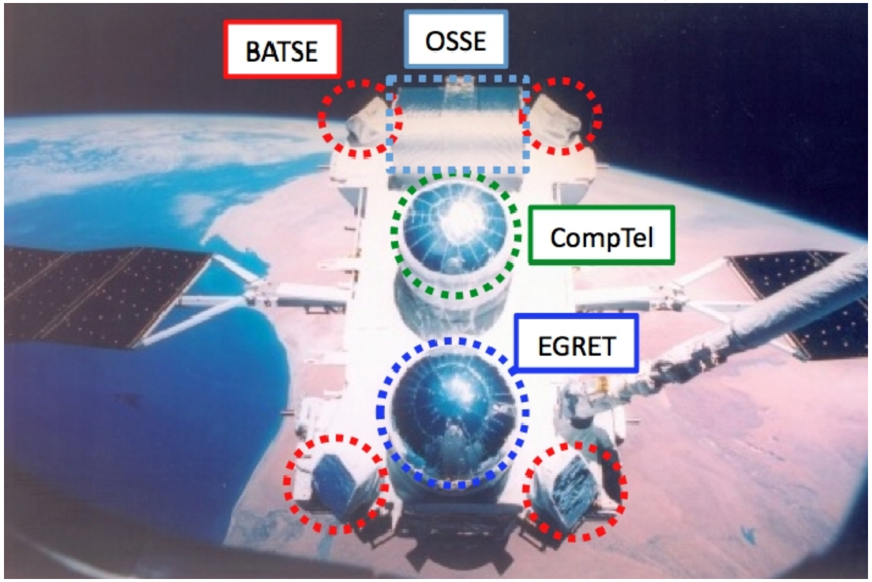

One of the 8 BATSE modules

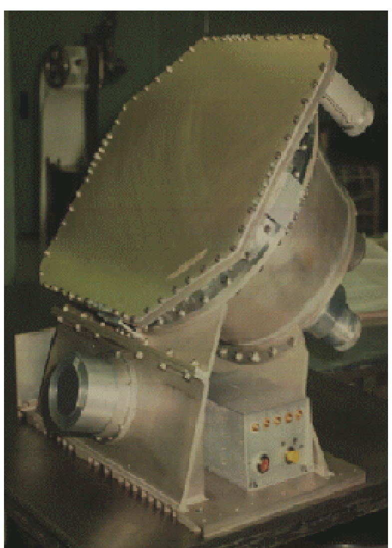

The 12+2 GBM detectors

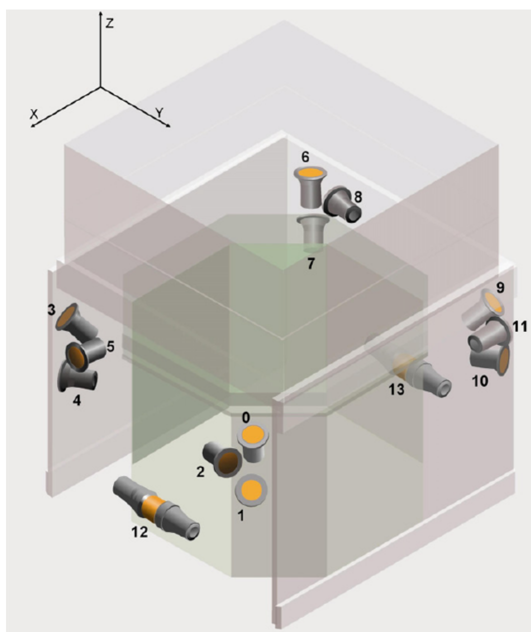

- **GRB positions determined from relative counts**
- **Fast, but typical error radius of a few degrees**

- ***CGRO*/BATSE**
  - Large Area Detectors (LADs)
    - NaI(TI) 0.5 inch thick, 2025 cm^2 each
    - 40-600 keV
  - Spectroscopy Detectors (SDs)
    - NaI(TI) 3 inch thick, 127 cm^2 each
    - 0.015-20 MeV
  - 8 modules (1 LAD + 1 SD) at each s/c corner

- ***Fermi*/GBM**
  - **12 NaI(Tl) detectors (0.08 keV – 1MeV)**
  - **2 BGO detectors (150 keV – 40 MeV)**
  - The onboard s/w compares the NaI rates to a table of calculated relative rates for each of the 1634 directions (5^o resolution) in s/c coord.
  - The location with the best chi2 fit is converted into (RA, Dec) using s/c attitude information and transmitted to the ground

Coded apertures (1/2)

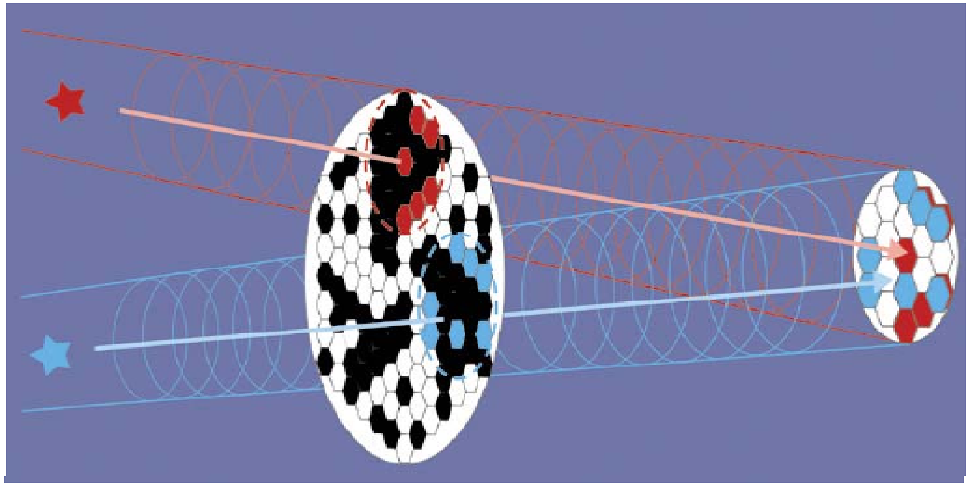

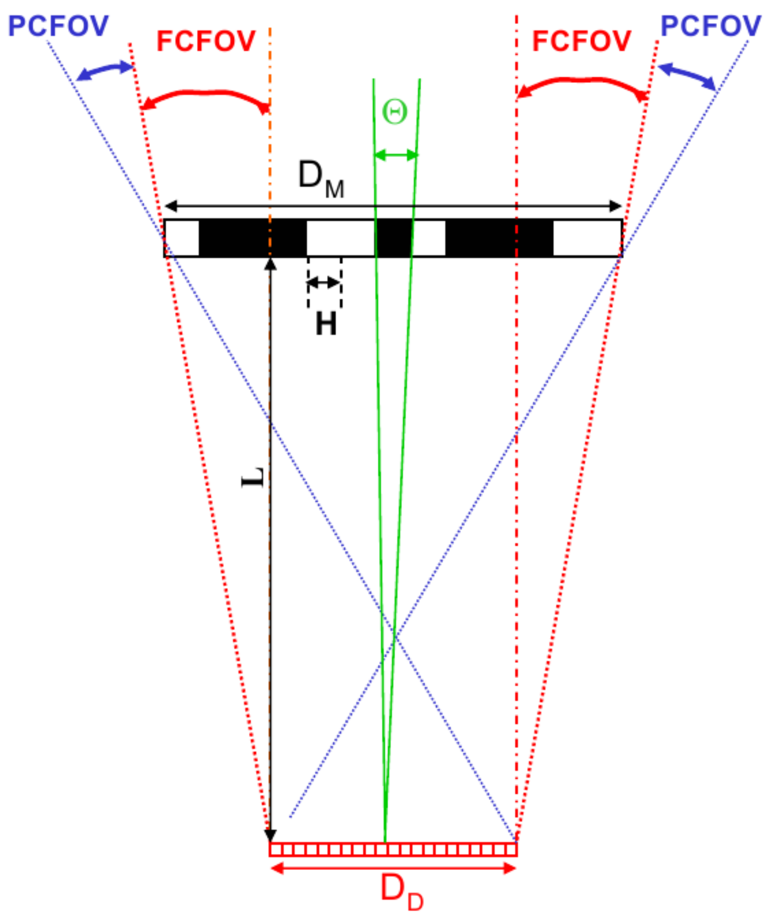

- **Coded mask technique**
  - Use photon straight propagation
  - Based on the **"camera obscura" principle**
- **Mask (opaque and transparent elements)**
  - Element size = H
  - Distance from detector = L
  - Mask dimension = D_M
- **Position sensitive detector (e.g., Ge or CdTe)**
  - Dimension < mask dimension ($D_D < D_M$)
  - Pixel size < mask element size
- **Two fields of view**
  - Fully coded: the mask-modulated source signal reaches all parts of the detector (~ constant sensitivity)

    Θ_{FC} = atan [(D_M-D_D)/L]
  - Partially coded (decreasing sensitivity)

    Θ_{PC} = atan [($D_{M+}D_D$)/L]
- **Angular resolution: $\Delta\theta$ = atan (H/L)**
  → few arcmin GRB positions

Coded apertures (2/2)

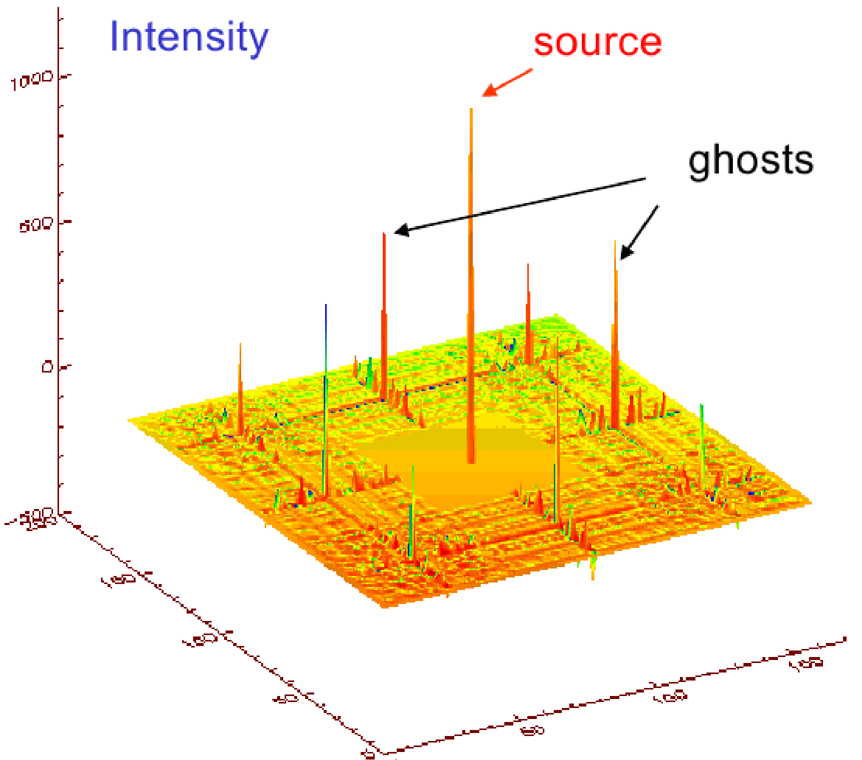

- **Encoding of a 2-dim source distribution (i,j) into a 2-dim data space (k,l)**
- **Imaging matrix algebra**
  - S = distribution of source intensities in the FoV
  - M = distribution of mask elements
  - B = background noise on the PSD
  - Intensity distribution on the PSD: D = S * M + B

    $D_{k,l} = \mathrm{Sum}_{i,j}$ [$S_{i,j}$. $M_{i+k,j+l}$ + $B_{k,l}$]
- **The sky image W can be constructed in a unique way if M is invertible**
  - i.e. there exists G such as M * G = δ
    - In practice M * G defines the PSF
  - The Uniformly Redundant Array (URA) meets the above conditions and minimizes the bkg
  - **W = D * G = S + B * G**
- **The deconvolution (source detection and ghost cleaning) is an iterative procedure**
  - Source models are decoded, normalized and subtracted from the sky image

Pair-conversion telescopes (tracker and calorimeter)

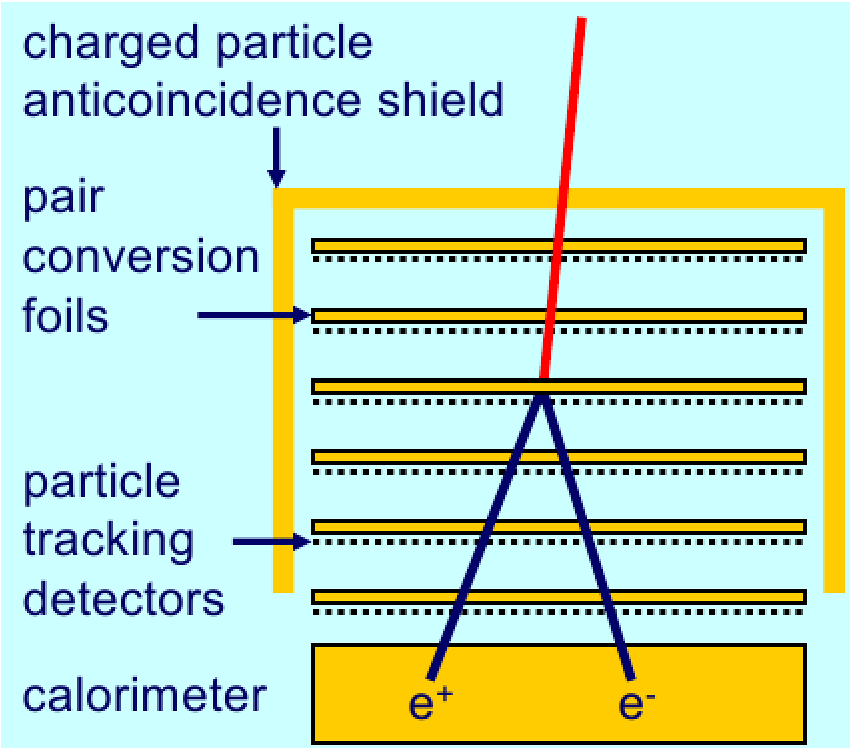

Click here to watch the video

- **Event reconstruction from CAL-TKR interplay,** e.g., for *Fermi*/LAT:
  - Sum energy in CAL, fit axis & moments, estimate leakage (parametric, profile fitting)
  - Link TKR hits into tracks & fit direction in 4 ways (VTX or not, w/ CAL constraint or not)
  - Project tracks to ACD & look for hits (not shown below)

- **Nearly ideal γ-ray candidate (*Fermi*/LAT)**
  - Starts in middle of TKR
  - Extra hits near track
  - CAL axis aligned with TKR track
  - CAL energy confined near axis

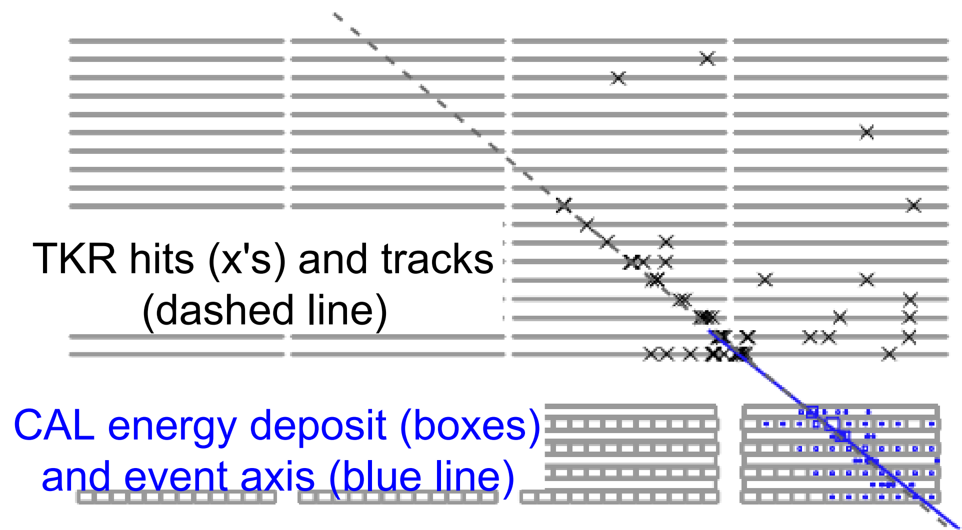

IRFs and likelihood formalism

- **Model fitting through (extended) Maximum Likelihood Estimation of source parameters**
  - Binned or unbinned (event by event) “forward-folding” analysis
  - Instrument Response Functions (IRFs): effective area, PSF and energy redistribution function
  - Telescope response is a function of photon (true, reconstructed) energies (E, E') and directions (v, v')

$$R(E',\hat{v}';E,\hat{v}) = A_{eff}(E,\hat{v})P(\hat{v}';E,\hat{v})D(E';E,\hat{v})$$

- **Expected count rate for a source flux *F* and an instrument response *R***

$$\frac{dM(E',\hat{v}')}{dt} = \int\int R(E',\hat{v}';E,\hat{v})F(E,\hat{v})d\hat{v}dE$$

- **Expected counts from the sum of the flux models**

$$M_{tot}(E',\hat{v}') = M_{gal}(E',\hat{v}') + M_{iso}(E',\hat{v}') + \Sigma^{src}M_{src}(E',\hat{v}')$$

- **Poisson probability to see *n* events given *M* expected, and log-likelihood function (binned fit)**

$$P(n;M) = \frac{M^n}{n!}e^{-M} \qquad \mathcal{L} = \log\Pi_i^{bin}P(n_i;M_i)$$

- **Uses lots of information optimally, which is a double-edge sword**
  - Issues with any of the IRFs can affect fits and can be difficult to disentangle
- **A *hypothesis* testing tool: it can only tell you about what you put into the model**
  - Everything you observe has to be accounted for by some aspect of the model

Orbital environment

- **Space devices are exposed to high fluxes of accelerated particles**
  - Produce ionization effects similar to those due to cosmic photons
  - Produce secondary photons in the surrounding material

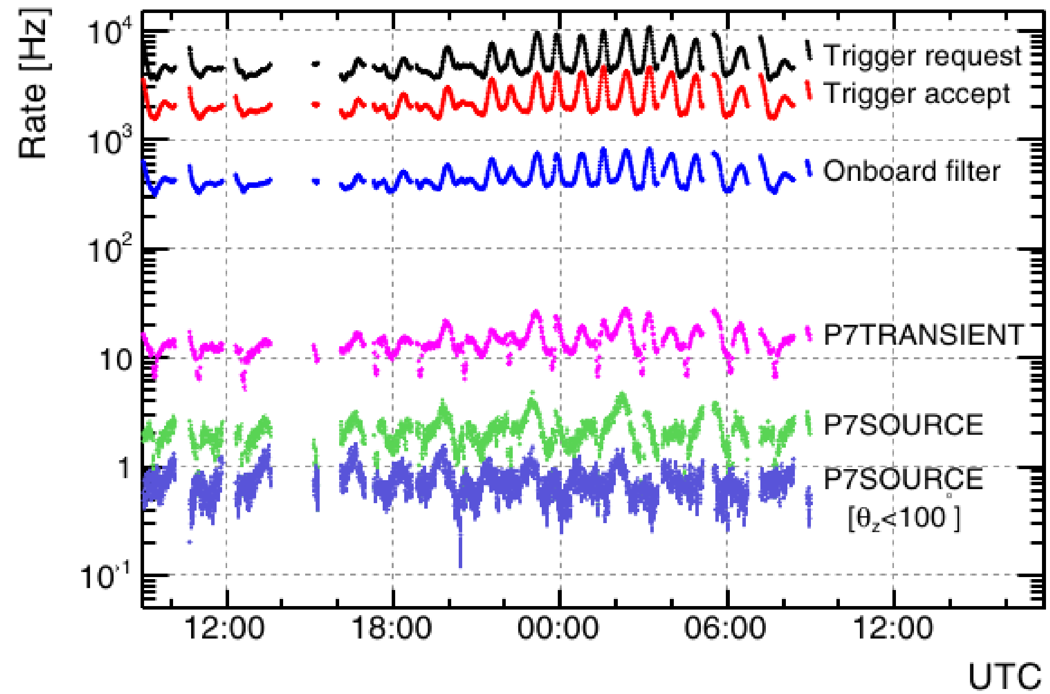

- ***Fermi:*** cosmic ray (CR) flux and LAT trigger rates vary with orbit
  - Related to rigidity cutoff
  - Many CR components, including γ-rays from back

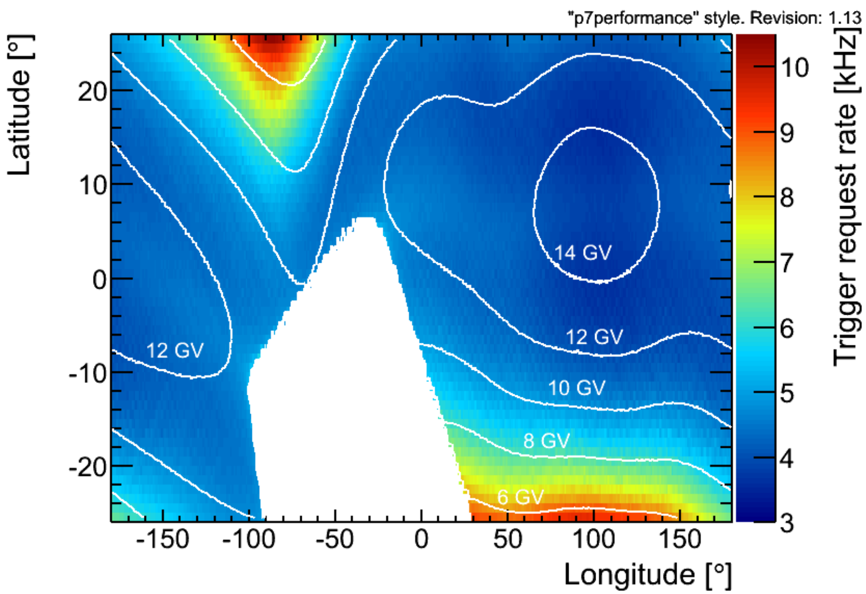

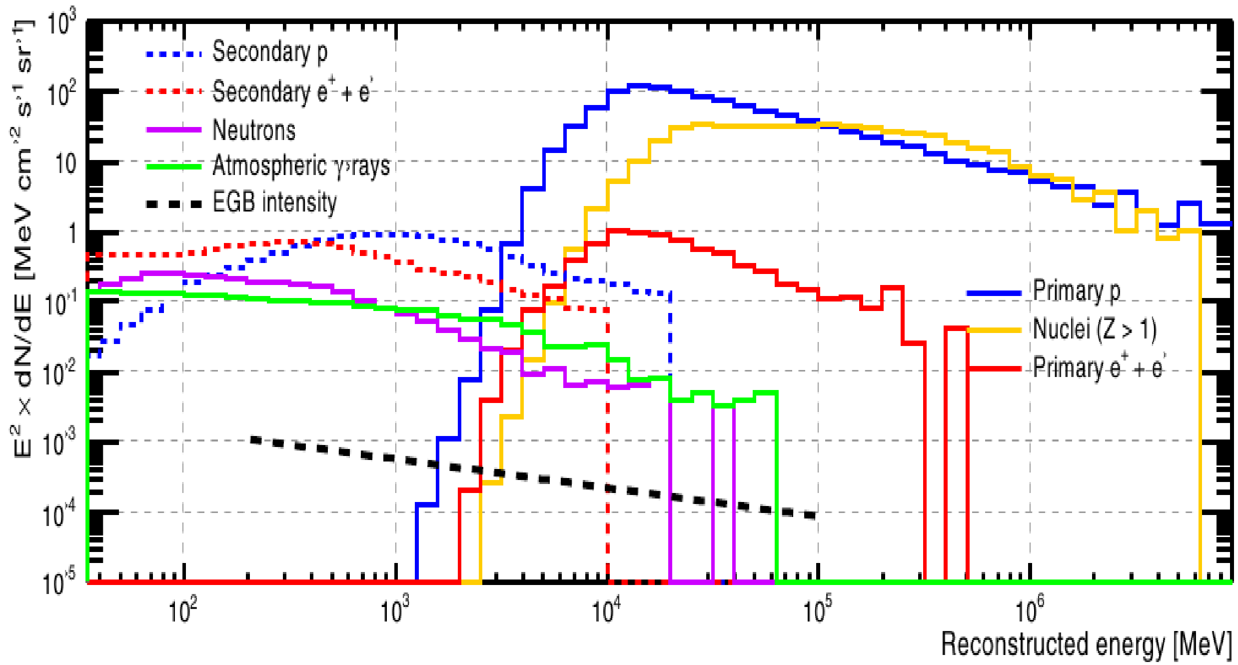

Dissemination of GRB alerts with the GCN

The **GRB Coordinates Network** system distributes:
(http://gcn.gsfc.nasa.gov/gcn/)

- **Notices: locations of GRBs and other transients detected by spacecrafts**
  - Most in real-time while the GRB is still bursting
  - Others are delayed due to telemetry down-link
- **Circulars and Reports:** follow-up observations and analyses made by ground-based and space-based radio to TeV (and astroparticle) observers

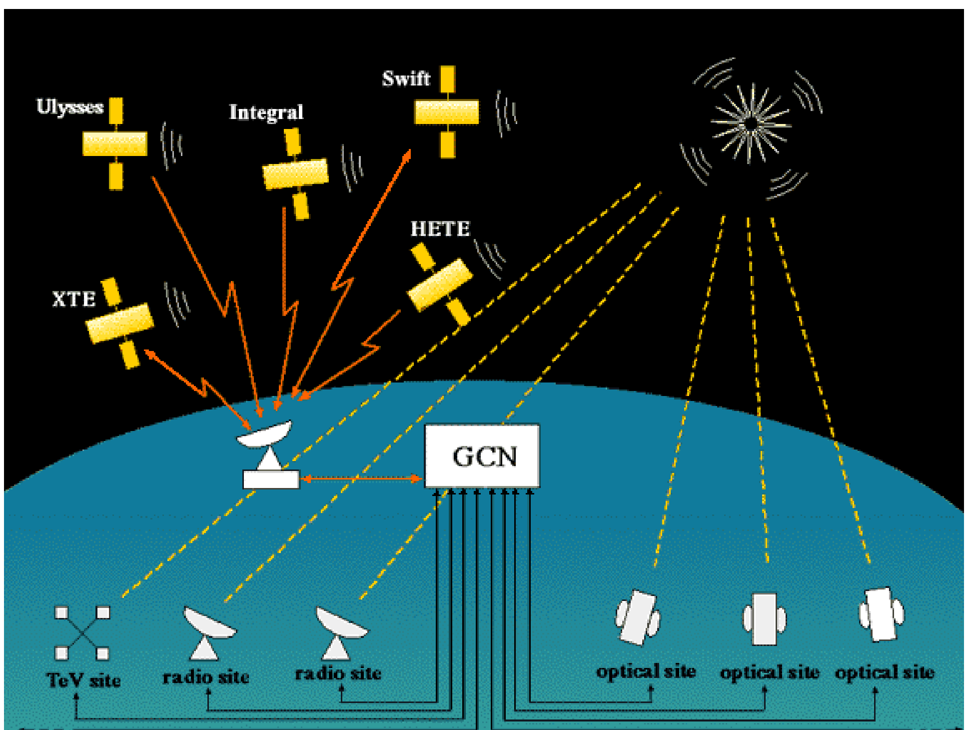

CIRCULARS and REPORTS (current)

Bursts of Special Interest (updated in real-time)
A set of links to information about recent bursts of special interest (the ones with follow-up activity).
Circulars (updated in real-time)
A sequential archive in serial number order of all GCN Circulars.
Reports (updated in near real-time)
A sequential archive in serial number order of all GCN Reports.

NOTICES (active missions)

MAXI GRB/Unknown/Known Information (updated in real-time)
This table contains information about detections by MAXI (GRBs and other Unknowun sources, and previously Known sources).

Fermi GRB Information (updated in real-time) and LAT Monitor and Transient Information
These tables contain information about GRBs, flares from known sources, and new sources detected by Fermi.

Swift GRB Information (updated in real-time, 10-200 sec) and Ground-processed (1-6 hrs delay)
These tables contain the results of the real-time processing and the off-line ground processing of the Swift triggers (bursts and non-bursts).

Swift-BAT Monitor Information (updated in near real-time, 1-6 hrs)
This table contains the results of the near-real-time automated processing of the Swift-BAT All-Sky Monitor program.

INTEGRAL GRB Positions (updated in real-time) and SPI-ACS Triggers, Lightcurves
These tables contains information about GRBs/Transients/noise detected by INTEGRAL.

AGILE GRB Information (updated in real-time)
This table contains information about GRBs detected by AGILE.

IPN_Raw Notices (updated in real-time) and IPN_Position Notices (discontinued 2003) and IPN_Segment Notices (archive)
These tables contain the GCN/IPN Position, Segment , and Lightcurve Notices.

Wind-KONUS Notices (updated in real-time)
This table contains the GCN/KONUS Notices (light curves from 1994 to current).

MOA Notices (updated in real-time)
This table contains the GCN/MOA gravitational lensing event Notices.

GCN circulars on GRB 130427A

- 14686 GRB 130427A / SN 2013cq: Hubble Space Telescope Observations
- 14673 VLT observations of GRB 130427A
- 14672 GRB 130427A: Konkoly optical observations
- 14669 GRB 130427A:: BTA spectroscopic observations on May 10/11.
- 14666 GRB 130427A: Continued RATIR Optical and NIR Observations - Photometric Evidence for a New Component
- 14662 GRB 130427A: Skynet detections of a possible supernova
- 14646 GRB 130427A: Spectroscopic detection of the SN from the 10.4m GTC
- 14645 GRB 130427A: optical observations
- 14631 GRB 130427A: Tautenburg 2nd epoch: No break, no clear SN
- 14617 GRB 130427A: host galaxy observations
- 14615 GRB 130427A: Keck/LRIS Observations
- 14608 GRB 130427A: Ten nights of Skynet/PROMPT/GORT observations
- 14606 GRB 130427A: Continued RATIR Optical and NIR Observations
- 14605 GRB 130427A, LBT optical spectrum
- 14598 GRB 130427A, Watcher afterglow detection
- 14597 GRB 130427A: Excess optical emission consistent with an emerging supernova
- 14596 GRB 130427A: Amateur observations from Sweden
- 14592 GRB 130427A: Tautenburg afterglow observations
- 14590 GRB 130427A: RHESSI observations
- 14582 GRB 130427A: optical observations in CrAO
- 14579 GRB 130427A: correction to GCN 14487
- 14549 GRB 130427A: Non-observation of VHE emission with HAWC
- 14538 GRB 130427A: Pan-STARRS 1 optical observations
- 14534 GRB 130427A: MITSuME Ishigakijima Optical Observation after 5 days
- 14526 GRB 130427A: Predictions about the occurrence of a supernova
- 14525 GRB 130427A: KAIT optical observations
- 14523 GRB 130427A: SARA-N optical observations
- 14522 GRB 130427A: VLA 20 GHz detection
- 14521 GRB 130427A: ABT optical observations
- 14520 GRB 130427A: High-energy neutrino search
- 14519 GRB 130427A: GMRT radio detection
- 14518 GRB 130427A: Continued GMG optical observations
- 14517 GRB 130427A: Nishi-Harima Optical Spectroscopic Observations
- 14516 GRB 130427A: photo-z of possible SDSS host galaxy
- 14515 GRB 130427A: high energy gamma-ray detection by AGILE
- 14514 GRB 130427A: Continued RATIR Optical and NIR Observations
- 14513 GRB 130427A: MITSuME Ishigakijima Optical Observation after 2 days
- 14511 GRB 130427A: Challis Observatory optical observations
- 14510 GRB 130427A: Continued Skynet/PROMPT Observations
- 14509 GRB 130427A: further GMG observations
- 14508 GRB 130427A: Fermi-LAT refined analysis
- 14507 GRB 130427A: SARA-N detection
- 14506 GRB 130427A: Continued RATIR Optical and NIR Observations
- 14505 GRB 130427A: CrAO RT-22 36 GHz observation
- 14503 GRB 130427A in the Ep,i - Eiso plane
- 14502 GRB 130427A: Improved Swift-XRT analysis
- 14498 GRB 130427A: MITSuME Okayama and Ishigakijima Optical Observation after 1 day
- 14497 GRB 130427A: Skynet/PROMPT Observations
- 14495 GRB 130427A: Nishi-Harima NIR Observations
- 14494 GRB 130427A: CARMA 3mm observations
- 14492 GRB 130427A : Xinglong TNT optical observation
- 14491 GRB 130427A: VLT/X-shooter redshift confirmation
- 14490 GRB 130427A optical time series
- 14489 GRB 130427A, Optical Observations
- 14488 GRB 130427A: Continued iTelescope T21 optical observations
- 14487 Konus-Wind observation of GRB 130427A
- 14486 GRB 130427A: Kanata/HOWPol optical imaging polarimetry
- 14485 GRB 130427A: Swift-XRT refined Analysis
- 14484 GRB 130427A: SPI-ACS/INTEGRAL observations
- 14483 GRB 130427A: Continued RATIR Optical and NIR Observations
- 14482 GRB 130427A: CARMA 85 GHz detection
- 14481 GRB 130427A: SNUO/SOAO/BOAO Observation
- 14480 GRB 130427A: VLA 5 GHz detection
- 14478 GRB 130427A: NOT optical photometry and redshift
- 14476 GRB 130427A: RAPTOR Bright Counterpart Before Swift Trigger
- 14475 GRB 130427A: T100 observations
- 14474 GRB 130427A: optical observations in CrAO
- 14473 GRB 130427A: Fermi GBM observation
- 14472 GRB 130427A: Swift/UVOT followup observations of an Optical Afterglow
- 14471 GRB 130427A: Fermi-LAT detection of a burst
- 14470 GRB 130427A: Swift-BAT refined analysis
- 14468 GRB 130427A: Zadko observatory - Gingin optical observations
- 14466 GRB 130427A: GMG optical observation
- 14465 GRB 130427A: MITSuME Okayama Optical Observation
- 14464 GRB 130427A: Optical Observations
- 14462 GRB 130427A: MAXI/GSC detection
- 14459 GRB 130427A: RATIR Optical and NIR Observations
- 14458 GRB 130427A: Weihai optical observations
- 14457 GRB 130427A: iTelescope T11 optical observations
- 14456 GRB 130427A: Continued P60 follow-up of an extremely bright optical afterglow
- 14455 GRB 130427A: Gemini-North redshift
- 14454 GRB 130427A: MITSuME Akeno Optical observation(T0+8000s~)
- 14453 GRB 130427A: PAIRITEL NIR Detections
- 14452 GRB 130427A: Faulkes Telescope North detection
- 14451 GRB 130427A: P60 early detection
- 14450 GRB 130427A: early optical observations
- 14449 GRB 130427A: P60 early nondetection
- 14448 GRB 130427A: Swift detection of a very bright burst with a likely bright optical counterpart

GCN circulars on GRB 130427A: detection / z determination

```
TITLE:   GCN CIRCULAR
NUMBER:  14448
SUBJECT: GRB 130427A: Swift detection of a very bright burst
         with a likely bright optical counterpart
DATE:    13/04/27 08:24:13 GMT
FROM:    David Palmer at LANL  <palmer@lanl.gov>

A. Maselli (INAF-IASFPA), A. P. Beardmore (U Leicester),
A. Y. Lien (NASA/GSFC/ORAU), V. Mangano (INAF-IASFPA),
C. J. Mountford (U Leicester), K. L. Page (U Leicester),
D. M. Palmer (LANL) and M. H. Siegel (PSU) report on behalf of the
Swift Team:

At 07:47:57 UT, the Swift Burst Alert Telescope (BAT) triggered and
located GRB 130427A (trigger=554620). Swift slewed immediately to the
burst.
The BAT on-board calculated location is RA, Dec 173.139, +27.692 which is
   RA(J2000) = 11h 32m 33s
   Dec(J2000) = +27d 41' 29"
with an uncertainty of 3 arcmin (radius, 90% containment, including
systematic uncertainty). The BAT light curve shows an extremely bright
complex peak about 20 seconds long starting at T-50, while Swift was
slewing from the previous pre-planned target, followed by a smaller
peak during the slew to the burst with emission through at least T+200.
The peak count rate was ~ 100,000 counts/sec (15-350 keV),
at T-40 sec, before the trigger.

The XRT began observing the field at 07:50:17.7 UT, 140.2 seconds after
the BAT trigger. XRT found a bright, uncatalogued X-ray source located
at RA, Dec 173.1362, 27.7129 which is equivalent to:
   RA(J2000)  = +11h 32m 32.69s
   Dec(J2000) = +27d 42' 46.4"
with an uncertainty of 4.7 arcseconds (radius, 90% containment). This
location is 75 arcseconds from the BAT onboard position, within the BAT
error circle. No event data are yet available to determine the column
density using X-ray spectroscopy.

UVOT took a finding chart exposure of 150 seconds with the White filter
starting 147 seconds after the BAT trigger. A blurred bright source
appears to be located near the XRT position in the initial 2.7'x2.7'
sub-image. However, the lack of reference stars and lack of star tracker
lock prevents a definitive identification and the measurement of a
position or magnitude.

This is an extremely bright burst in all three instruments,
and it was also seen by Fermi/GBM.

After the slew to the burst, the star trackers had trouble
locking on to give a spacecraft attitude, so the XRT position
may be inaccurate at the arcminute level.

The apparent optical counterpart appears extremely blurred,
possibly due to the lack of star tracker lock, but more likely to be
due to instrumental effects on a very bright optical counterpart.

Further follow-up is warranted for all ground-based observatories.

Burst Advocate for this burst is A. Maselli (maselli AT ifc.inaf.it).
Please contact the BA by email if you require additional information
regarding Swift followup of this burst. In extremely urgent cases, after
trying the Burst Advocate, you can contact the Swift PI by phone (see
Swift TOO web site for information: http://www.swift.psu.edu/too.html.)
```

```
TITLE:   GCN CIRCULAR
NUMBER:  14455
SUBJECT: GRB 130427A: Gemini-North redshift
DATE:    13/04/27 11:43:31 GMT
FROM:    Andrew Levan at U.of Leicester  <A.J.Levan@warwick.ac.uk>

A.J. Levan (U. Warwick), S.B. Cenko (U.C. Berkeley), D.A. Perley
(Caltech) and N.R. Tanvir (U. Leicester) report for a larger
collaboration:

We obtained spectroscopy of the afterglow of GRB 130427A (Maselli
et al. GCN 14448, Elenin et al. GCN 14450, Perley et al. GCN 14451)
with Gemini-North / GMOS, begininnig at 09:19 UT roughly 1.5 hours
after the burst. Two different central wavelengths were observed
giving a coverage from ~3100-6700 A. The resulting spectra are of
very high signal to noise given the brightness of the afterglow.
In these spectra we identify absorption lines due to Ca H and K,
Mg I as well as the Mg II doublet at a common redshift of z=0.34.
We suggest this to be the redshift of GRB 130427A.

We do not see evidence for emission lines from an underlying host,
although given the brightness of the afterglow this is not surprising.
The absolute magnitude of object in SDSS, if at z=0.34 is M_R ~
-19.7, relatively bright for a GRB host.

We thank the Gemini-staff for their help in rapidly obtaining these
observations.
```

Fermi GCN circulars on GRB 130427A

TITLE: GCN CIRCULAR
NUMBER: 14473
SUBJECT: GRB 130427A: Fermi GBM observation
DATE: 13/04/27 20:27:19 GMT
FROM: Andreas von Kienlin at MPE <azk@mpe.mpg.de>

A. von Kienlin (MPE) reports on behalf of the Fermi GBM Team:

"At 07:47:06.42 UT on 27 April 2013, the Fermi Gamma-Ray Burst Monitor triggered and located GRB 130427A (trigger 388741629/130427324) which was also detected by the Swift/BAT and Fermi/LAT (Maselli et al. 2013, GCN 14448 and S. Zhu et al., GCN 14471) The GBM on-ground location is consistent with the Swift position.

The angle from the Fermi LAT boresight is 48 degrees.

Based on hard and intense emission in a GBM BGO detector, GBM initiated an Autonomous Report Request. This request caused Fermi to reorient towards this GRB (GBM flight location).

The GBM light curve consists of a bright structured peak followed at ~T0+120 s by a FRED-like pulse. The overall duration (T90) is about 138s s (50-300 keV).

Owing to the brightness of the burst, systematic effects are very large and no single model gives an adequate fit in this preliminary analysis. A Band function fit in the interval from T0+0.002 s to T0+18.432 s yields the following parameters Epeak = 830 +/- 5 keV, alpha = -0.789 +/- 0.003, and beta = -3.06 +/- 0.02.

The event fluence (10-1000 keV) in this time interval is (1.975 +/- 0.003)E-03 erg/cm^2. The 1.024 sec peak photon flux measured starting from T0+7.48808 s in the 8-1000 keV band is 1052 +/- 2 ph/s/cm^2, making this the most intense and fluent GRB detected by Fermi GBM.

Further analysis is being performed"

TITLE: GCN CIRCULAR
NUMBER: 14471
SUBJECT: GRB 130427A: Fermi-LAT detection of a burst
DATE: 13/04/27 20:10:41 GMT
FROM: Judith Racusin at GSFC <judith.racusin@nasa.gov>

S. Zhu, J. Racusin, D. Kocevski, J. McEnery (NASA/GSFC), F. Longo (Univ of Trieste and INFN), J. Chiang (SLAC), G. Vianello (Stanford) report on behalf of the Fermi-LAT team:

At 07:47:06 UT on 27 April 2013, Fermi LAT detected high energy emission from GRB 130427A, which was also detected by Fermi-GBM (trigger 388741629/130427324) and by Swift (Maselli et al. GCN 14448). The GBM detection triggered an autonomous repoint of the spacecraft.

The LAT on-ground location is consistent with the optical position reported in Elenin et al. (GCN 14450). The burst was about 47 deg from the LAT boresight at the time of the trigger and within the LAT field of view for the next 700 seconds.

The data from the Fermi LAT show a multi-peaked light curve consistent with the GBM trigger. More than 200 photons above 100 MeV are observed within 100 seconds with a TS of >1000. Using the non-standard LAT Low Energy (LLE) data selection, thousands of counts above background were detected within a 100 s interval coinciding with the time of the GBM emission, with a significance of ~40 sigma.
The highest energy LAT photon has an energy of 94 GeV.

A GBM circular is forthcoming.

The Fermi LAT point of contact for this burst is Sylvia Zhu (s.jc.zhu@gmail.com).

The Fermi LAT is a pair conversion telescope designed to cover the energy band from 20 MeV to greater than 300 GeV. It is the product of an international collaboration between NASA and DOE in the U.S. and many scientific institutions across France, Italy, Japan and Sweden.

[GCN OPS NOTE(30apr13): Per author's request, time in the first sentence was changed from "07:47:15" to "07:47:06".]

2.a. Current high-energy space missions

Konus-Wind (1994-?)

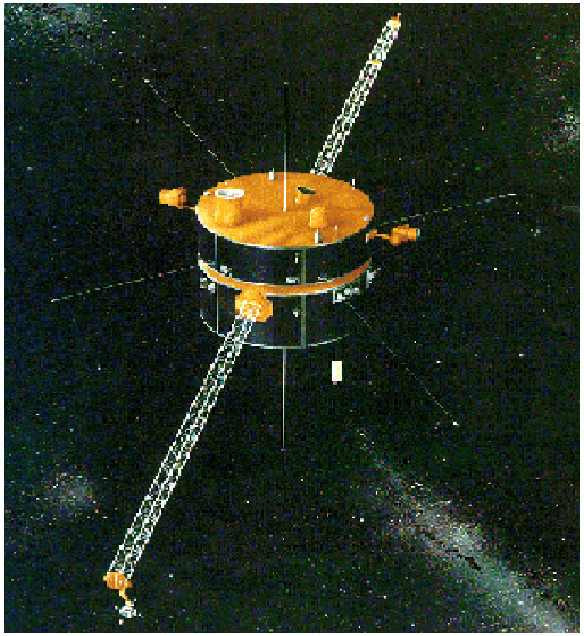

- **Joint Russian-American experiment**
- **Two NaI(Tl) detectors:** 13 cm diameter, 7.5 cm height
  - Opposite faces of s/c → **full sky coverage**
  - ~20 keV – 15 MeV energy range (present time)
  - Effective area: ~100-160 cm^2
- **Triggers (Nov. 1994 – May 2012)**
  - **2145 GRBs – 1782 long (83%), 363 short (17%)**
  - **145 *Swift*/BAT GRBs (21%), including GRB 080319B!**
  - **92 GRBs with measured redshift**

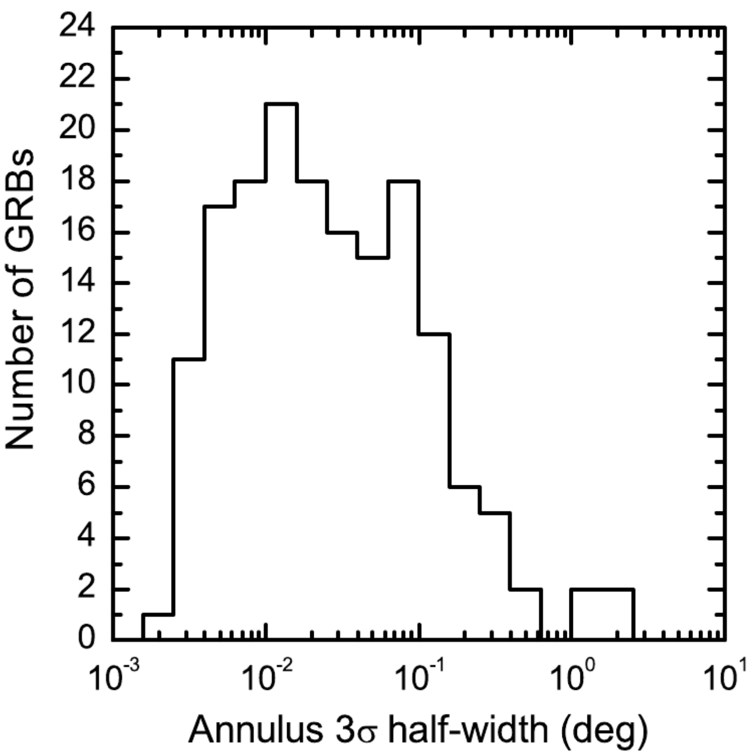

- **Will be followed by Konus-UF (10 keV – 15 MeV) onboard Spectr-UF / World Space Observatory (to be launched in 2016)**

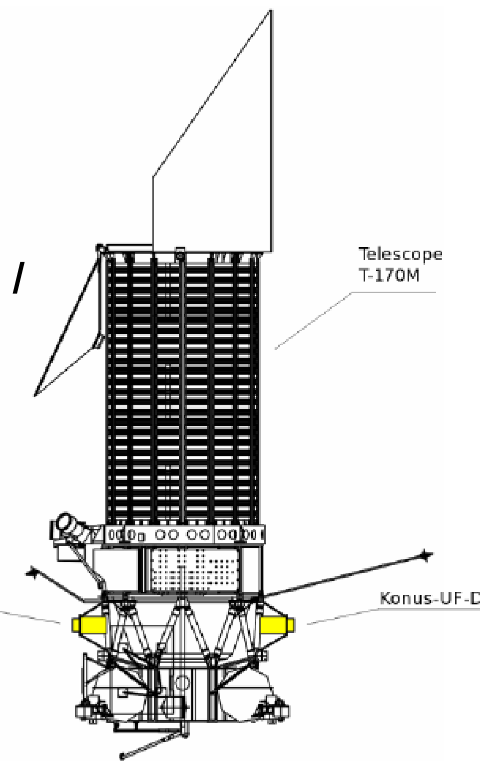

Pal'shin et al. 2013, arXiv:1301.3740

- **IPN localizations of Konus short GRBs:** distribution of 3σ half-widths of the 164 triangulation annuli obtained using the distant s/c data

IPN localizations of Konus short GRBs

Pal'shin et al. 2013, arXiv:1301.3740

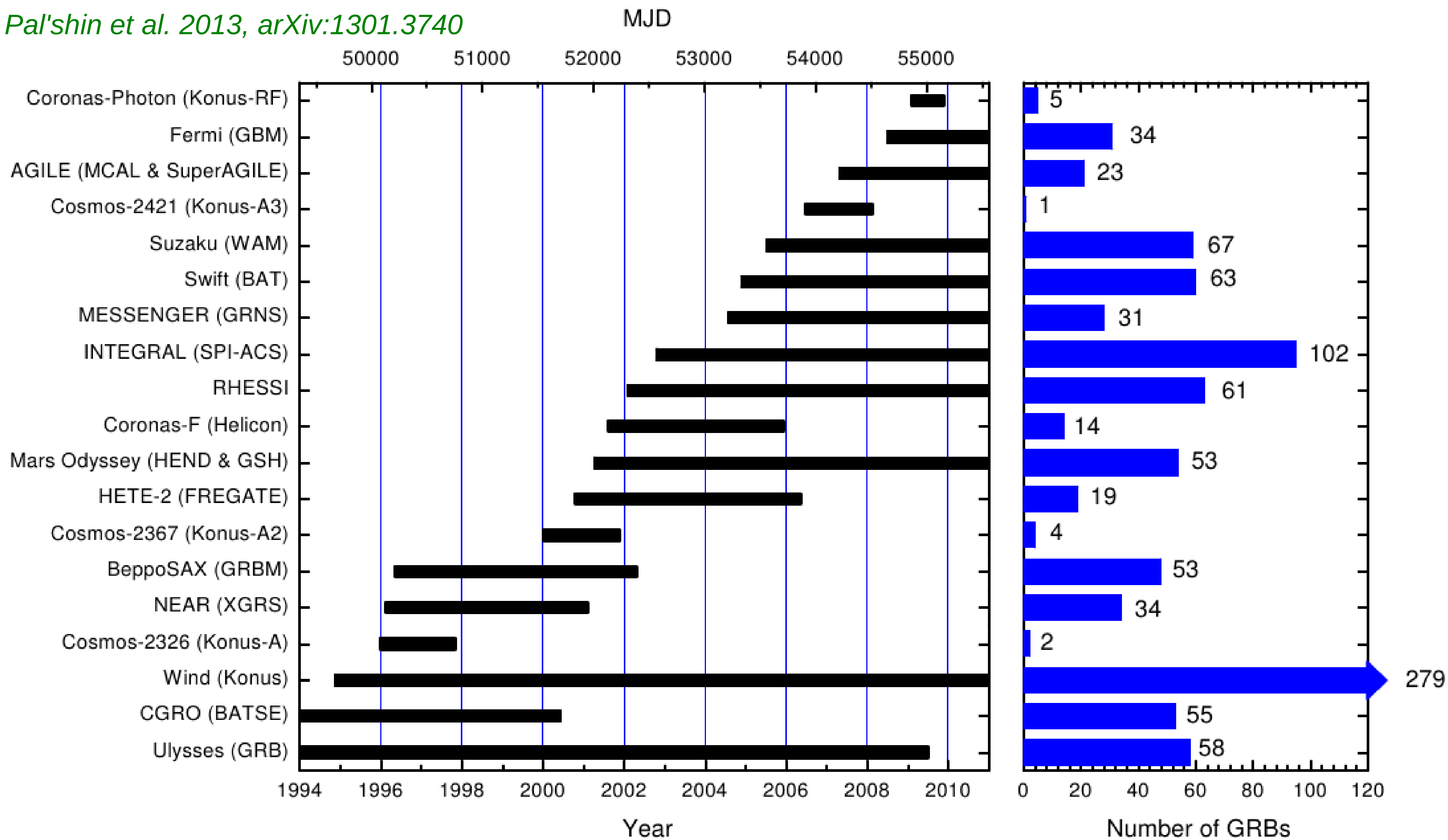

- **Left:** timelines of the IPN missions / instruments since the launch of Wind in 1994
- **Right:** number of Konus short bursts observed by each mission
  - For Konus-Wind: number of bursts observed by at least one other IPN s/c

The INTEGRAL mission (2002-?)

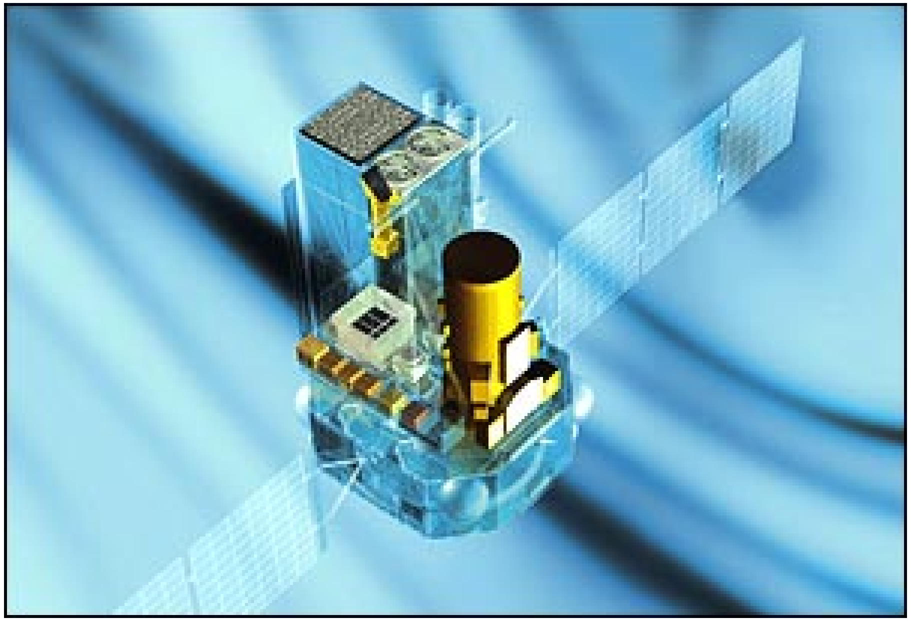

- **INTErnational Gamma-Ray Astrophysics Laboratory**
  - Launched in Oct. 2002 (ESA M2 mission)
  - Combines imaging and spectroscopy
- **SPI spectrometer:** emphasis on spectroscopy
  - Coded mask + 19 high-purity Ge detectors (85 K)
- **IBIS imager:** emphasis on imaging
  - Coded mask + 2 layers of pixel detectors: ISGRI (CdTe) and PICsIT (CsI)
- **X-ray monitor JEM-X**
  - 3-35 keV, 4.8° FoV, localization <20″
- **Optical monitor OMC**
  - 5° FoV, localization <8″
- **Science operations <u>currently</u> approved until 12/31/2014**

Instrument	**SPI**	**IBIS**
Energy range	15 keV - 8 MeV	20 keV - 10 MeV
$\Delta E/E$	**0.2% @ 1 MeV**	7% @ 100 keV
Field of view	16° fully coded	9°x9° fully coded
Angular resolution	2°	**12'**
Source location	20'	**<1'**
Timing accuracy	100 μs	67 μs
Sensitivity (10^6 s) $cm^{-2}\ s^{-1}\ keV^{-1}$	7×10^{-8} @ 1 MeV	4×10^{-7} @ 1 MeV

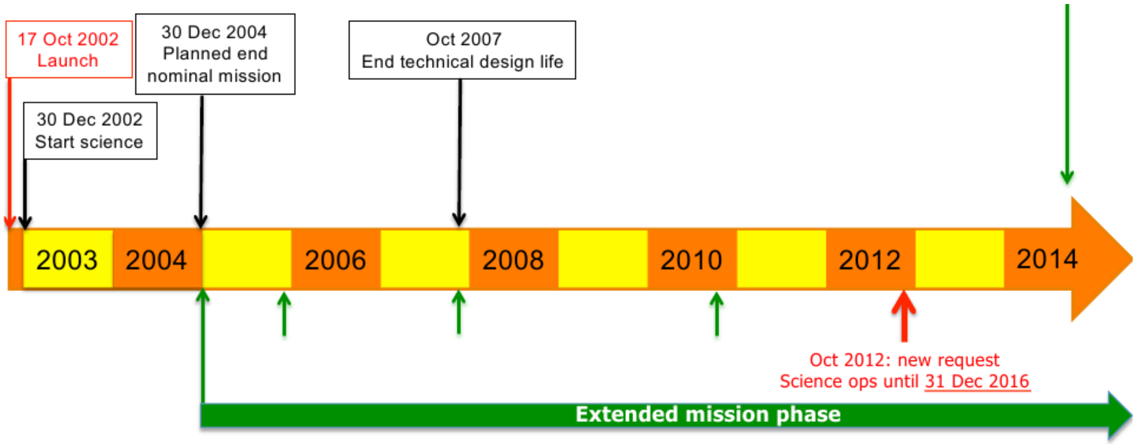

GRB observations with INTEGRAL

- **INTEGRAL Burst Alert System:** real-time localizations
  - Rate increase and imaging algorithms (15-200 keV)
  - Time scales from 2 ms to 100 s are searched for
- **More than 90 GRBs localized** in real-time (a few exceptions), **7 redshifts**

- **GRB 041219A polarization**
  - IBIS used as a Compton polarimeter (200-800 keV)
  - Events interacting once in the upper layer (ISGRI) and once in the lower layer (PICsIT)
  - Polarization dependency of the differential cross section for Compton scattering

$$\frac{d\sigma}{d\Omega} = \frac{r_0^2}{2}\left(\frac{E'}{E_0}\right)^2\left(\frac{E'}{E_0} + \frac{E_0}{E'} - 2\sin^2\theta\cos^2\phi\right)$$

    - E_0 (E') energies of the indicent (scattered) photon
    - ϕ azimuthal angle w.r.t. polarization direction:

$$N(\phi) = S[1 + a_0 \cos 2(\phi - \phi_0)]$$

  - Polarization angle: P.A. = $\phi_0 - \pi/2 + n\pi$
  - Polarization fraction: $\Pi = a_0 / a_{100}$, where a_{100} is the amplitude expected for a 100% polarized source

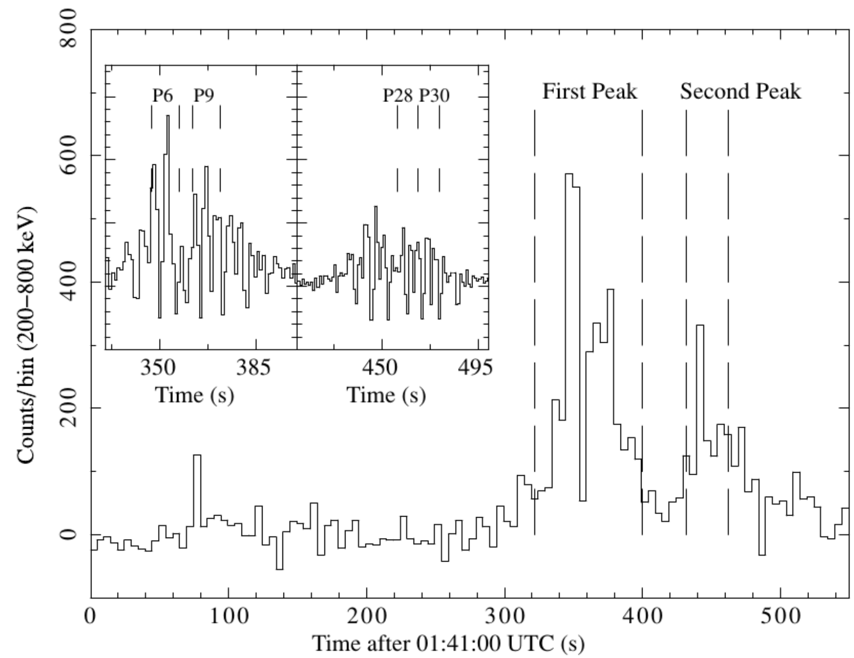

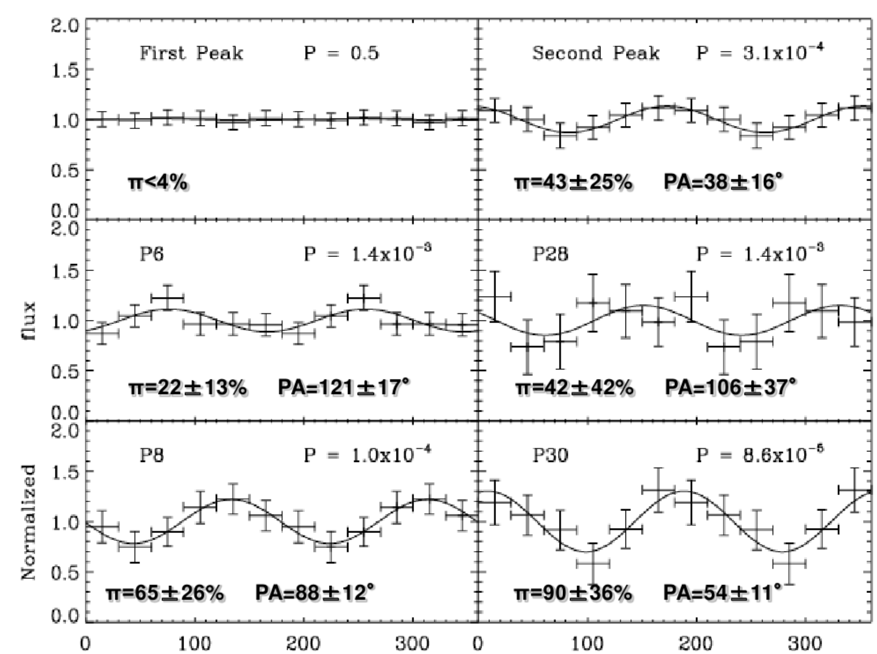

The *Swift* observatory (2004-?)

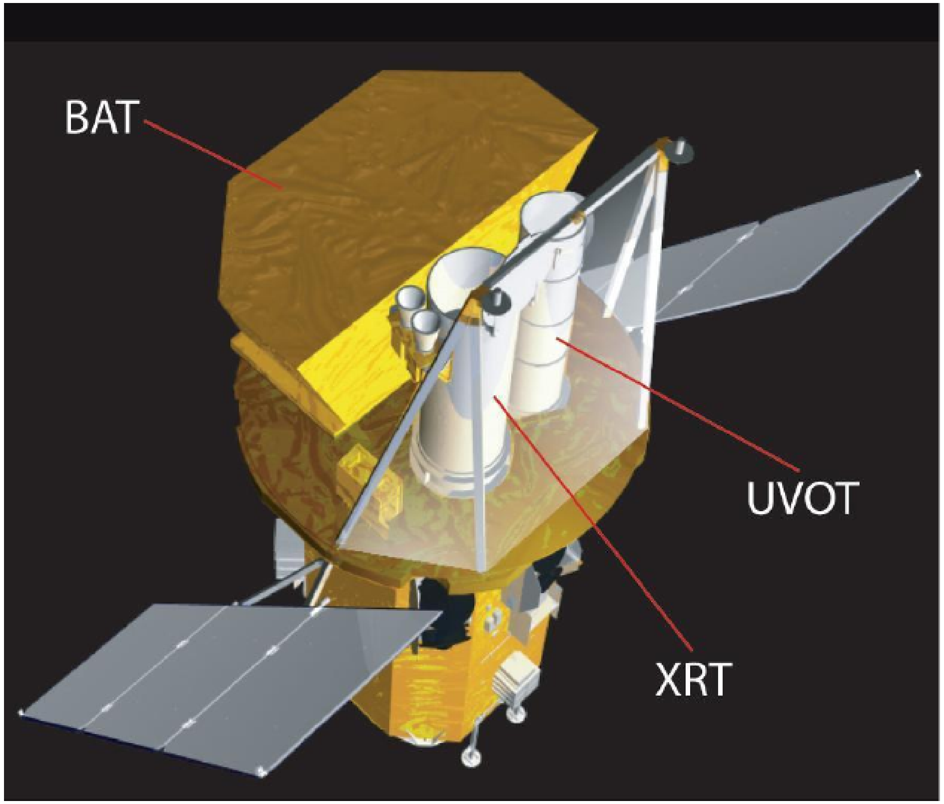

Gehrels et al. 2004, ApJ 611, 1005

- **Burst Alert Telescope (BAT)**
  - Coded mask + CdZnTe
  - 15-150 keV, 2 sr FoV
  - Detects >100 GRBs / yr
  - Centroid accuracy: 1' - 4'
- **X-Ray Telescope (XRT)**
  - Grazing incidence imaging telescope
  - 0.2-10 keV, narrow-field (24'x24') camera
  - Centroid accuracy: 5”
- **UV/Optical Telescope (UVOT)**
  - 30 cm telescope, 6 filters, 24 mag sensitivity
  - Centroid accuracy: 0.5”
- **Autonomous repointing (20-100 s)**

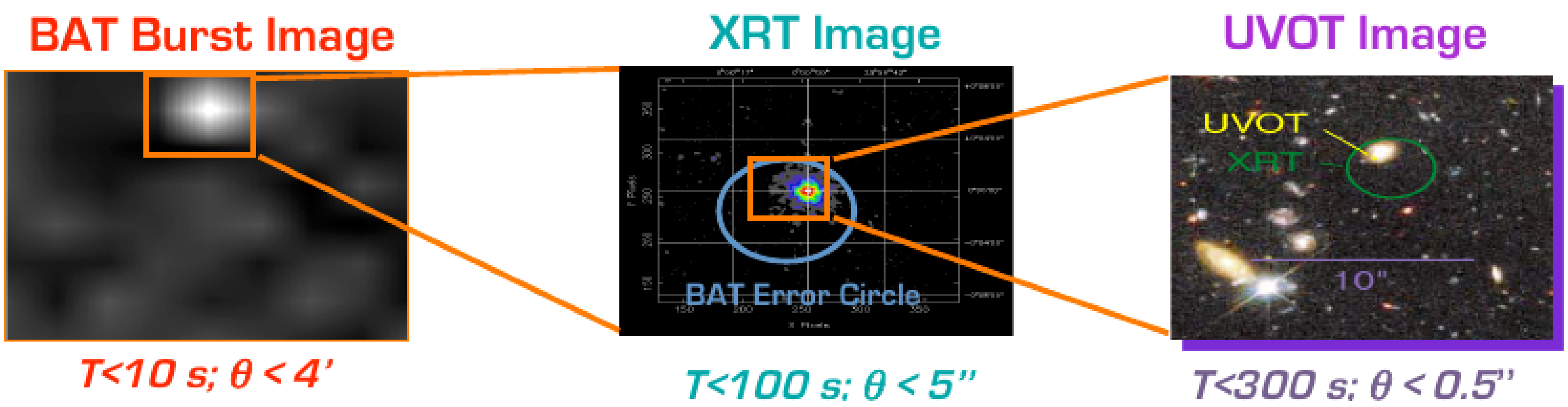

The Burst Alert Telescope (1/2)

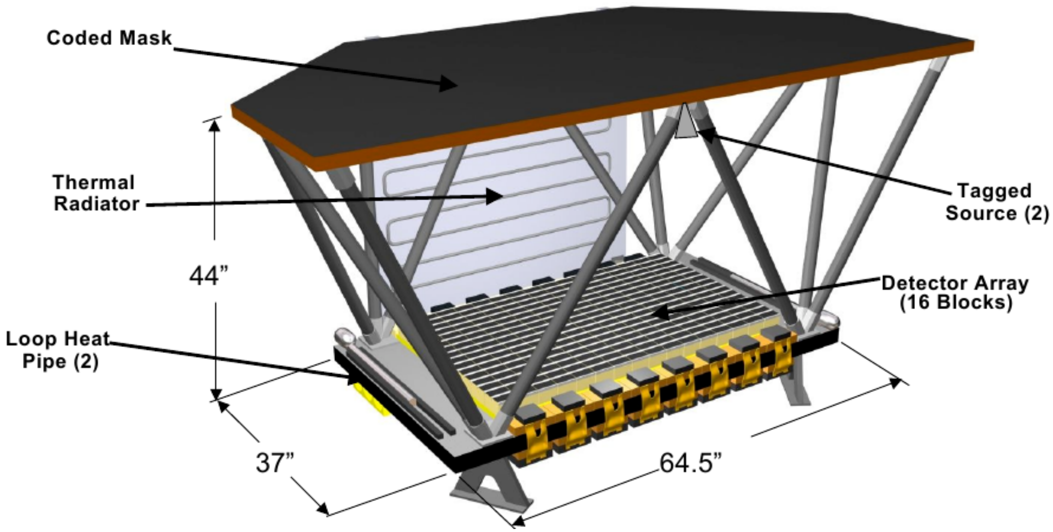

- **Coded mask**
  - 2.7 m^2, random pattern (50% open, 50% closed)
  - 50 000 lead tiles opaque to γ rays
- **Detectors**
  - 32 768 fine pixels
  - 128 pixels / modules, 256 modules
  - 5240 cm^2 detector area

BURST ALERT TELESCOPE CHARACTERISTICS

BAT Parameter	Value
Energy range	15–150 keV
Energy resolution	~7 keV
Aperture	Coded mask, random pattern, 50% open
Detection area	5240 cm^2
Detector material	CdZnTe (CZT)
Detector operation	Photon counting
Field of view	1.4 sr (half-coded)
Detector elements	256 modules of 128 elements module^{-1}
Detector element size	$4 \times 4 \times 2$ mm^3
Coded-mask cell size	$5 \times 5 \times 1$ mm^3 Pb tiles
Telescope PSF	<20″
Source position and determination	1″–4″
Sensitivity	$\sim 10^{-8}$ ergs cm^{-2} s^{-1}

1 BAT detector module

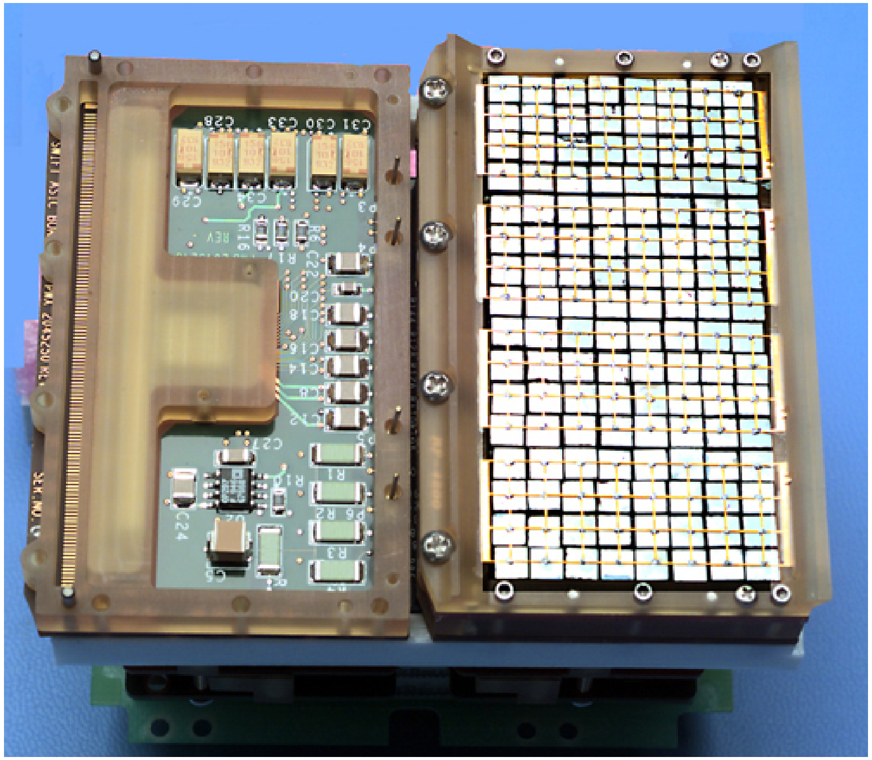

The Burst Alert Telescope (2/2)

The X-Ray Telescope

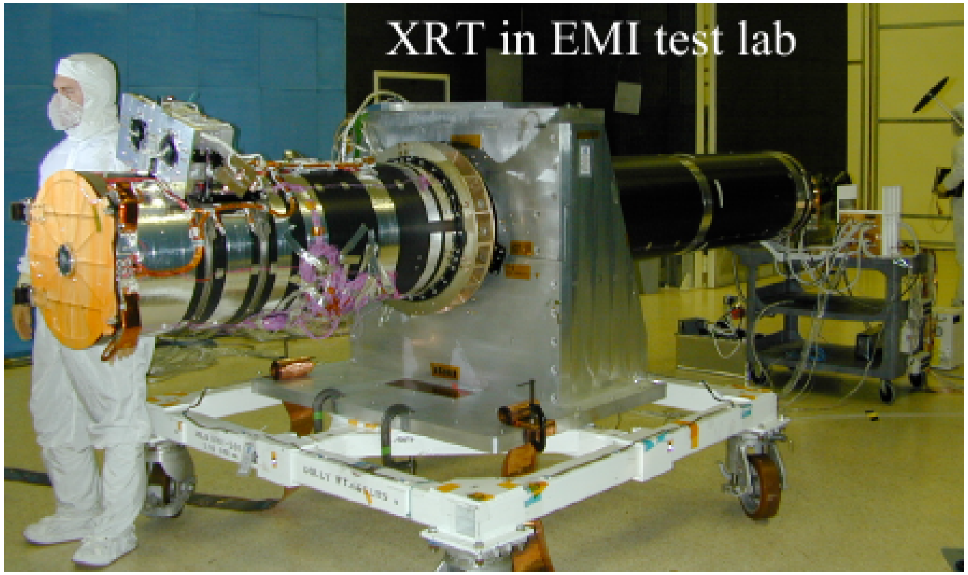

XRT parameters

Energy range	0.2–10 keV
Telescope	JET-X Wolter 1
Effective area	110 cm^3 @ 1.5 keV
Field of view	$23.6 \times 23.6'$
Detection elements	600×600 pixels
Telescope PSF	18″ HPD @ 1.5 keV
Sensitivity	2×10^{-14} $erg\,cm^{-2}\,s^{-1}$

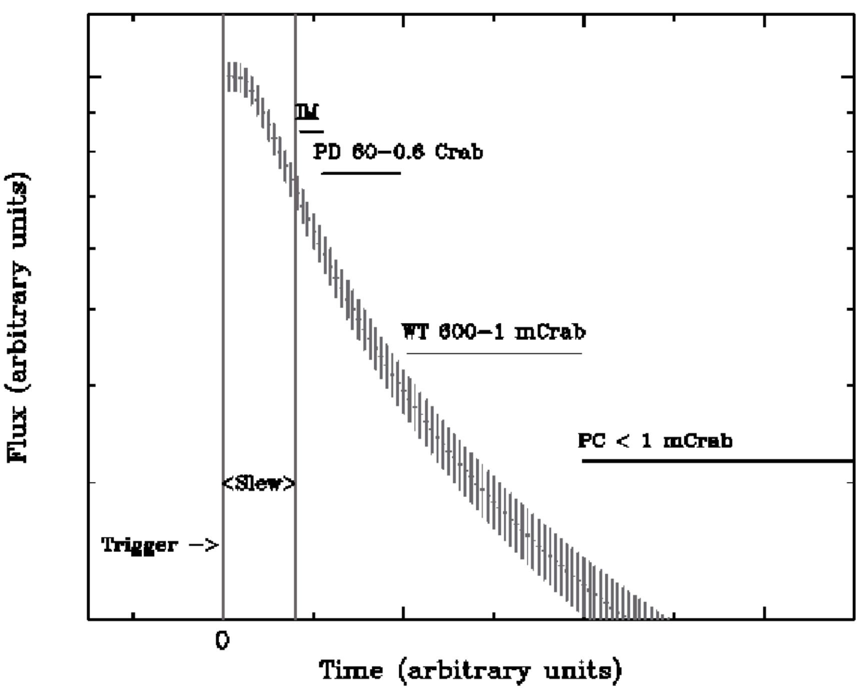

- The XRT must autonomously select readout modes suited to observations of GRBs and afterglows
- More details in K. Page's lecture

Mode	Image capability	Spectral Capability	Time resolution	Cal sources in FOV	On-board Event reconstruction	Flux level mode switch
PU & LR	no	Yes	0.14 ms	yes	no, done on-ground	0.6-60 Crab
WT	1D	Yes	1.7 ms	no	no, done on ground	1-600 mCrab
PC	2D	Yes	2.5 s	See window size	yes	< 1 mCrab
IM	2D	No	0.1 s (short)	yes	not applicable	> 140 mCrab
		No	2.5 s (long)			< 5.6 mCrab

Swift triggers

- **BAT rate triggers**
  - Take a rate history in a specific energy range and region
  - Look on many time scales for an increase that exceeds threshold and pick the most significant
  - Then use that Δt, E to make a detector map
  - Short (<64 ms) & long rate triggers

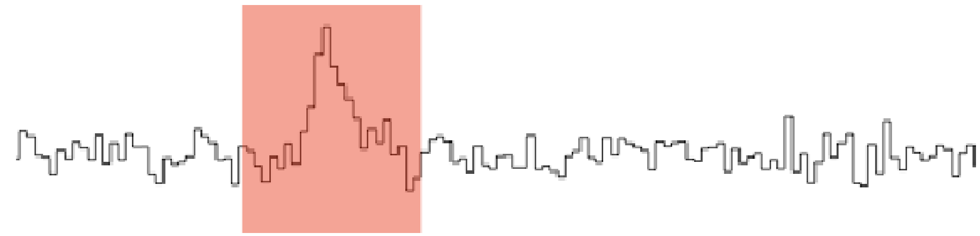

- **BAT image triggers, 15-50 keV (FFT analysis)**
  - 64 s image: anything new found is called a GRB
  - Images of 320 s or 5-42 min: anything new found is called a transient

- **Initial image (rather than rate) triggers may be indicative of high-z bursts (b/c of time dilatation)**

- **747 BAT GRBs as of March 2013**
  - 85% with X-ray observations <300 s
  - 77% with X-ray detections
  - 60% with optical detections (UVOT, ground)
  - **237 with redshift (41 prior to Swift), 9 above z=5**
  - **>60 short GRBs localized (0 prior to Swift)**

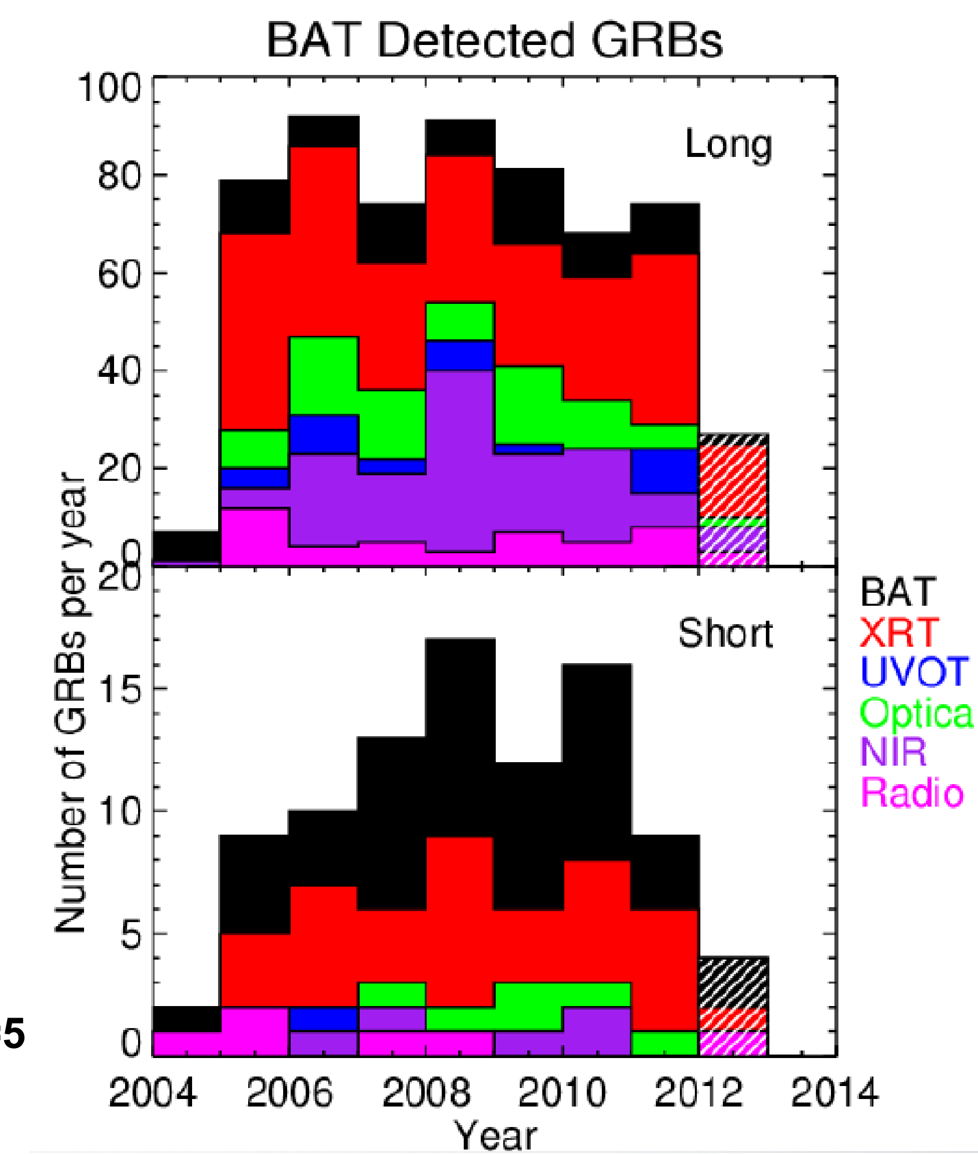

Swift evolving observing time

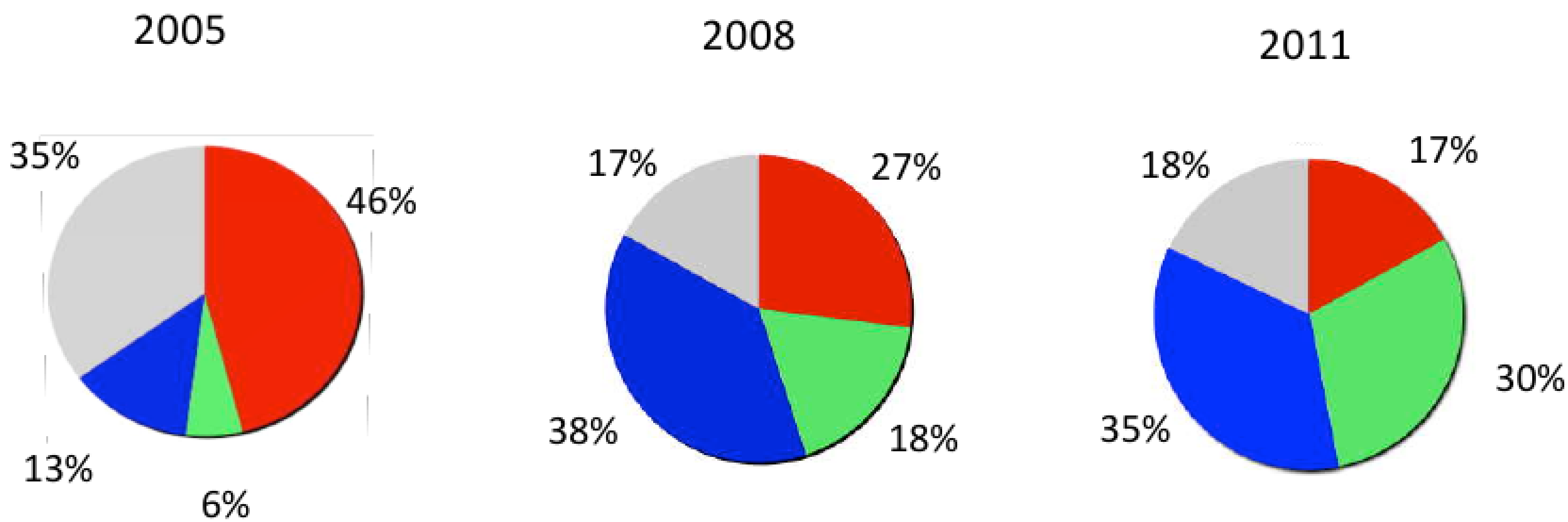

GRBs

Target of Opportunities (TOOs)

Guest Investigator targets / Fill-ins

SAA & Calibration

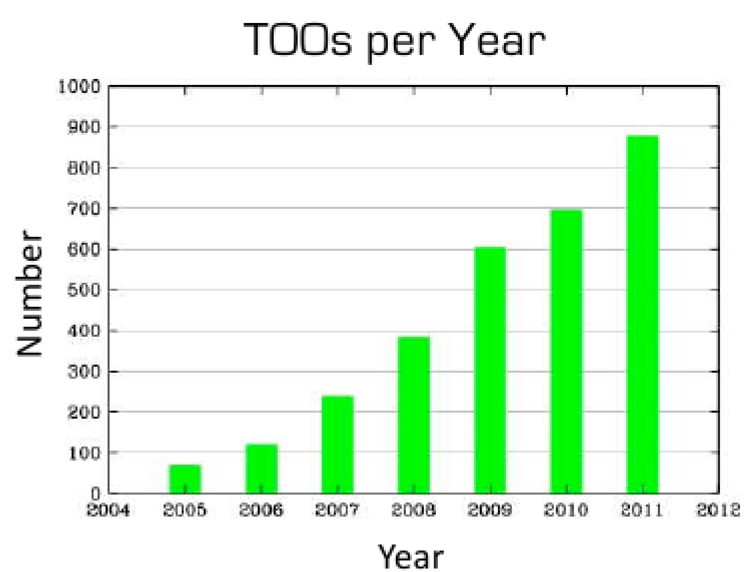

Swift new operations initiatives

- **Enhanced BAT triggering**
  - Fluence triggering for long transients
  - Galaxy position in BAT onboard catalog

- **Automated / rapid tiling observations for large error boxes**
  - *Fermi*/LAT low significance bursts
  - Advanced Ligo / Virgo triggers
  - Inter-Planetary Network
  - Observe all tiles within one orbit (rather than multiple TOOs)
  - 4 configurations
    - 2x2 (~0.3 deg radius)
    - 7 (~0.5 deg radius)
    - 19 (~0.7 deg radius)
    - 37 (~1 deg radius)
  - Significant observing campaign, but worthwhile for high priority targets

- **BAT sub-threshold catalog to be released and real-time release from then on**

Auto Sky Tiling

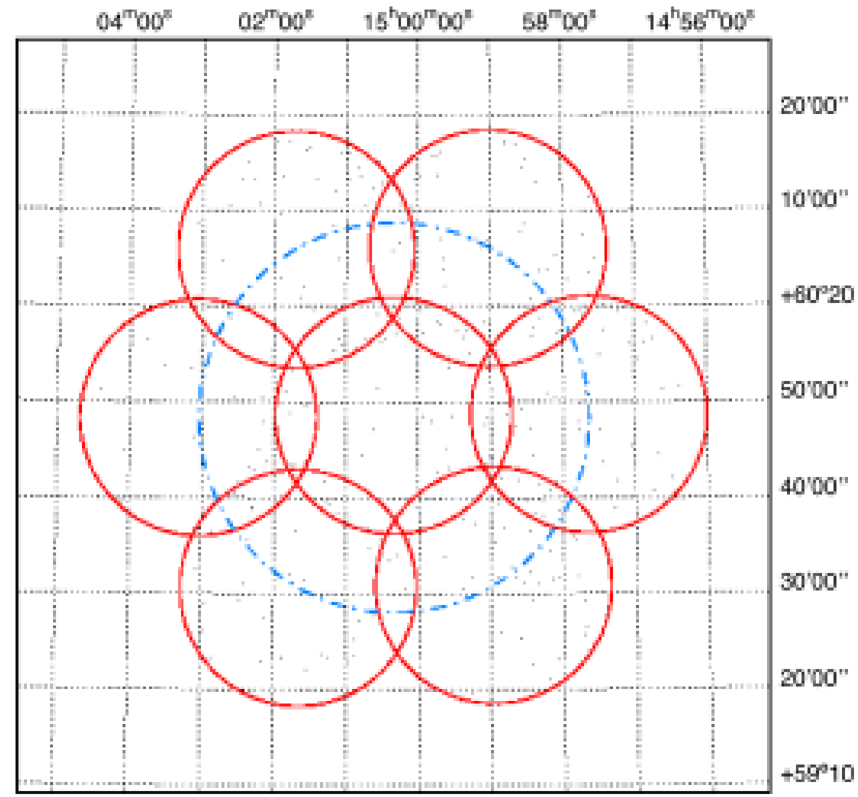

The *Fermi* observatory (2008-?)

Atwood et al. 2009, ApJ 697, 1071

- **Large Area Telescope (LAT)**
  - Large field of view (2.4 sr @ 1 GeV)
  - Sees the entire sky every 3 hours
  - 20 MeV to >300 GeV
  - Onboard and ground burst triggers
  - Localization, spectroscopy

Meegan et al. 2009, ApJ 702, 791

- **Gamma-ray Burst Monitor (GBM)**
  - Sees the entire unocculted sky (>9.5 sr)
  - 8 keV to 40 MeV
  - 12 NaI detectors (8 keV to 1 MeV)
    - Onboard trigger, onboard and ground localizations, spectroscopy
  - 2 BGO detectors (150 keV to 40 MeV)
    - Spectroscopy

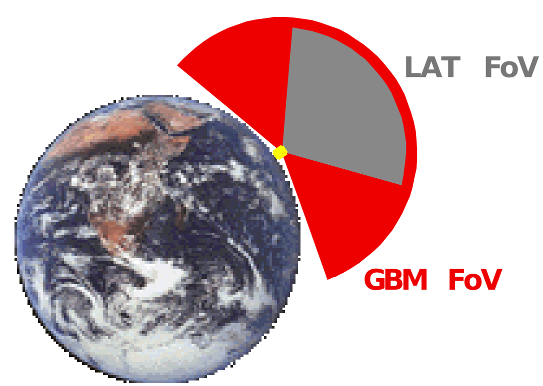

Response of GBM detectors

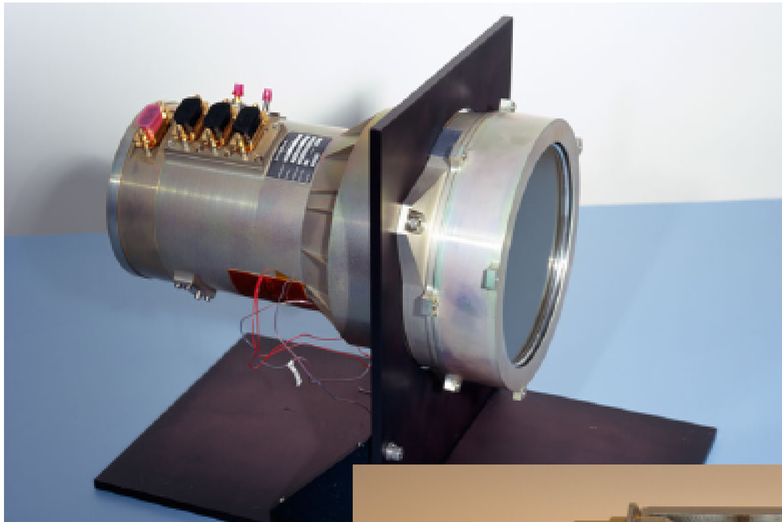

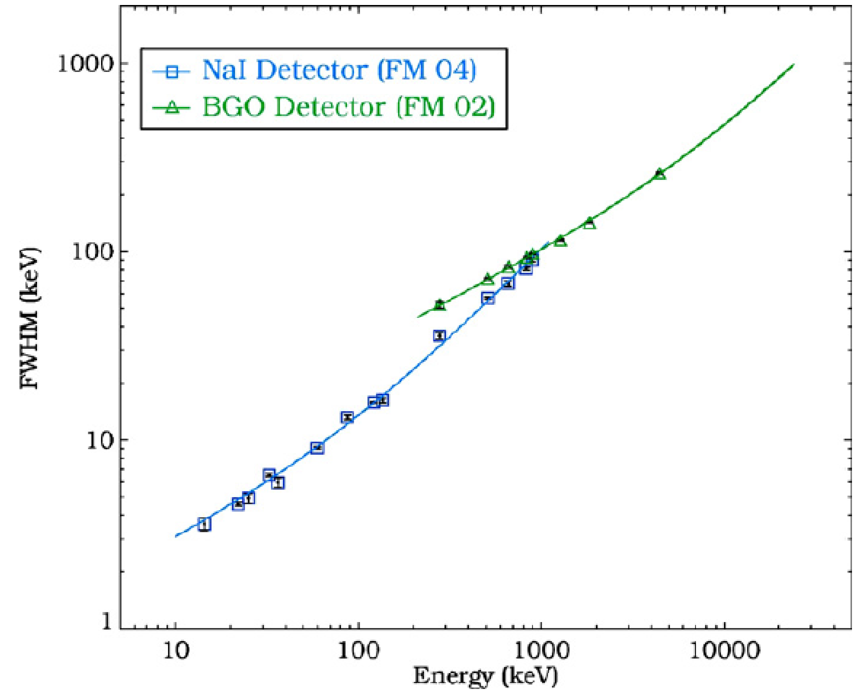

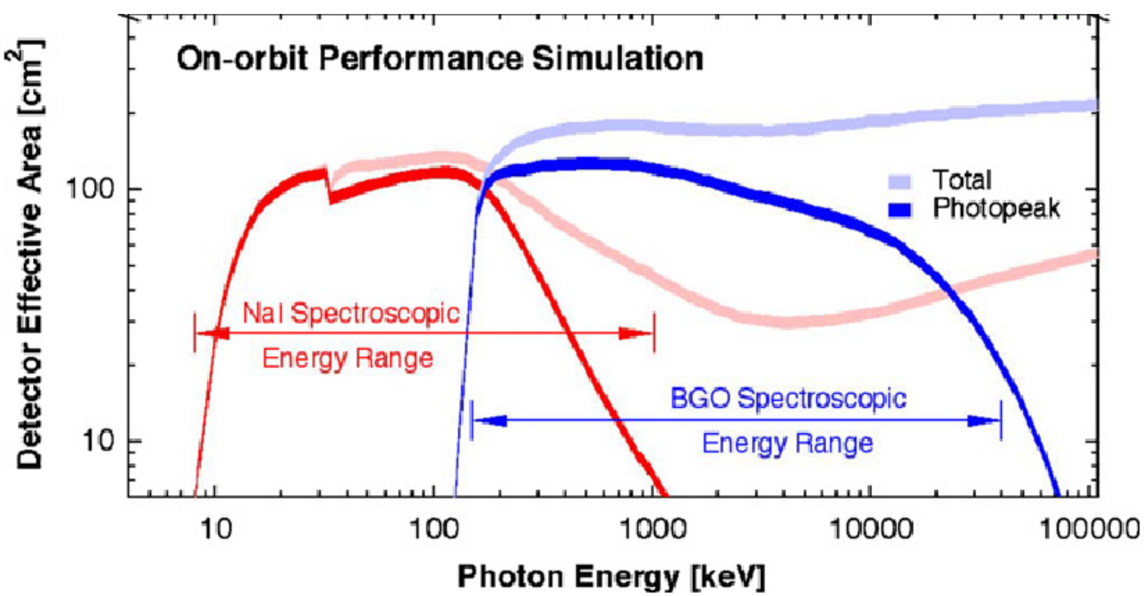

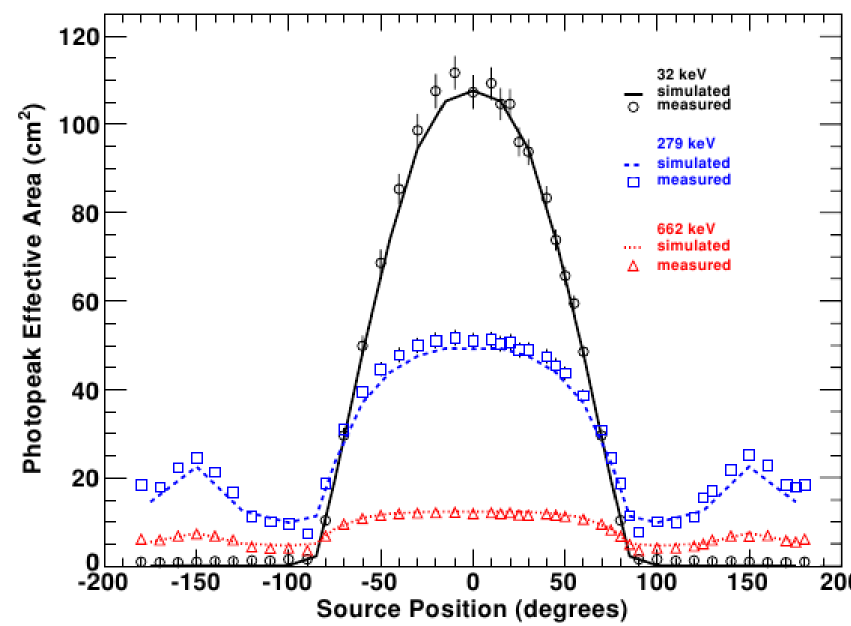

GBM triggers and alerts

GBM triggers over the mission

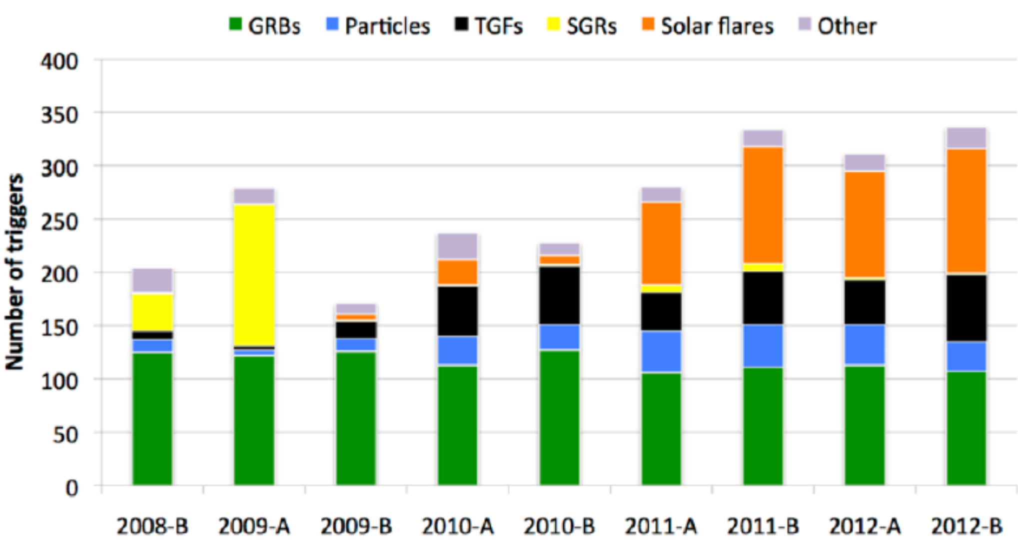

GBM actions on triggering

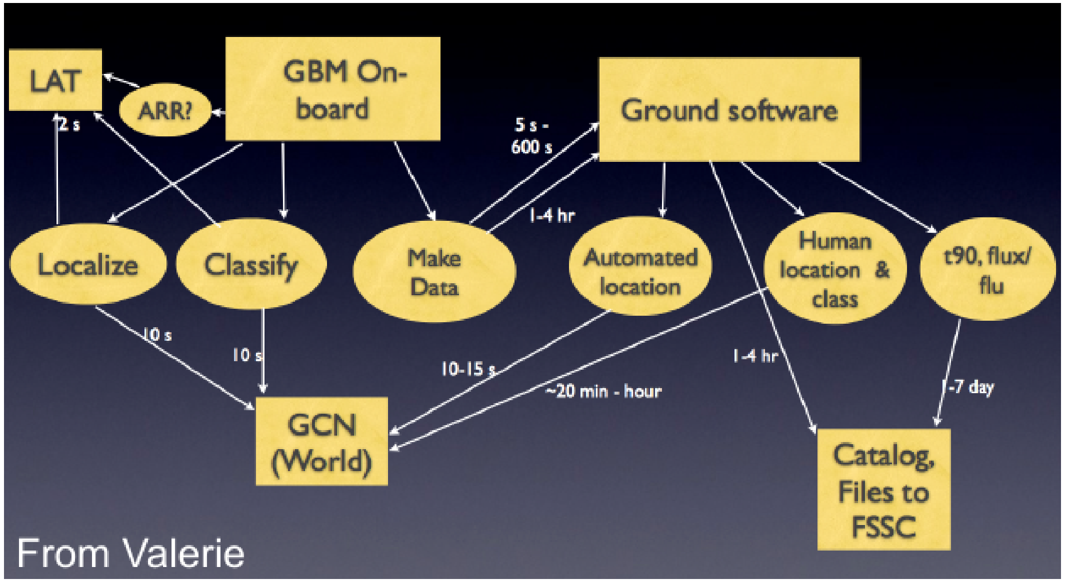

- **Increase of the solar cycle**
- **New TGF algorithm on Nov. 2009**

- **Onboard GRB trigger**
  - Two or more detectors over threshold
  - More flexible algorithm compared with BATSE → better sensitivity to very short GRBs and long soft GRBs
  - Onboard trigger classifications (solar flare, particle event, GRB, etc)

- **Localization of GRBs by GBM**
  - GRB locations computed onboard (<2 s) to allow re-orienting the s/c in view of LAT afterglow observations
  - On-board locations transmitted to the ground and distributed (GCN notices), with a typical latency of ~10 s
  - On-ground automated locations: more accurate, typical latency of few 10's s
  - Somewhat longer latency using human intervention

GBM localizations

- **Bright GBM-detected bursts:** location accuracy is limited by the incomplete knowledge of **systematic effects** (e.g., scattering in the s/c and the Earth's atmosphere)

- **Flight software (FSW):** at least one sky location for each trigger
  - May compute more, depending on the intensity and duration of the event
- **Automated on-ground locations:** same timescales as chosen by the FSW but GCN notices are distributed only if the calculated error is smaller
- **One or more on-ground locations** by operations personnel

W. S. Paciesas, M. S. Briggs, V. Connaughton, C. A. Meegan, GRB 2013 conference (Nashville)

- **FSW → on-ground improvement:**
  - Different binning of angular response tables (5° onboard, 1° on ground)
  - 3 spectral models instead of 1
  - Improved treatment of scattering from the Earth's atmosphere

- **Systematic errors of 6.6° and 3.9°** for the on-ground automatic and manual localizations
- **Indication of non-Gaussian errors**, with an extended tail of large outliers

	FSW	On-Ground Automatic	On-Ground Final
Total GRBs	130	128	129
Median reported error[@]	10.6°	5.0°	3.2°
Median true error	9.0°	7.3°	4.3°
Fraction with true error < reported error	57%	31%	40%
Fraction with true error < 2x reported error	84%	73%	69%
Systematic error[#]		6.6°	3.9°

[@] The reported FSW errors include a systematic error term; on-ground errors are statistical only

[#] Add in quadrature to reported error to obtain 68% confidence error

The IPN supplement to the GBM catalog of GRBs

Hurley et al. 2013, arXiv:1301.3522

Table 1. Recent IPN catalogs of gamma-ray bursts.

Years covered	Number of GRBs	Description
1990–1992	16	*Ulysses, Pioneer Venus Orbiter,* WATCH, SIGMA, PHEBUS GRBs[a]
1990–1994	56	*Granat*-WATCH supplement[b]
1991–1992	37	*Pioneer Venus Orbiter, Compton Gamma-Ray Observatory, Ulysses* GRBs[c]
1991–1994	218	BATSE 3B supplement[d]
1991–2000	211	BATSE untriggered burst supplement[e]
1992–1993	9	*Mars Observer* GRBs[f]
1994–1996	147	BATSE 4Br supplement[g]
1994–2012	~300	Konus short bursts[h]
1996–2000	343	BATSE 5B supplement[i]
1996–2002	475	*BeppoSAX* supplement[j]
2000–2006	226	HETE-2 supplement[k]
2008–2010	146	GBM supplement[l]

Table 4. Number of GBM bursts observed by each IPN spacecraft.

Konus	Suzaku	INTEGRAL	Swift	MESSENGER	RHESSI	AGILE	Odyssey	MAXI	RXTE
281	199	184	151	126	86	67	56	4	1

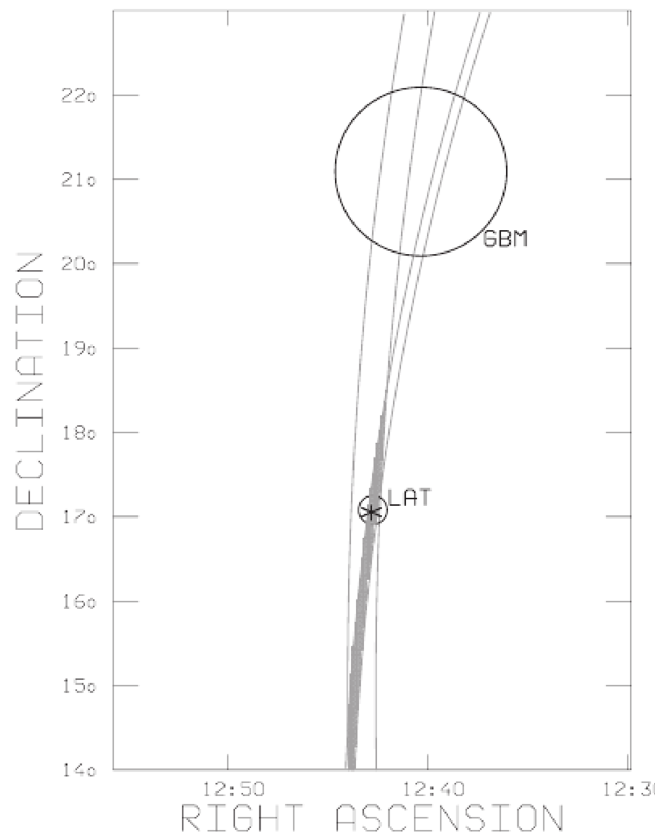

- **491 bursts examined**, 393 observed by at least one other instrument in the 9-s/c IPN
- **Localizations of 146 GRBs could be improved by triangulation**
- IPN localizations intersect the 1σ GBM error circles in only 52% of the cases, if no GBM systematic uncertainty assumed → **87% agreement if 6° GBM systematic uncertainty assumed**
- IPN 1σ error boxes: areas **between ~1 square arcmin and 110 square degrees**
  - **On average, a factor of 180 smaller than the corresponding GBM localizations**

The Large Area Telescope

- **Sub-systems work together** to identify and measure the flux of cosmic gamma rays
- **Precision Si-strip Tracker**
  - 18 XY tracking planes
  - Single-sided silicon strip detectors: 228 µm pitch, 880 000 channels
  - Tungsten foil converters (1.5 X_0)
  - Measures the photon direction; gamma ID
- **Hodoscopic CsI Calorimeter**
  - Array of 1536 CsI(Tl) crystals in 8 layers
  - 3072 spectroscopy channels (8.5 X_0)
  - Hodoscopic array supports bkg rejection and shower leakage correction
  - Measures the energy; images the shower
- **Segmented Anti-Coincidence Detector**
  - 89 plastic scintillator tiles
  - Rejects background of charged cosmic rays
  - Segmentation minimizes self-veto effects at high energy
- **Electronics System**
  - Includes flexible, robust hardware trigger and software filters

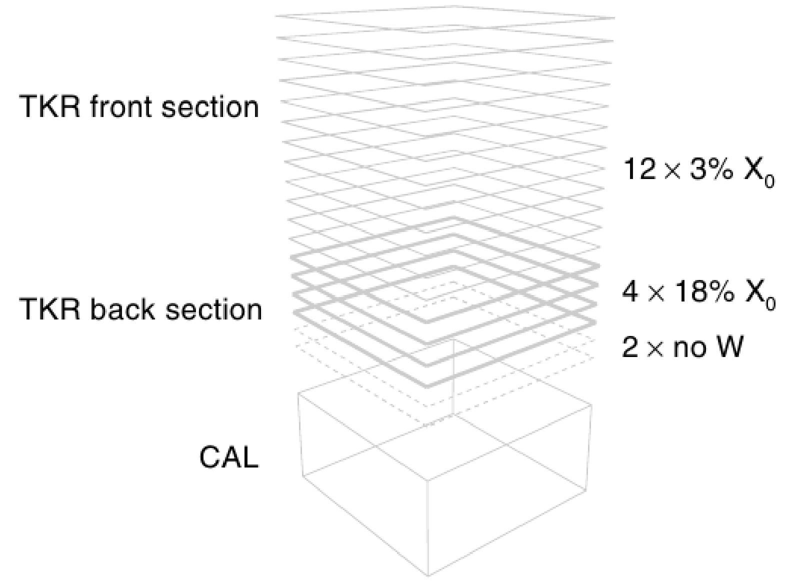

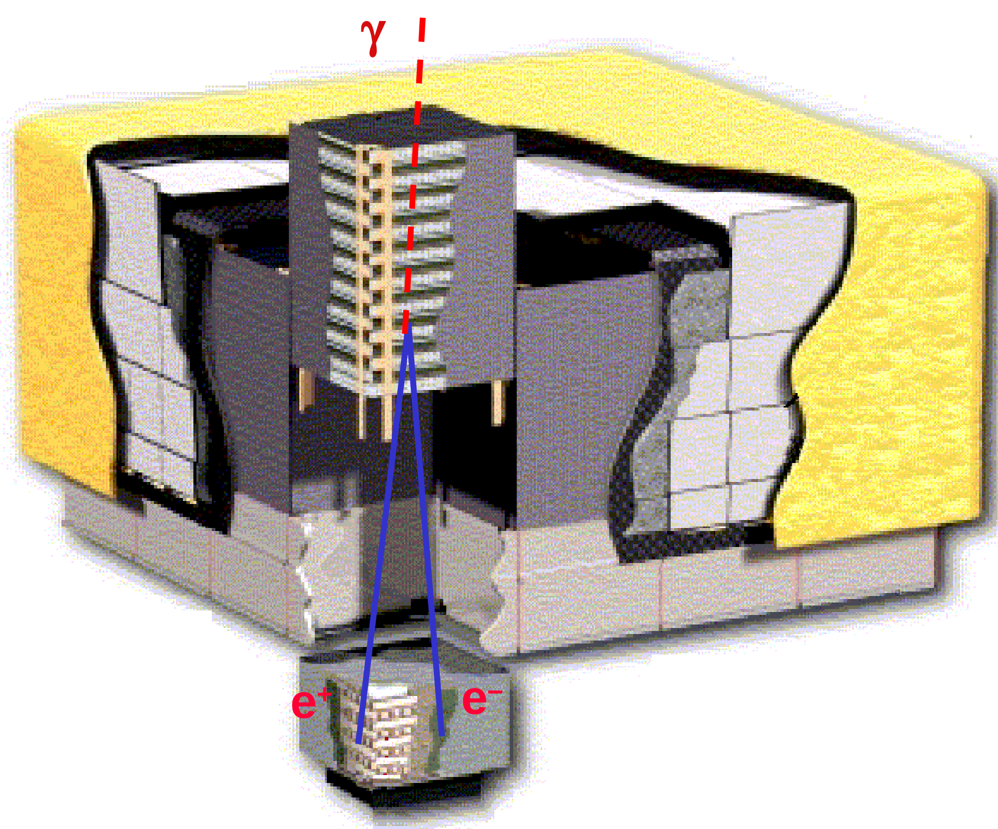

The LAT sub-systems during integration

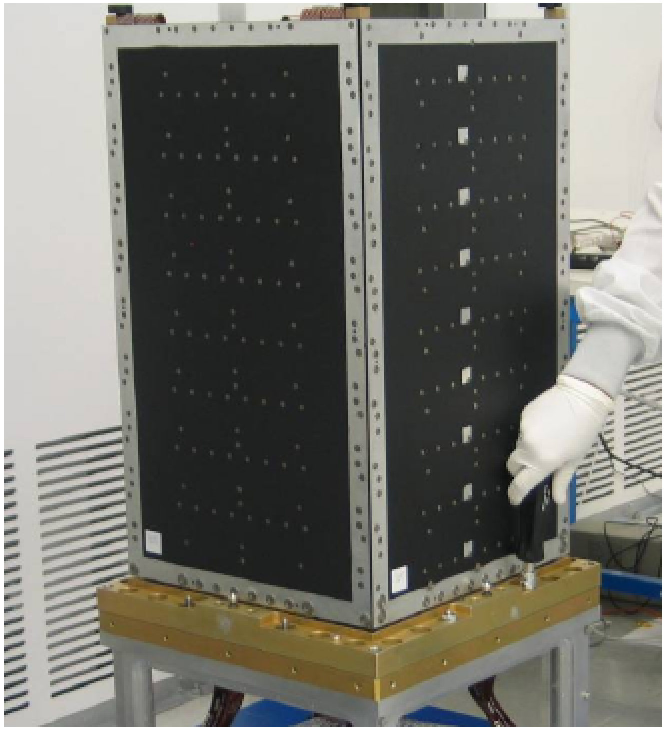

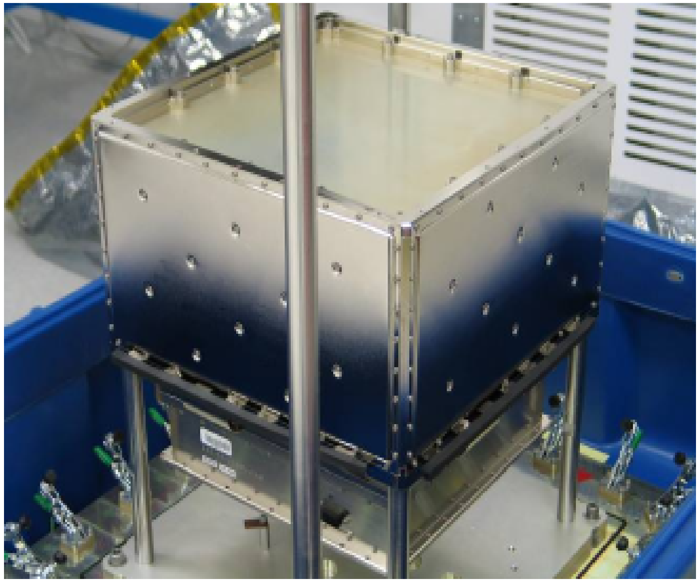

1 CAL module

ACD

1 TKR module

LAT Instrument Response Functions

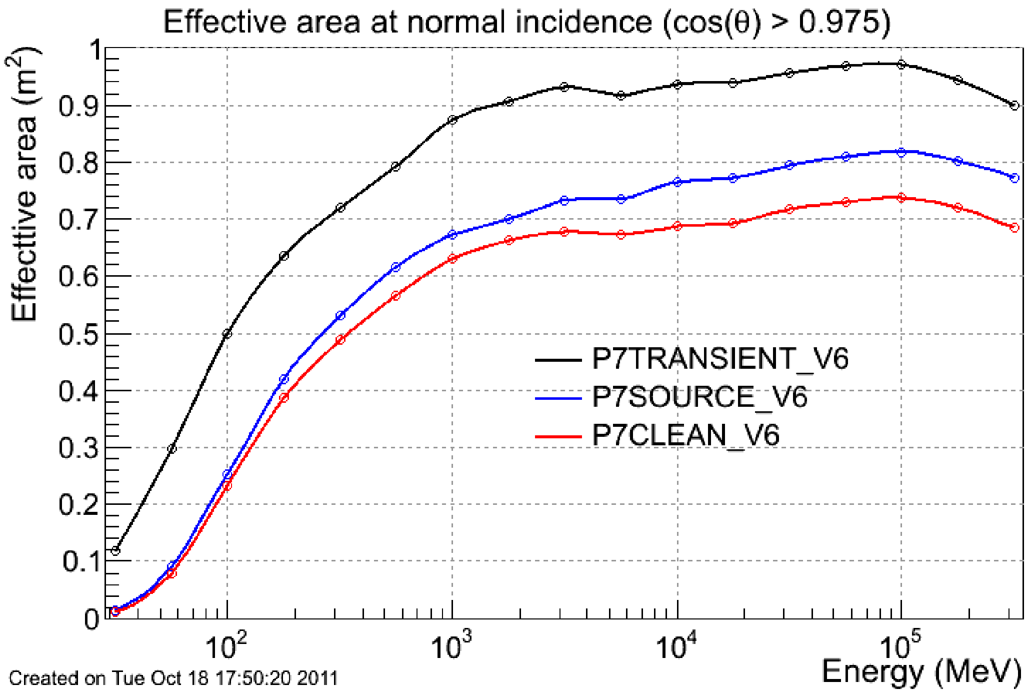

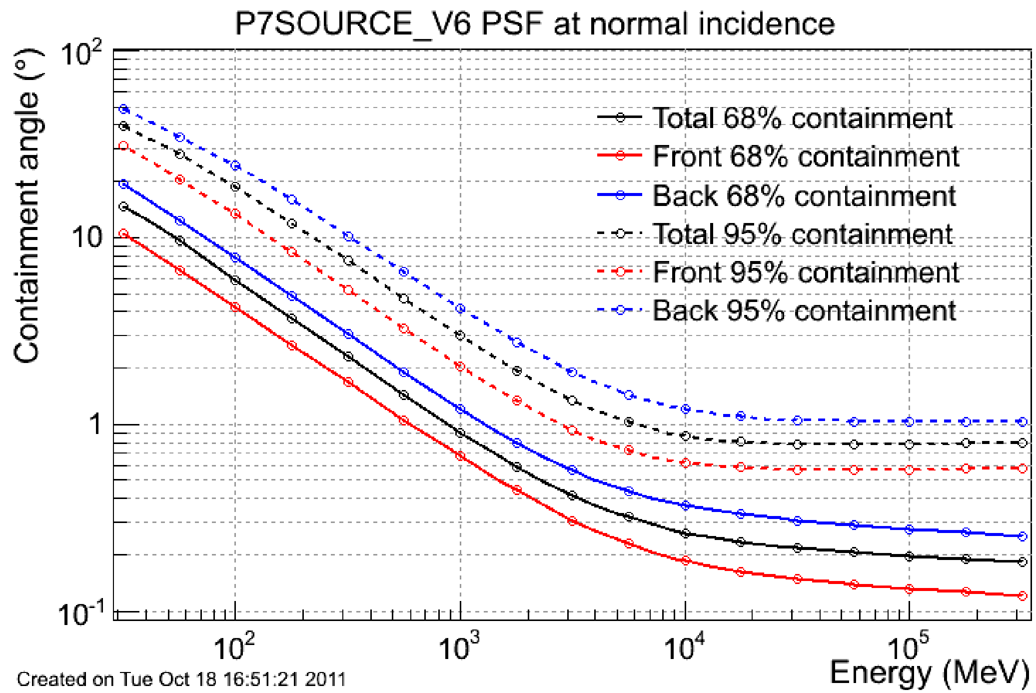

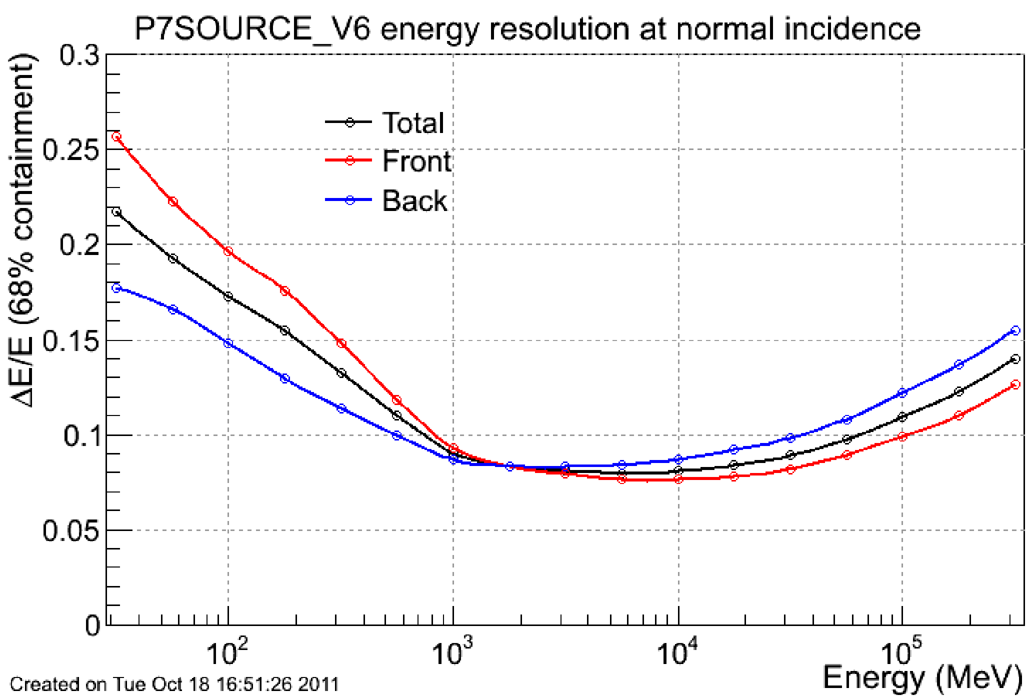

	LAT	EGRET
Energy range	20 MeV to >300 GeV	20 MeV – 30 GeV
Energy resolution (on axis, 0.1-10 GeV)	<18%	10%
Peak effective area	~ 9000 cm^2	1500 cm^2
Angular resolution (single photon, 10 GeV)	0.25°	0.54°
Field of view	~2.4 sr (@ 1 GeV)	0.4 sr
Deadtime per event	27 us	100 ms

LAT localizations

GRB NAME	R.A. Deg., J2000	Dec. Deg., J2000	68% Deg.	90% Deg.	95% Deg.
080825C	233.95	−4.55	0.77	1.24	1.55
080916C	119.87	−56.58	0.07	0.10	0.12
081006	136.43	−62.10	0.51	0.76	0.89
081024B	322.94	21.05	0.29	0.46	0.56
090217	204.79	−8.41	0.35	0.51	0.59
090323	190.64	17.03	0.10	0.16	0.20
090328	90.54	−42.01	0.13	0.17	0.19
090510	333.50	−26.53	0.04	0.06	0.07
090626	169.97	−33.34	0.23	0.32	0.37
090720B	203.08	−54.26	0.33	0.53	0.65
090902B	264.99	27.32	0.04	0.05	0.06
090926A	353.57	−66.33	0.04	0.07	0.08
091003	251.40	36.57	0.15	0.22	0.25
091031	71.40	−57.70	0.24	0.35	0.41
091208B	29.02	17.74	0.88	1.47	1.76
100116A	304.96	14.48	0.17	0.25	0.29
100325A	330.18	−26.40	0.60	0.86	1.00
100414A	192.16	8.64	0.12	0.18	0.22
100620A	86.98	−50.96	0.71	1.08	1.28
100724B	120.54	76.60	1.03	1.56	1.81
100728A	88.91	−15.01	0.10	0.19	0.23
110120A	61.55	−11.95	0.35	0.53	0.62
110428A	5.47	64.80	0.16	0.23	0.27
110625A	286.68	6.81	0.27	0.42	0.51
110709A	236.28	41.74	1.51	2.37	2.99
110721A	333.49	−38.62	0.53	0.80	0.93
110731A	280.42	−28.56	0.19	0.27	0.31

GRB NAME	Interval (t_0-t_1) s	Trans. Ev. in the ROI	Trans. Ev. Predicted
080825C	GBM (1.2–23.4)	7	6.8
	LAT (3.2–29.4)	11	10.1
	JOINT (3.2–23.4)	7	6.8
	EXT (23.4–29.4)	4	3.5
	LATTE (3.2–56.2)	14	11.5
080916C	GBM (1.3–65.5)	156	150.3
	LAT (5.0–209.8)	201	180.0
	JOINT (5.0–65.5)	146	140.2
	EXT (65.5–209.8)	55	40.9
	LATTE (2.4–562.3)	264	201.2

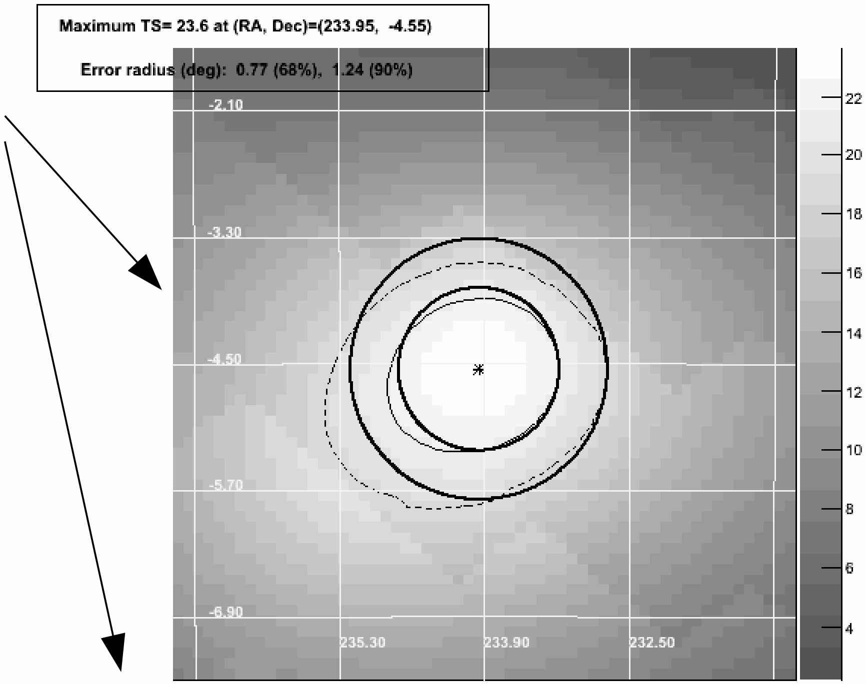

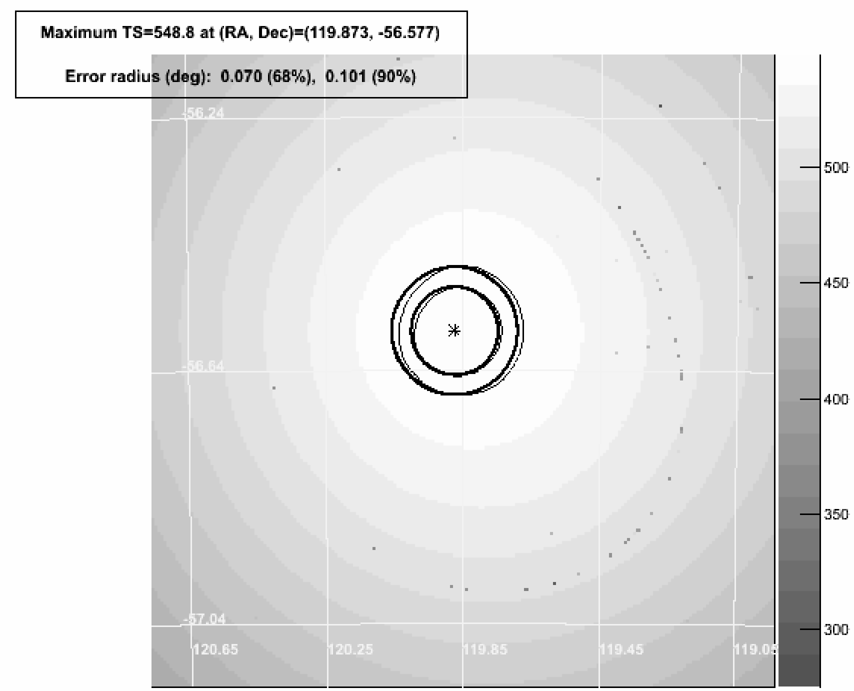

Fermi GRB detection statistics

GBM 2-year catalog
LAT 3-year catalog

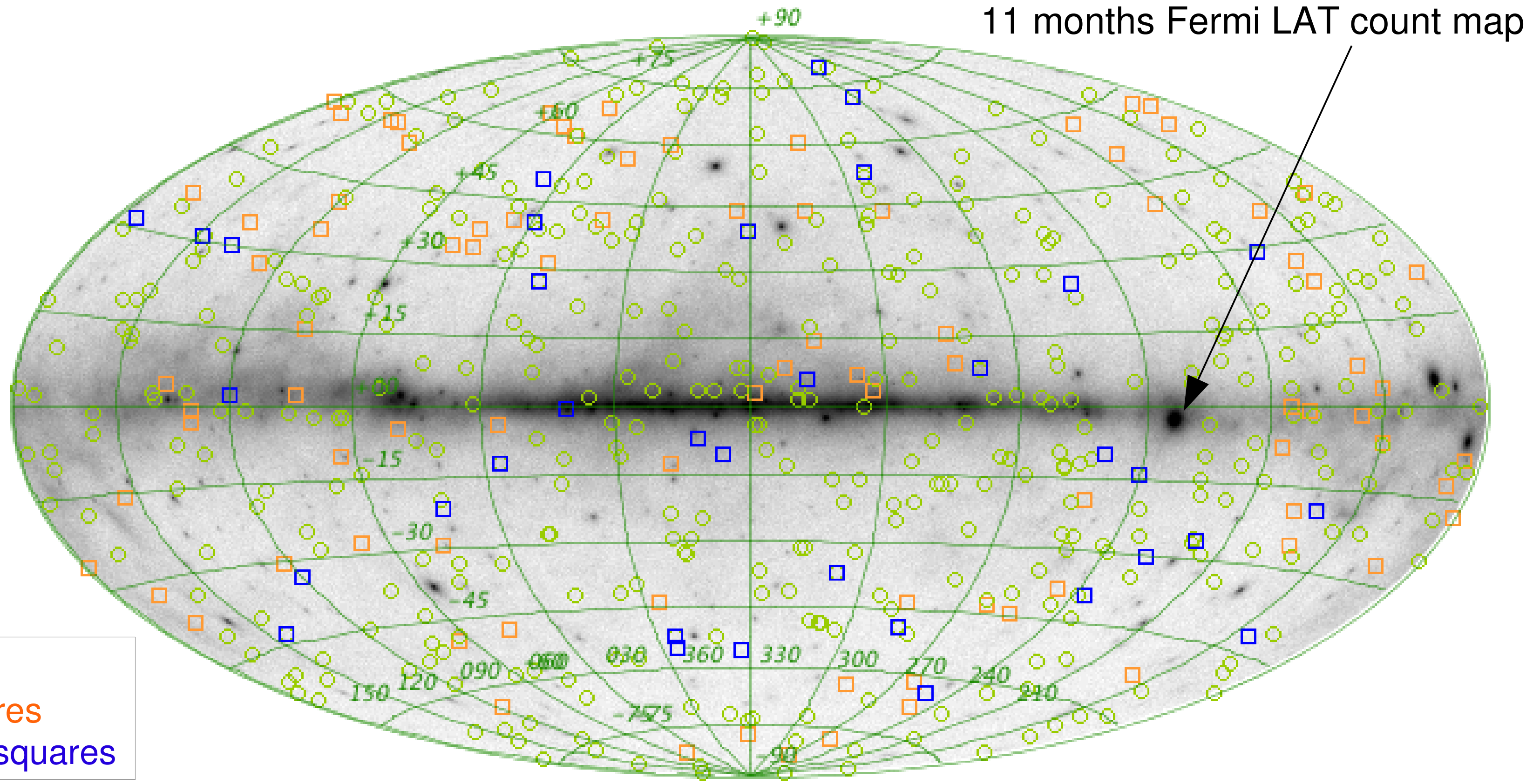

GBM LGRB: green circles
GBM SGRB: orange squares
LAT detections (35): blue squares

- **The GBM detects ~250 GRBs / year**, ~half in the LAT FoV

Paciesas et al. 2012, ApJS 199, 18; Goldstein et al. 2012, ApJS 199, 19

- **The LAT detected 35 GRBs in 3 years** (30 long, 5 short), including 7 “LLE-only” GRBs
  - Bright LAT bursts with good localizations are all followed-up by Swift
  - 10 redshift measurements, from z=0.74 (GRB 090328) to z=4.35 (GRB 080916C)
  - 4 joint BAT-GBM-LAT detections: GRBs 090510, 100728A, 110625A, 110731A

Ackermann et al. 2013 (submitted to ApJS, arXiv:1303.2908)

Comparing *Swift* and *Fermi* GRB samples

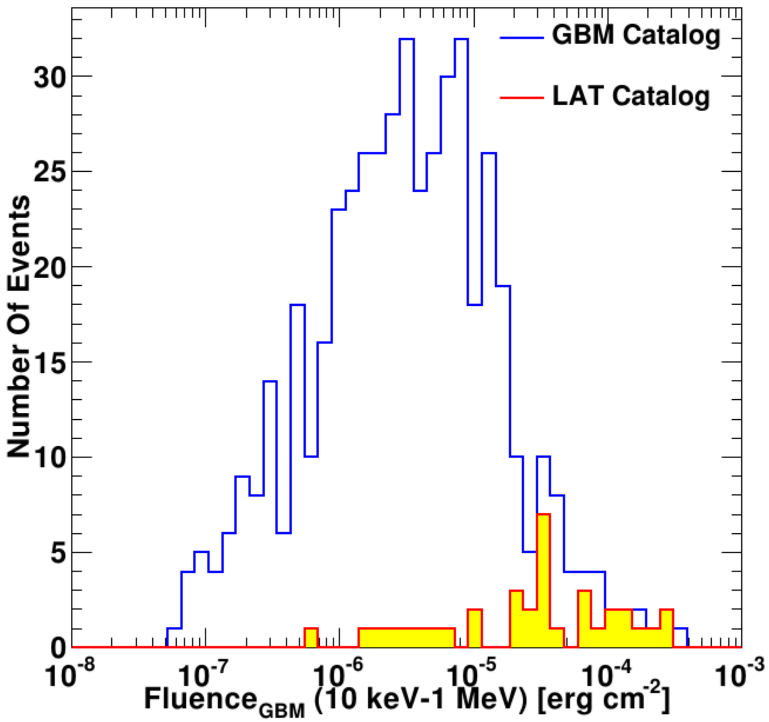

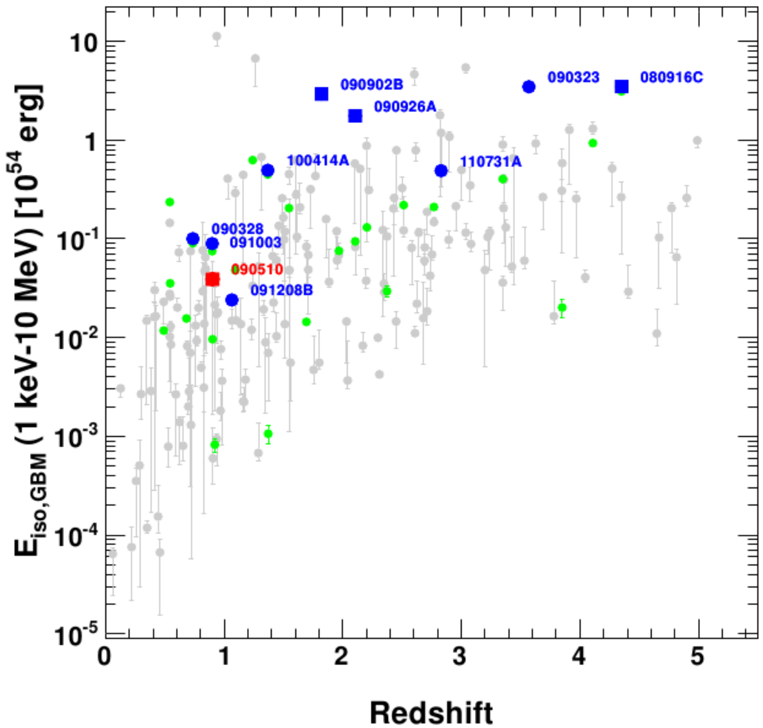

- *Butler et al. 2007, ApJ 671, 656 (see also Sakamoto et al. 2011, ApJS 195, 2)*
- *Racusin et al. 2011, ApJ 738, 138*
- *Goldstein et al. 2012, ApJS 199, 19*
- *Ackermann et al. 2013, arXiv:1303.2908*

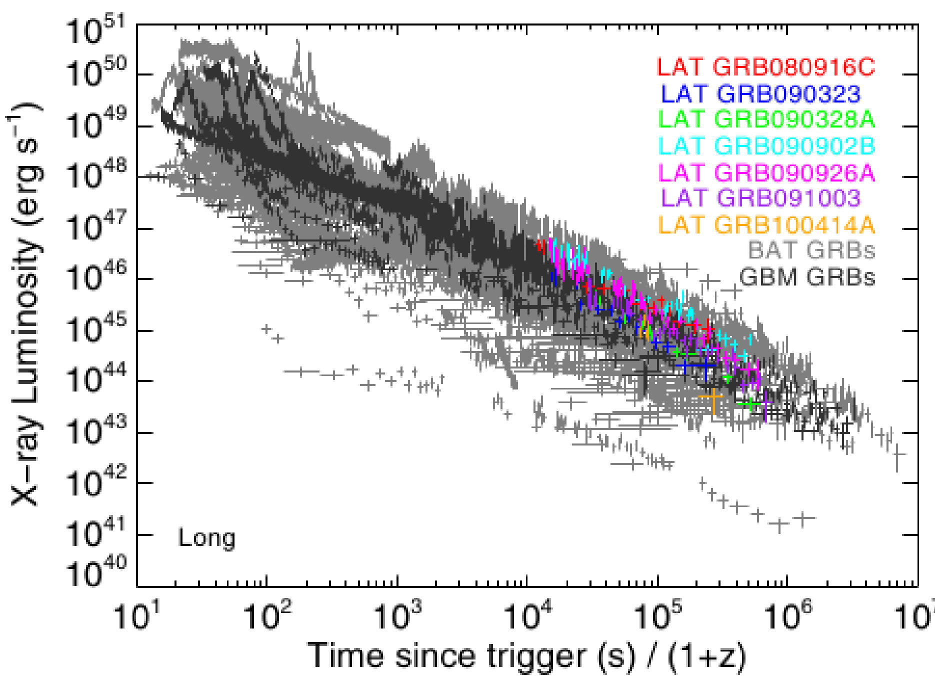

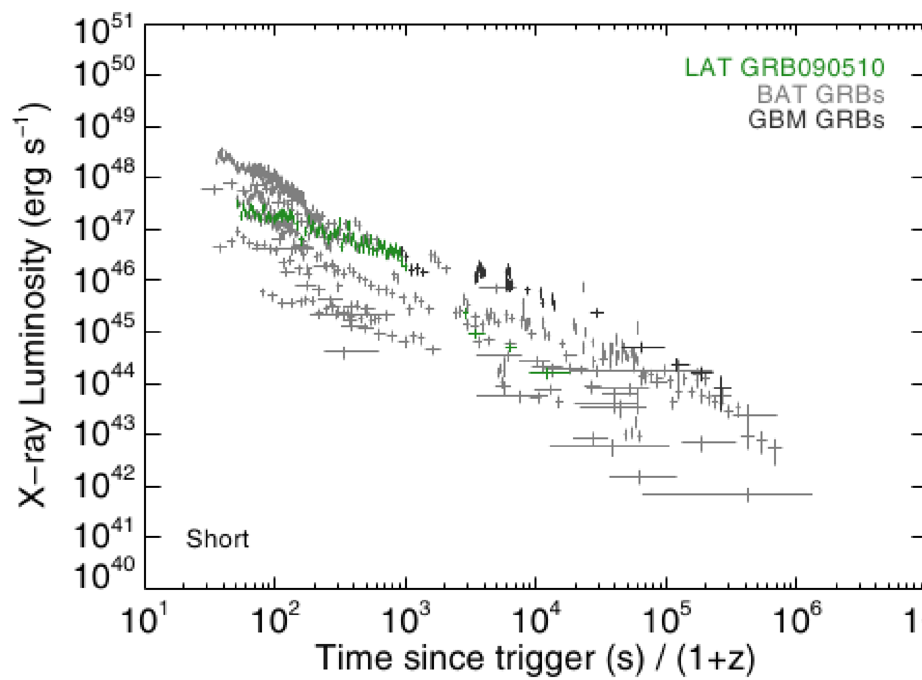

GRB 090926A multi-detector light curve

- **Correlated variability** in various bands, with a sharp spike at T_0+10 s
  - All energy ranges synchronized (<50 ms)
  - Low and high energies are co-located or even causally correlated
- **LAT >100 MeV emission is delayed** (~4 s)
  - Delay > spike widths
- **LAT >100 MeV emission is temporally extended**
  - Well after the GBM prompt phase
  - 19.6 GeV photon detected at T_0+24.8 s

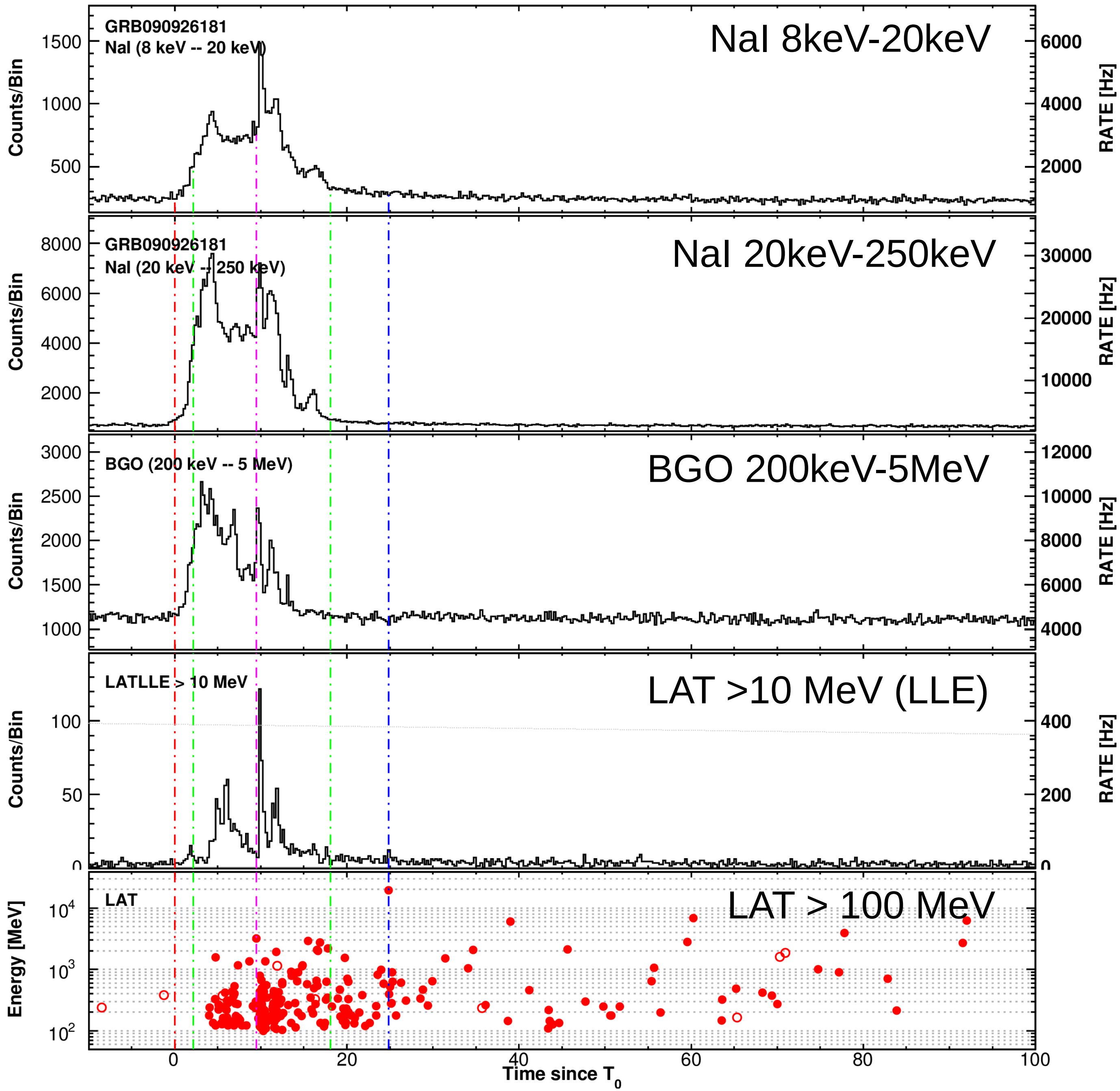

GRB 090926A broad-band spectrum

- Fluence = 2.2 x 10^{-4} erg cm^{-2} (10 keV - 10 GeV)
- E_{iso} = 2.2 x 10^{54} erg
- **Extra component (power law)**
  - Starts delayed (~9 s)
  - Persists at longer times
  - Dominates > 10 MeV
- **Spectral cutoff**
  - Significant in bin c, marginally in bin d
  - Shape not constrained
- **First direct measurement of the jet Lorentz factor:** Γ ~ 200-700
  - If cutoff due to $\gamma\gamma$ absorption
  - Model dependent

Ackermann et al. 2011, ApJ 729, 114

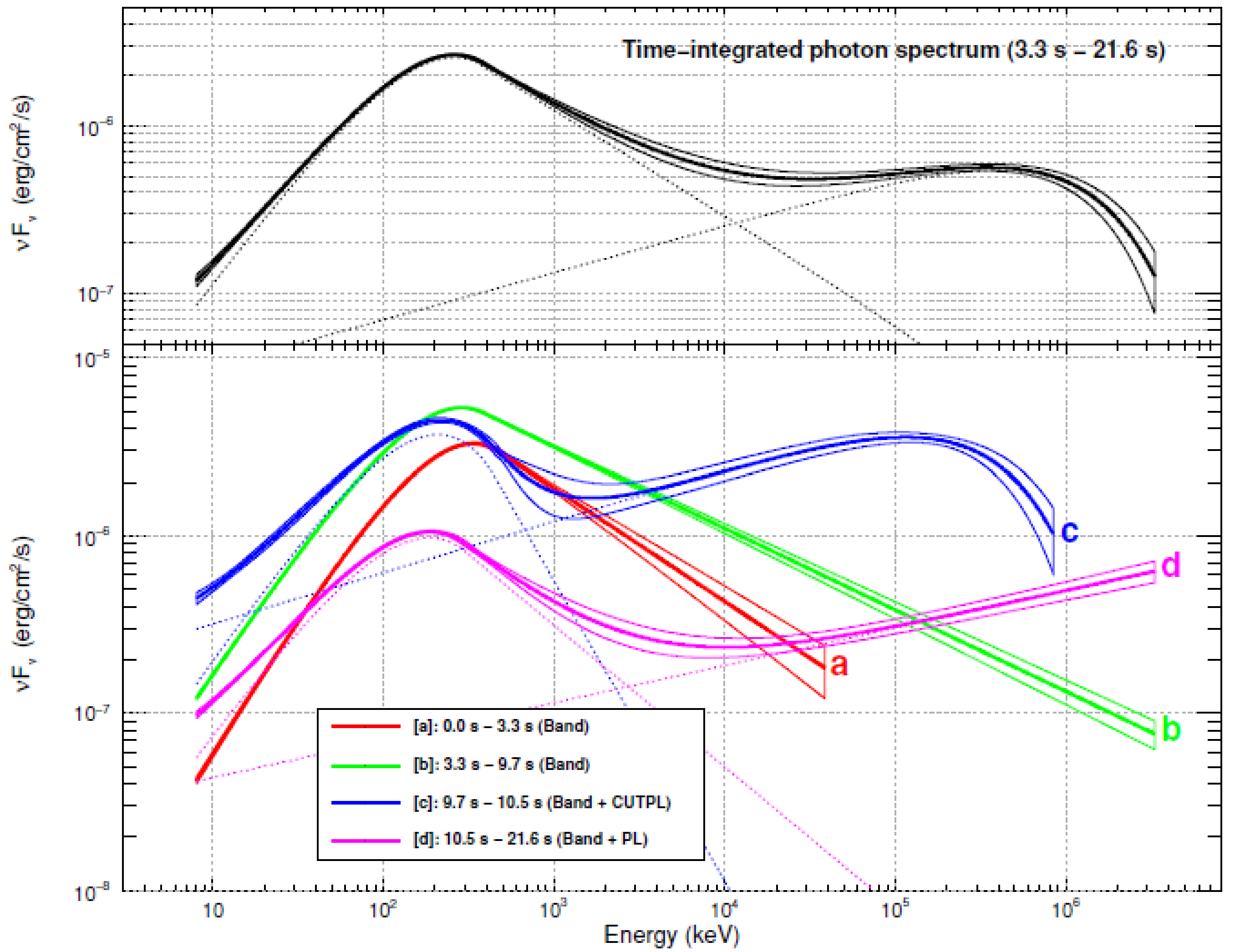

LAT Low-Energy event class & Pass 8 data

- **Most GRBs** detected using the standard event selection above 100 MeV (and likelihood technique)
- **LAT Low-Energy (LLE) event class**
  - Higher background, higher effective area in the 10-100 MeV range and at larger off-axis angles
  - Worse PSF than standard event classes (no localization possible)

- **Pass 6:** release in Aug. 2009, pre-flight
- **Pass 7:** release in Aug. 2011, fix for so-called “ghosts”
- **Pass 8: a radical revison of event-level analysis → a “new” LAT in 2014!**
  - Experience gained in first phase of the mission
  - Includes every aspect of the data-reduction process

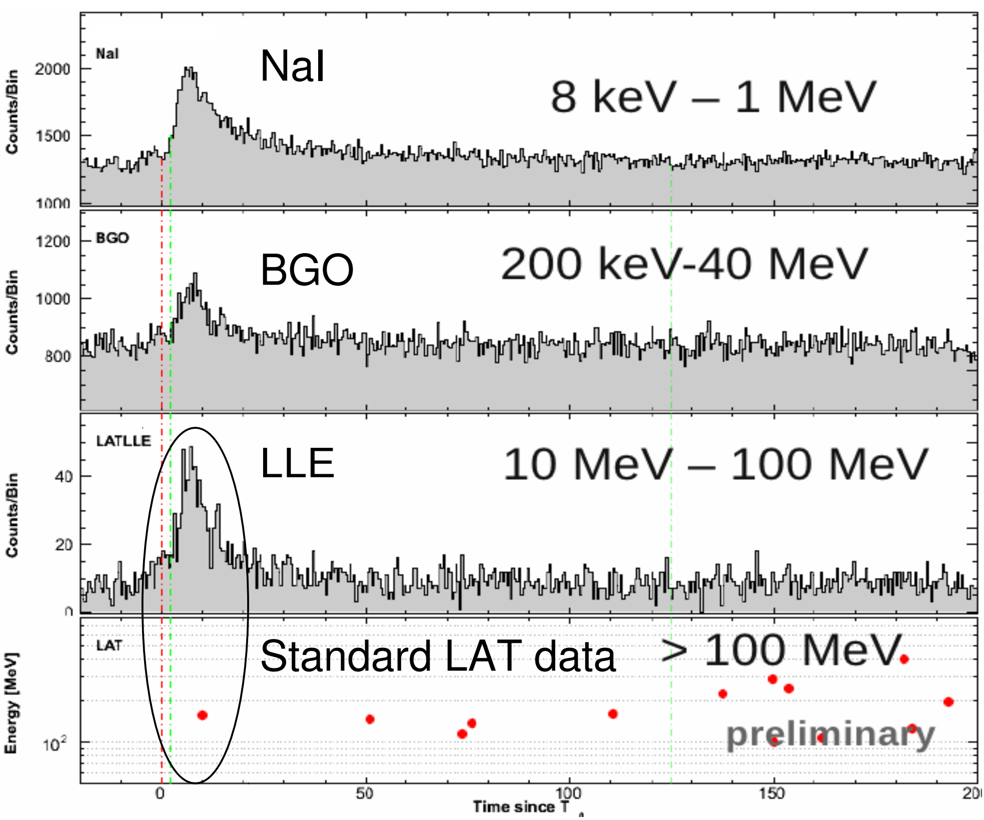

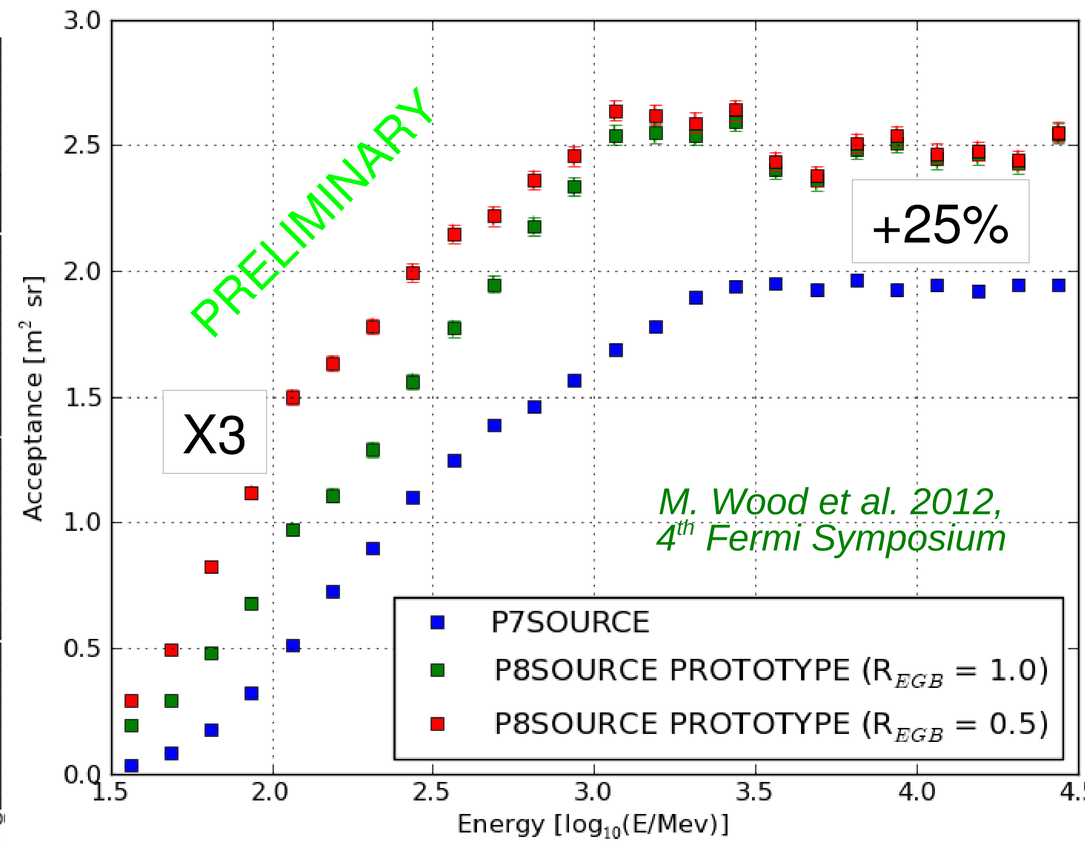

Instrument timing and the ghost effect

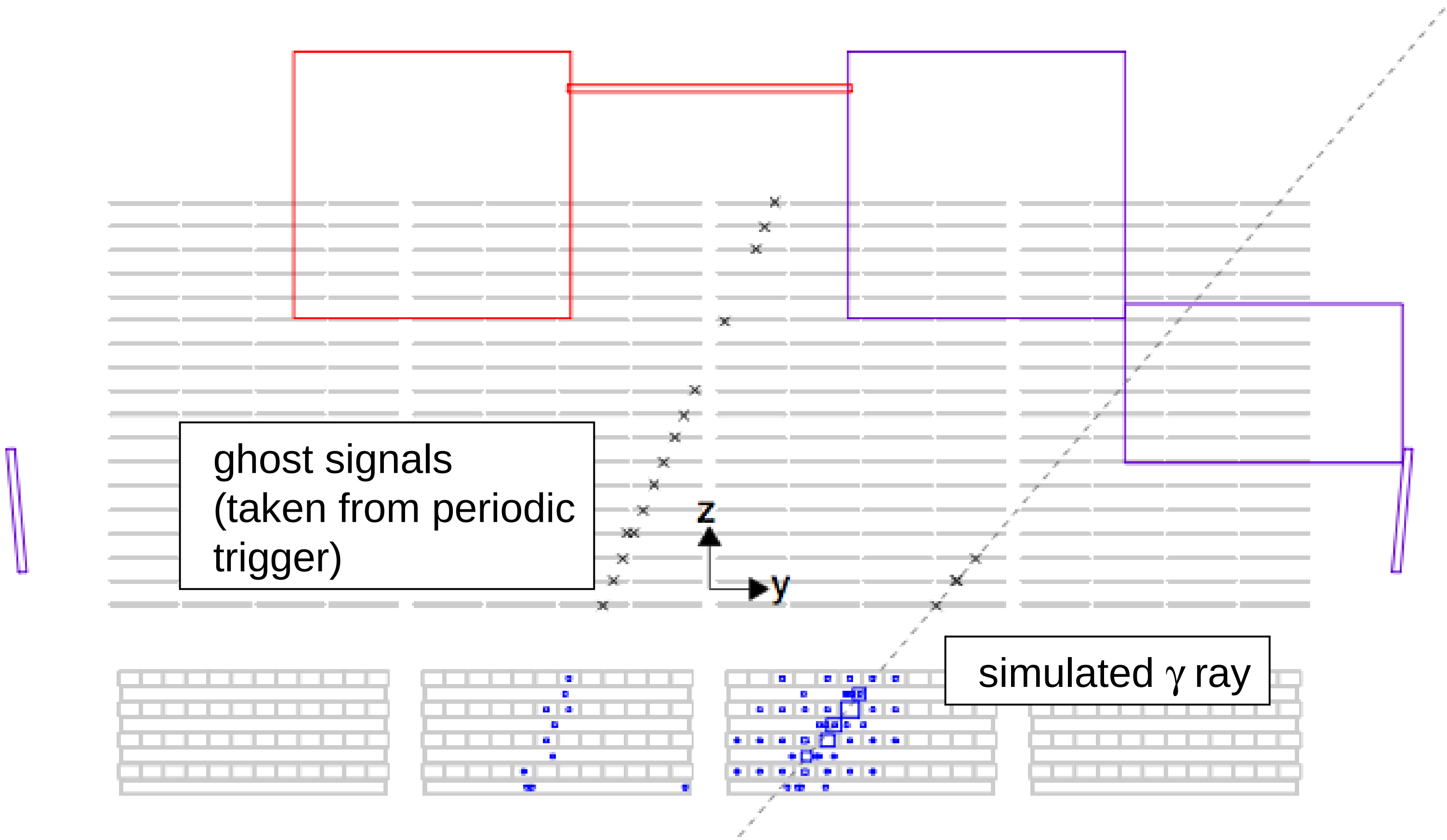

- Low power budget → μs (not ns) electronics
- Sensitive to signals from out-of-time cosmic rays
- Depends on CR rate which varies with orbit

Subsystem	Fast signal (trigger)	Slow signal (event data)
ACD	400 ns	4 μs
CAL	500 ns	3.5 μs
TKR†	1.5 μs	10 μs

2.b. Future high-energy space missions

Status of the *Swift* and *Fermi* missions

- **Report of the 2012 Senior Review of the Astrophysics Division Operating Missions**
  - **http://science.nasa.gov/astrophysics/2012-senior-review**

- ***Swift*** **(excerpts):**
  - *"All instruments and systems are operating normally and there are* ***no issues with expendables that would limit the lifetime. The orbit lifetime is beyond 25****."*
  - *"****Using triggers from Swift and Fermi will greatly increase LIGO sensitivity, and coincidences would confirm the association****. Only Swift can provide the accurate positions required for redshift determination, which unlocks analysis of the physics of the gravitational wave detections."*
  - *"The team has responded admirably as the mission has evolved, maintaining the priority, quality, and quantity of observations for the primary GRB mission even as it has become a reduced part of the observing program."*
  - *"We recommend an* ***extension through 2016 with review in 2014****."*

- ***Fermi*** **(excerpts):**
  - *"****Planned as a 10-year mission, designed for a 5-year prime phase that ends August 2013****."*
  - *"Fermi is at the forefront of Time Domain Astronomy (TDA) and enables great flexibility in performing multi-wavelength observations with other telescopes."*
  - *"****Overlap with ALIGO will enable GBM to provide electromagnetic confirmation for ALIGO candidate detections of GWs from coalescing binaries****."*
  - *"The first three years of Fermi have been very productive, and the committee believes* ***we have yet to see the peak of Fermi's science output.****"*
  - *"We recommend an* ***extension through 2016 with a review in 2014****."*

ISS-LOBSTER (2017?)

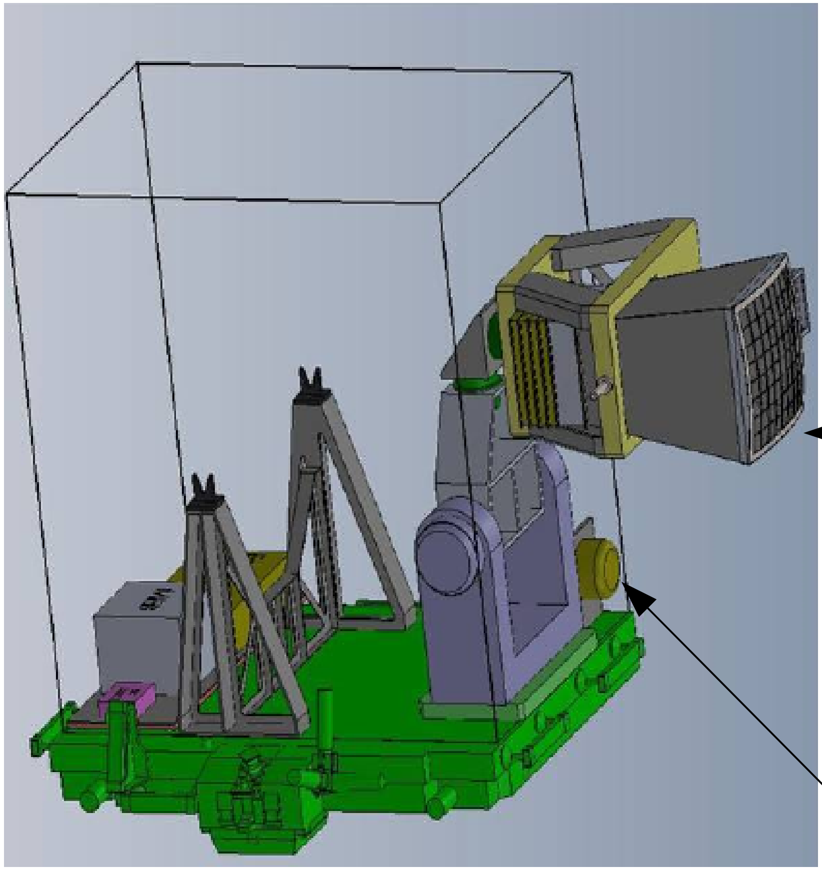

Objects Type	ISS-Lobster Predicted Rate (yr^{-1})
GW NS-NS Merger	1-2
GW NS-BH Merger	6-18
ccSN Shock Breakout	1-2
Tidal Disruption Flares	>14
Long GRBs	>100
High-z GRBs (z>5)	~5
Short GRBs	>30
Other transients will be observed including: AGN, Blazars, Novae, Stellar Super Flares, and Thermonuclear bursts	

- **Submitted to the 2012 NASA Astrophysics Explorer Mission of Opportunity AO**
  - Selection results pending
- **Wide Field Imager (WFI)**
  - Curved Microchannel plate optic (40 x 40 cm)
  - Focal plane CCD with 100 eV energy resolution
  - 0.3-5 keV, 30^o x 30^o FoV
  - 1 arcmin position resolution
  - Fast repointing capability (1.5^o / s)
  - Will follow-up Advanced Virgo/LIGO GW position contours within minutes
- **Gamma-ray Transient Monitor (GTM)**
  - Single NaI scintillator identical to *Fermi*/GBM
  - 10-1000 keV
  - View 2π sr unocculted by Earth and ISS
  - Provides GRB triggers
  - No positional information

J. L. Racusin et al.,
GRB 2013 conference (Nashville)

SVOM (2018?)

- **"Space-based multi-band astronomical Variable Objects Monitor", launch 2018(?), >3 years**
- **Chinese Space Agency & CNES**
- **Spacecraft**
  - LEO orbit, 30^{o}, nearly anti-solar pointing
  - Repointing in <5 min
  - VHE transmission to ground (like HETE-2)
- **ECLAIRs (low-energy threshold)**
  - Coded mask + 80 x 80 CdTe detectors
  - 4-150 keV, ~2 sr FoV
  - **~80 GRBs / yr** with fast loc. (~10 arcmin, 90%)
  - Positions <1 min to ground
- **Gamma-Ray Monitor (GRM)**
  - 0.05-5 MeV (NaI/CsI), ~2 sr FoV
  - Non-imaging spectro-photometer → GRB Epeak
- **Micro-channel X-ray Telescope (MXT)**
  - 0.2-10 keV, 64'x64'
  - <17" loc. (50% GRBs)
- **Visible Telescope (VT)**
  - 400-950 nm, 24'x24'
  - <1" loc., 22.5 mag in 300 s (better than *Swift*/UVOT)

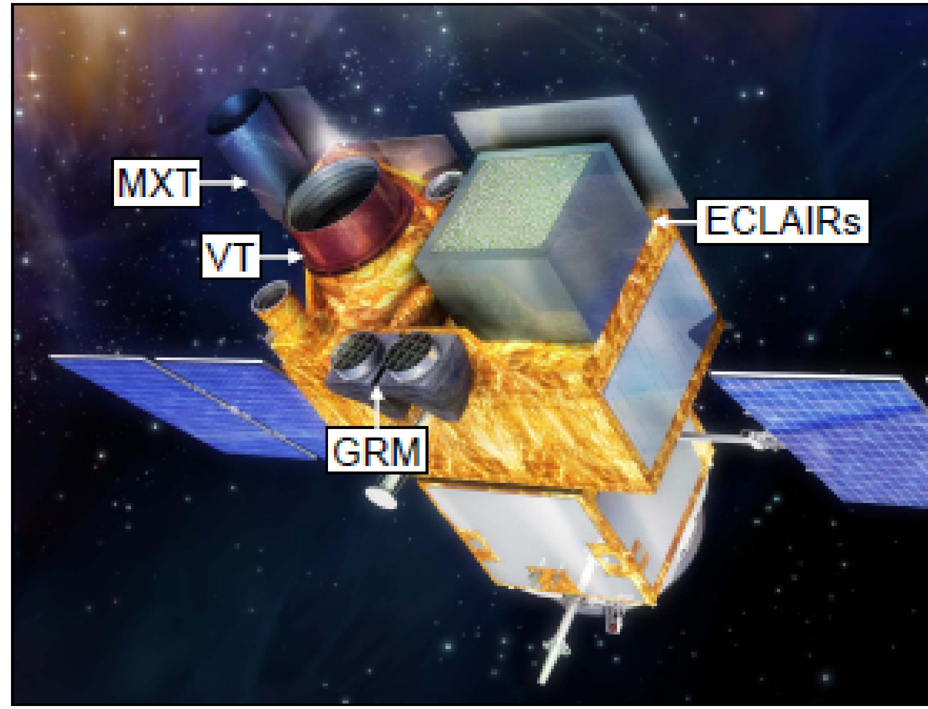

- **Ground Segment (~20% of SVOM GRBs)**

Ground-based Wide Angle Camera (GWAC):
  - ~8000 deg^2, monitors ECLAIRs FoV
  - 400-950 nm, 15 mag in 10 s

Two robotic Ground-based Follow-up Telescopes (GFTs):
  - <0.5" loc., photometric z (+NIR for the French GFT)

SVOM (2018?)

Godet et al. 2012, SPIE 84431O

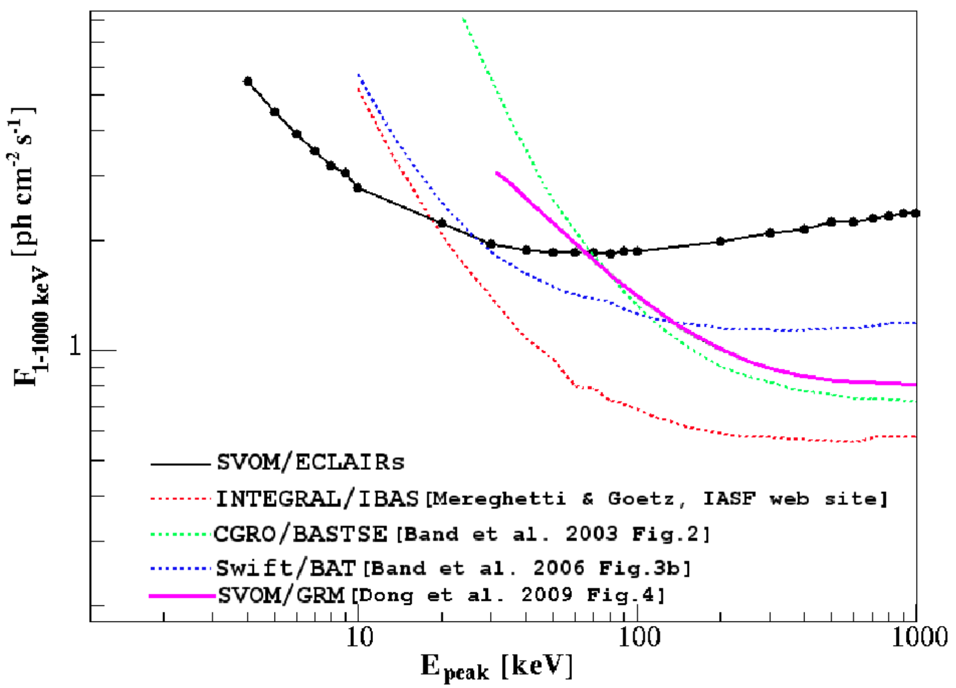

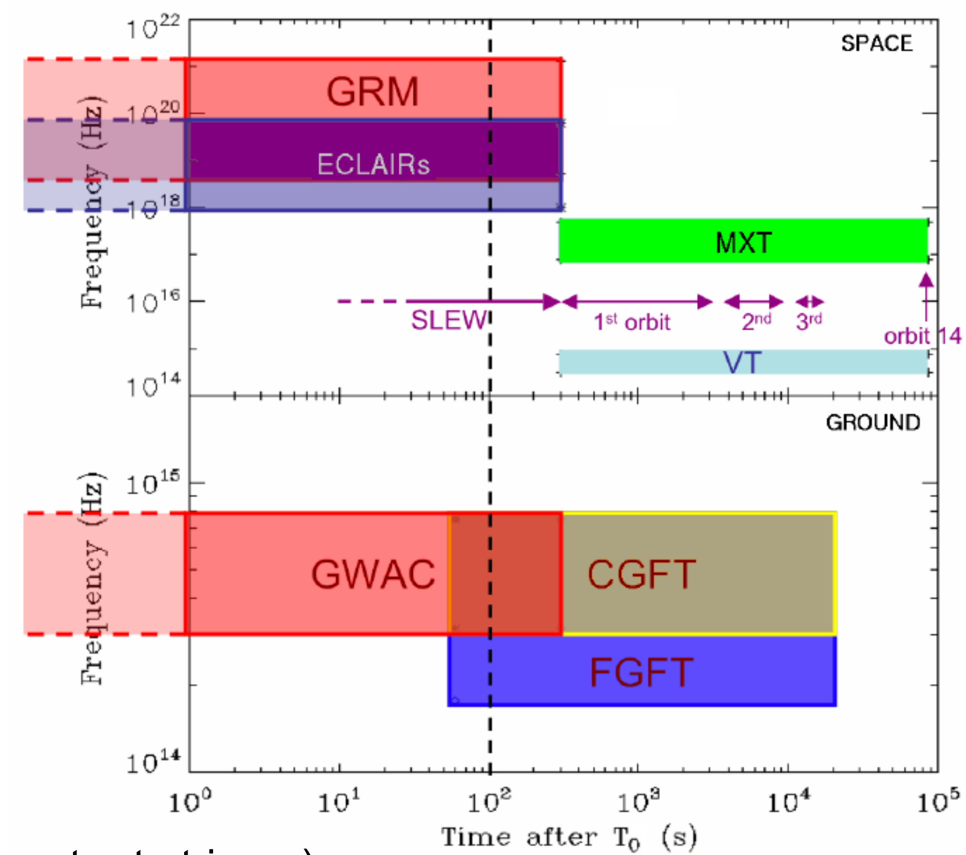

- **Synergy between the SVOM instruments**
  - ECLAIRs: GRB detection & localization (image / count-rate trigger)
  - GRM: E_{peak} measurement up to 500 keV
  - MXT: refine the GRB position, afterglow follow-up observations
  - VT: refine the GRB position, afterglow follow-up observations, photo-z, dark GRBs, GRB SNe
  - GWAC: prompt optical emission
  - GFTs: prompt optical emission of long GRBs, identification & localization of afterglow, localization of dark GRBs, follow-up of the early afterglow in NIR/optical
- **Optimized pointing strategy** will facilitate observations and redshift measurements
  145 redshifts in 3 years, ~12 with z>5

SVOM (2018?)

Godet et al. 2012, SPIE 84431O

ECLAIRs		Gamma-Ray Monitor	
Type	coded mask camera mask aperture fraction: 40% mask-to-detector distance: 46 cm	Type	non-imaging spectrometer
Consortium	IRAP, CEA-Saclay (France) APC (France)	Consortium	IHEP Beijing (China)
Field of view	~ 2 sr (89×89 deg^2) Fully coded: 0.15 sr (22.1×22.1 deg^2)	Field of view	~ 2 sr
Energy band	4 – 150 keV	Energy band	50 keV – 5 MeV
Effective area	~ 1000 cm^2 @ 20-50 keV ~ 150 cm^2 @ 4 keV	Effective area	280 cm^2 @ 200 keV ~ 160 cm^2 @ 5 MeV
Detector	6400 Schottky CdTe detectors Pixel: 4×4 mm^2 – 1 mm in thickness	Detector	2× Phoswich NaI/CsI
FWHM	< 2 keV @ 60 keV		
Readout time	10 μs	Readout time	-

Micro channel X-ray Telescope		Visible Telescope	
Type	Wolter-I telescope	Type	Ritchey-Chrétien telescope
Consortium	IRAP, CEA-Saclay, LAM (France) University of Leicester (UK) MPE, IAAT (Germany)	Consortium	NAOC Beijing (China)
Field of view	64×64 arcmin^2	Field of view	21×21 arcmin^2
Energy band	0.2 – 10 keV	Energy band	V & R band
Effective area	~ 50 cm^2 @ 1.5 keV		
PSF FWHM	3.7 arcmin @ 1.5 keV	Resolution	0.6 arcsec
Focal length	1 m	Focal length	450 cm
Diameter	~ 21 cm	Diameter	45 cm
Detector	256×256 pn-CCD pixel: 75×75 μm^2	Detector	Two 2048×2048 CCDs
FWHM	75 eV @ 1 keV		
Readout time	100 ms	Exposure time	15 s

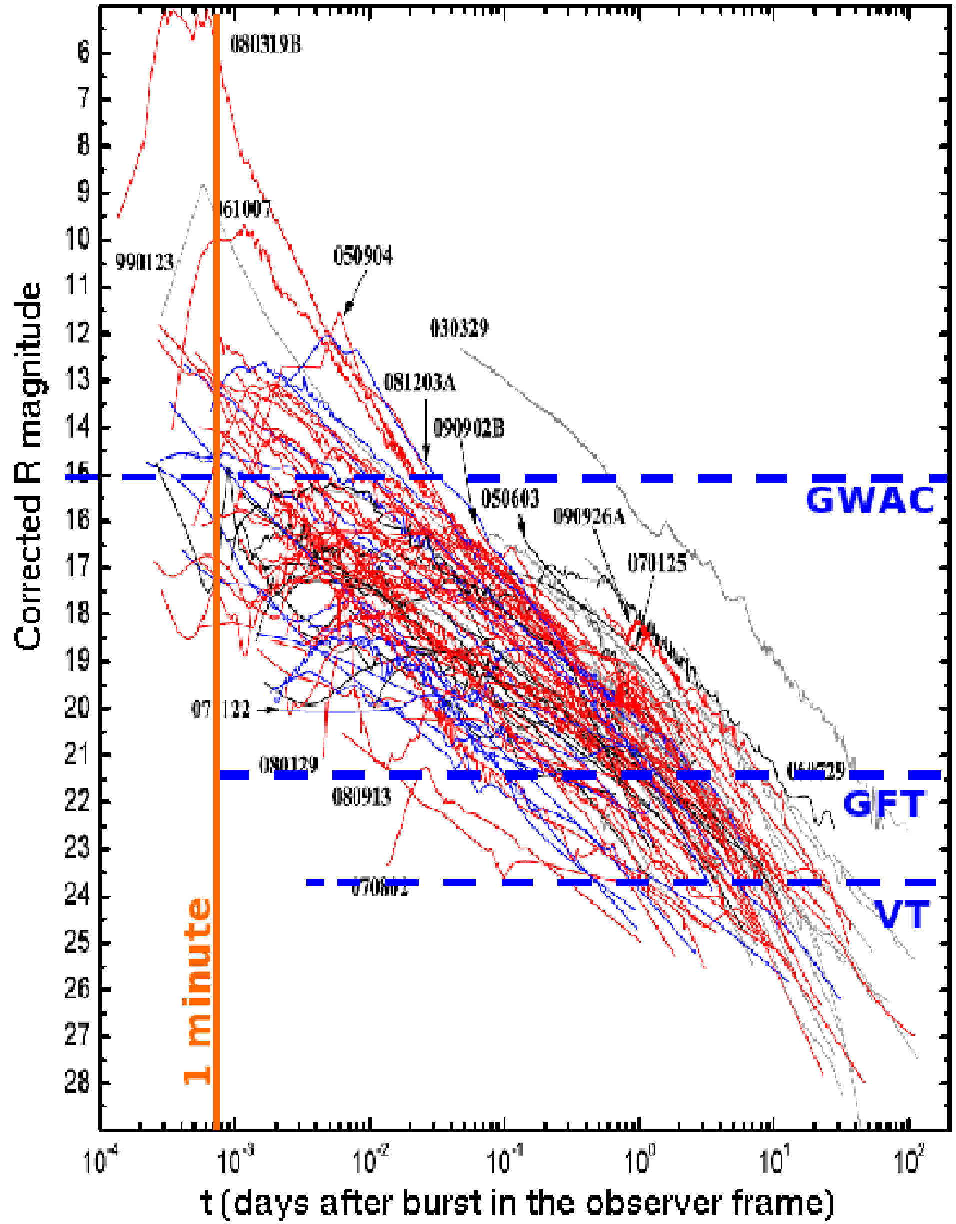

- See also the review of robotic optical telescopes in A. Klotz's lecture

GAMMA-400 (2019?)

Galper et al. 2013, AdSpR 51, 297

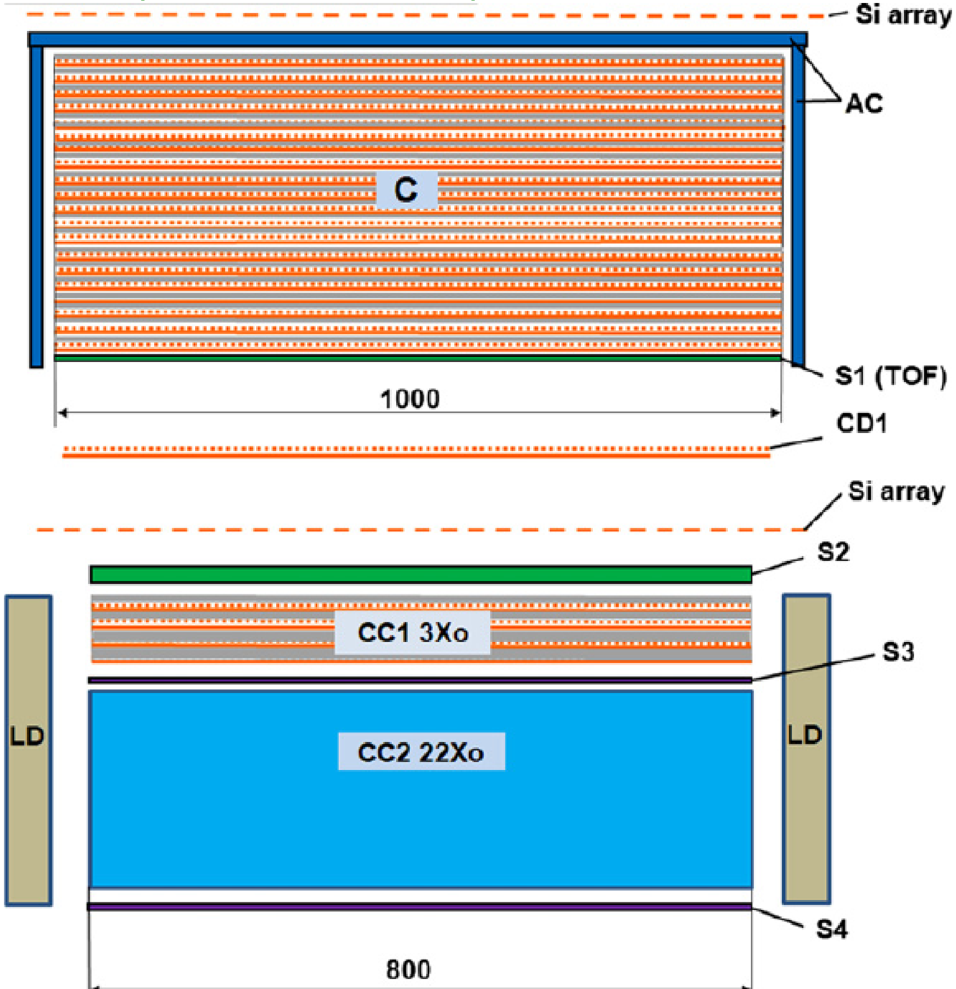

	Fermi/LAT	GAMMA-400
Energy range	20 MeV to >300 GeV	0.1-3000 GeV
Energy resolution (>100 GeV)	10%	~1%
Angular resolution (>100 GeV)	0.2°	**~0.02° ?**

- **Mission confirmed by Russian Federal Space Agency (Roscosmos) – launch end of 2018**
  - L2 or high elliptical orbit, >7 years
- **Astroparticle space experiment**
  - **Gamma rays: ~4000 cm^2 at 100 GeV 100 MeV (or lower) – 3 TeV, ~1.2 sr FoV**
  - Electrons / positrons 1-3000 GeV
  - Nuclei 250 GeV/n to 10^{15} eV/n
- **Design being improved**

- **ACD:** scintillators (AC)
- **TKR: converter-tracker (C) of ~25 double Si layers interleaved with W conversion foils**
- Time of flight system (S1 / S2), scintillators (S3 / S4), lateral detectors (LD), Si strip coordinate detector (CD1)
- **CAL (25 X_0 total at normal incidence):**
  - CC1 (imaging): 4 layers of double Si layers interleaved with W planes
  - CC2: EM calorimeter (BGO crystals)

- **Konus-FG GRB monitor**

LOFT (2022?)

Feroci et al. 2012, Exp Astron 34, 415

- **“Large Observatory For x-ray Timing”**
- **ESA M3 mission candidate (assessment phase)**

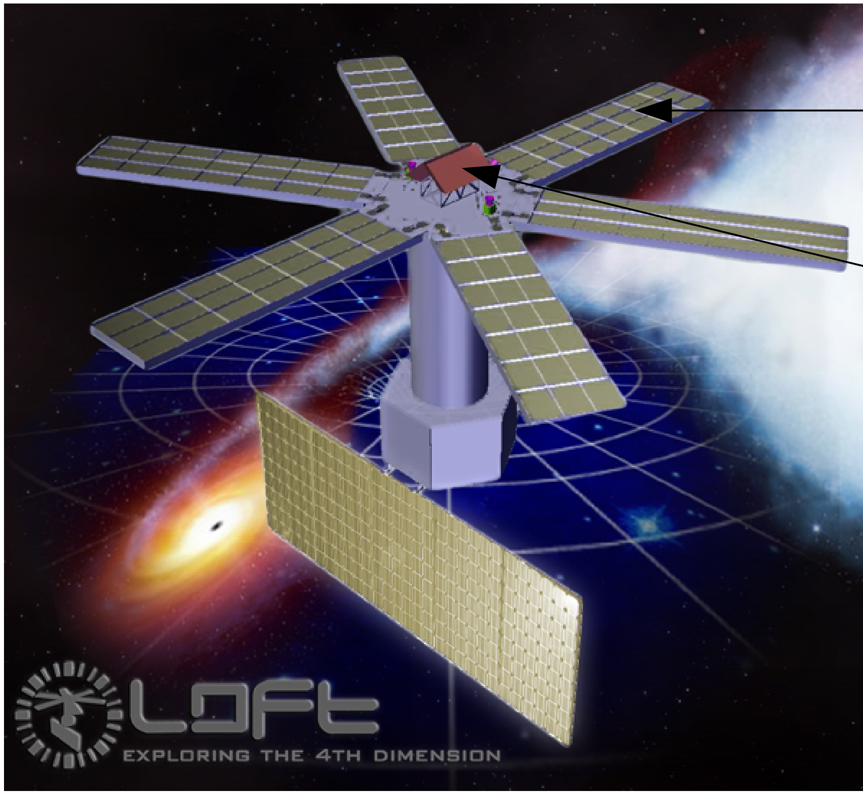

- **Large Area Detector (LAD)**
  - 2–50 keV, peak effective area of **~10 m²**
- **Wide Field Monitor (WFM)**
  - Coded mask imager
  - 2-50 keV, ~4 sr FoV

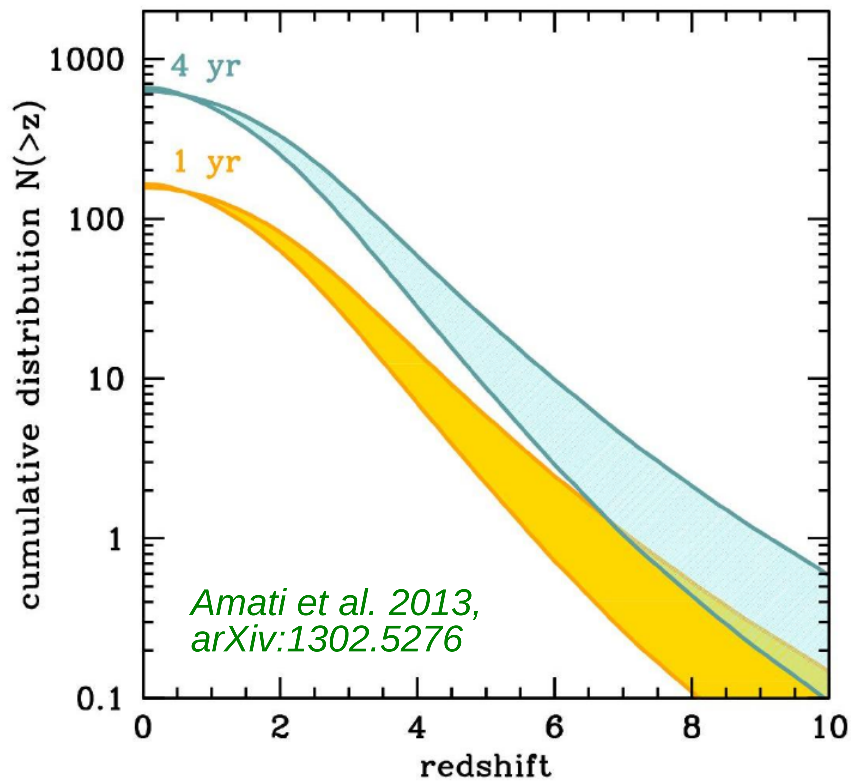

WFM	Energy range	2–50 keV	1–50 keV
	ΔE (FWHM)	<300 eV	<200 eV
	FoV (FWHM)	>3 steradian	>4 steradian
	Ang. res.	5 arcmin	3 arcmin
	PSLA	1 arcmin	0.5 arcmin
	Sens. (5σ, 50 ks)	2 mCrab	1 mCrab
	Sens. (5σ, 1 s)	0.5 Crab	0.2 Crab

Future telescopes for MeV gamma-ray astronomy?

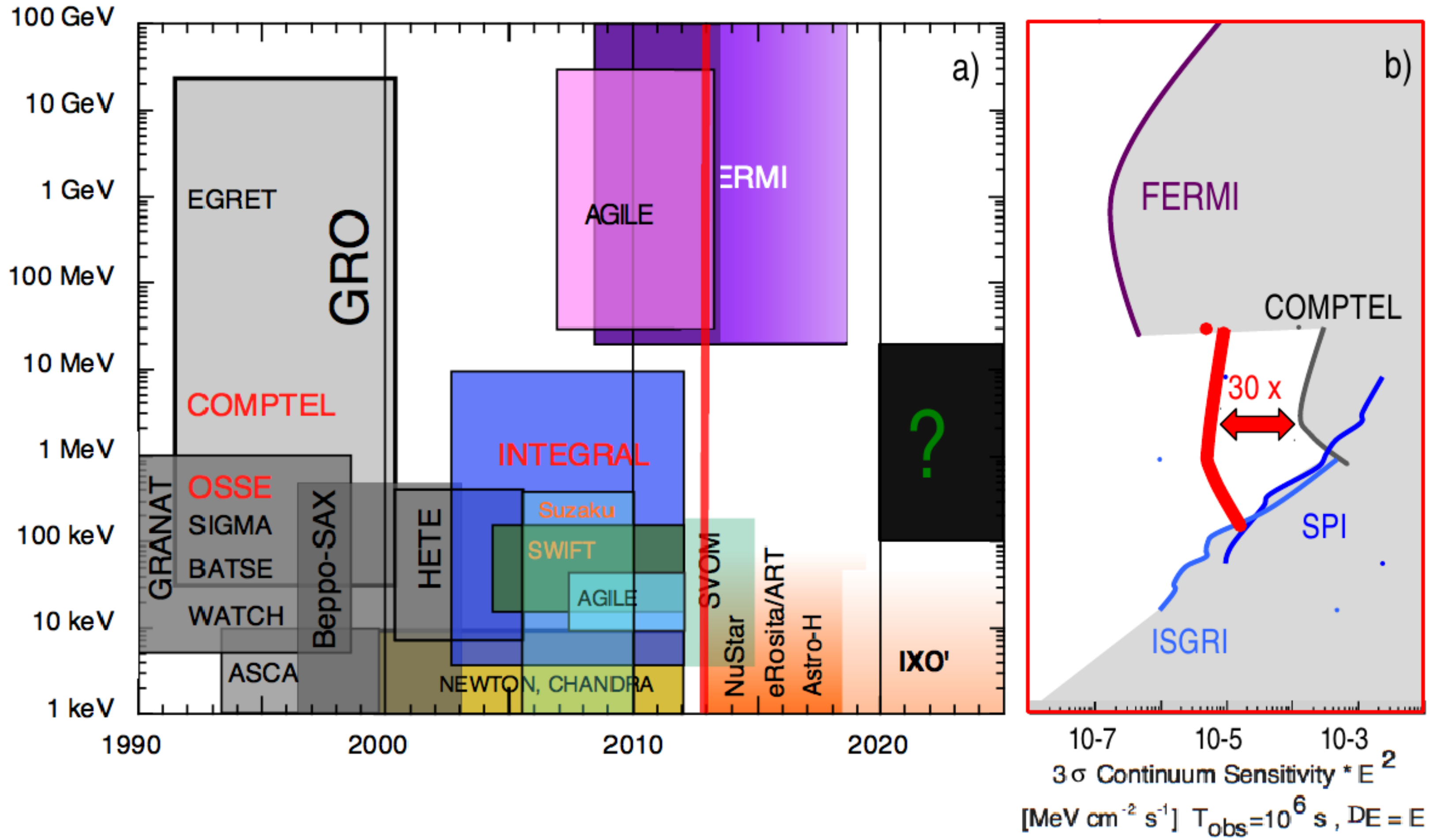

- **Post-Integral area: a white spot on the high-energy astrophysics roadmap**
- **Some Compton telescope / mission concepts**
  - ESA M3 call: GRIPS/GRM *(Greiner+07)*, CAPSiTT *(Lebrun+11)*, DUAL/ASCI *(von Ballmoos+11)*
  - ACT *(Boggs+06)*: NASA mission concept study
  - HARPO *(Bernard+12, arXiv:1211.1534)*
  - Etc

Scientific perspectives in the MeV domain?

- **"Scientific perspectives in the MeV domain" – January 2013 Workshop (APC)**
  - **https://indico.in2p3.fr/conferenceDisplay.py?confId=7243**
- **Performance requirements for GRB studies:**

Performance parameter	Goal value	Remarks and notes
Field-of-view (FWHM, deg)	$>2\pi$ (a few sr)	As large as possible, to monitor the sky and to provide many GRB triggers.
Angular resolution (FWHM, deg)	A few tens of arcmin	Would provide arcmin positions, but arcsecond positions are needed for follow-up observations by large optical telescopes...
Spectral resolution ($\Delta E/E$ @ Energy)	$\leq$10% @ 300 keV	Accurate E_{peak} measurement. Should not be less than ~10% at other energies (0.1-100 MeV).
Line sensitivity (@ Energy) ($cm^{-2}.s^{-1}$, 3σ, 1 Ms)		
Continuum sensitivity (in which energy band?) (cm-2 s^{-1} keV^{-1}, ΔE=E, 3σ, 1 Ms)	5.10^{-5} in 1 s (LGRBs) 2.10^{-4} in 100 ms (SGRBs) At 1 MeV	For time-resolved spectroscopy in the 0.1-100 MeV range: identification of spectral components and their time evolution.
Timing performances	$\leq$10 μs	Low deadtime needed for sensitive timing analysis, especially for SGRBs.
Polarimetric capability (Minimum Polarization Fraction for a Crab source in 1 Ms)	$\leq$10%	As a function of energy, to distinguish spectral components.
Real-time data ?	Yes	To promptly (within a few tens of s) disseminate GRB alerts, positions, and preliminary spectral analyses (e.g., SGRBs with high E_{peak}).

3. Prospects for GRB observation at very high energies with ground-based gamma-ray experiments

Fermi/LAT highest-energy detected photons

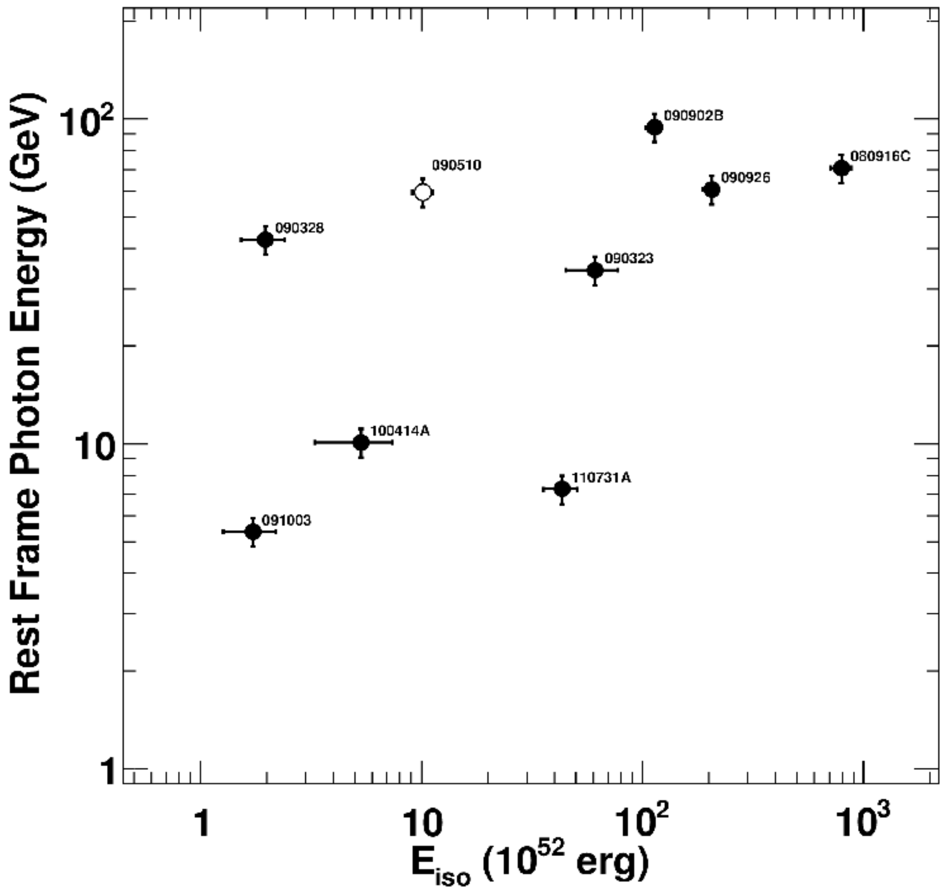

Event list from time-resolved likelihood analysis

GRB NAME	Number of events (> 100 MeV, P>0.9)	Energy GeV	Arrival time s	Probability
080825C	10	0.57	28.29	0.997
080916C	181	13.22	16.54	1.000
081006	10	0.79	12.08	0.955
081024B	11	3.07	0.49	1.000
090217	16	1.23	179.08	0.907
090323	28	7.50	195.42	1.000
090328	23	5.32	697.80	0.926
090510	186	31.31	0.83	1.000
090626	15	2.09	111.63	0.999
090720B	2	1.45	0.22	0.997
090902B	276	33.39	81.75	0.949
090926A	239	19.56	24.83	1.000
091003	20	2.83	6.47	1.000
091031	7	1.19	79.75	0.999
091208B	4	1.18	3.41	0.956
100116A	14	13.12	296.43	0.993
100325A	5	0.84	0.35	0.990
100414A	19	4.72	288.26	1.000
100620A	6	0.27	3.77	0.994
100724B	16	0.22	61.75	0.988
100728A	5	13.54	5461.08	0.987
110120A	6	1.82	72.46	0.999
110428A	6	2.62	14.79	1.000
110625A	6	2.42	272.44	0.986
110709A	5	0.42	41.75	0.921
110721A	22	1.73	0.74	0.998
110731A	64	3.39	435.96	0.998

- **Several tens-of-GeV photons in the rest frame**
- **GRB 080916C: 27.5 GeV photon at T_0+40.5 s** (~150 GeV rest frame, z=4.35) from Pass 8 analysis
- **GRB 090902B: 33.4 GeV photon at T_0+81.8 s**
- **Encouraging for VHE observatories** (HAWC, CTA)

Extrapolating *Fermi*/LAT spectra to VHE?

- **9.3 GRBs expected / year >100 MeV with >10 photons**
  - Pre-launch estimates (Band et al. 2009)
- **6.3 GRBs observed / year >100 MeV with >10 photons**
  - Number of "predicted" photons from likelihood fit

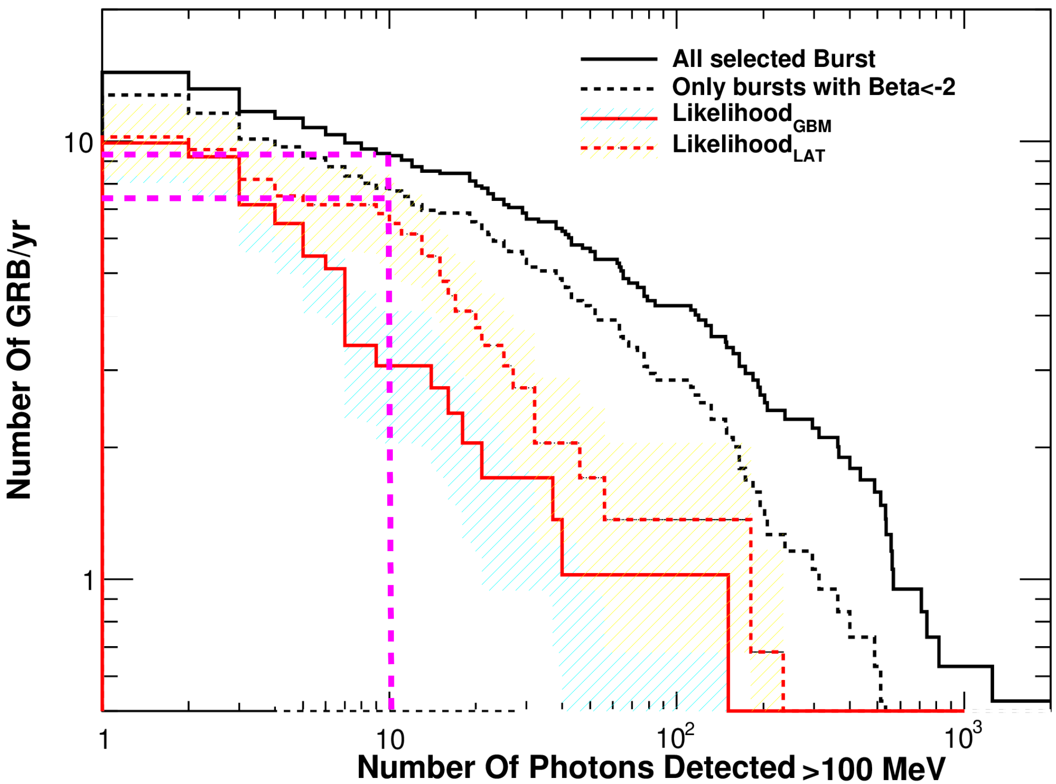

- **Fewer GRBs than anticipated**
  - Extra PL components must be rare
- **Is the prompt high-energy emission suppressed?**
  - Like for GRB 090926A

- **Afterglows of LAT bursts are bright**
  - Photon spectral index ~ -2
  - Rest-frame luminosity (100 MeV – 10 GeV) decays as t^{-1} at late times

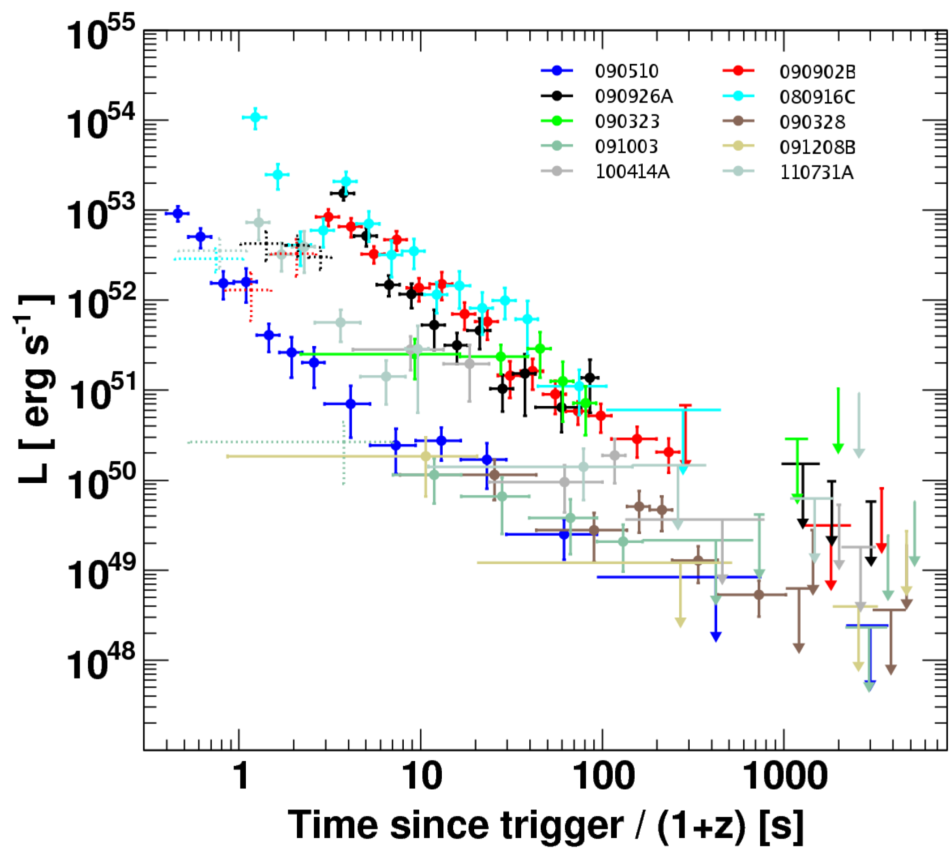

The development of Extended Air Showers

- **Interaction of a γ–ray or hadron in the atmosphere (~10 km)**
  - Cascade develops, then decays through bremsstrahlung and other losses
  - Hadronic showers are the main background

- **Gamma-ray showers**
  - Electromagnetic cascade is simpler than hadronic:
    - $e^{\pm}$ pair created by γ–ray
    - γ-ray production by $e^{\pm}$ bremsstrahlung
  - γ-ray showers more regular and smooth than hadronic showers (larger transverse momentum and electromagnetic sub-showers, more fluctuations)

- **Emission of Cherenkov light** by charged secondary particles (relativistic speed v>c/n)

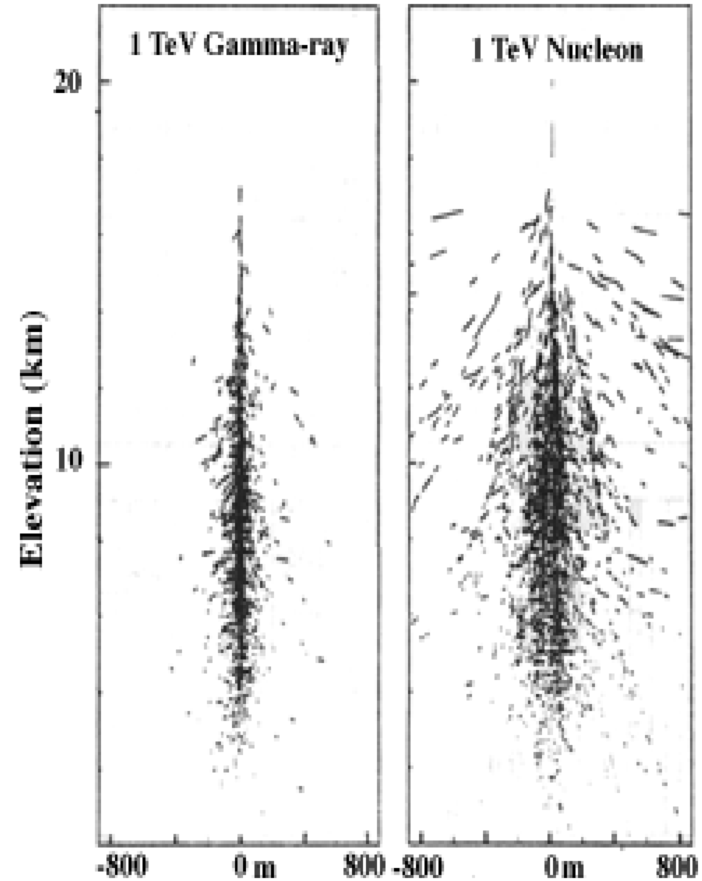

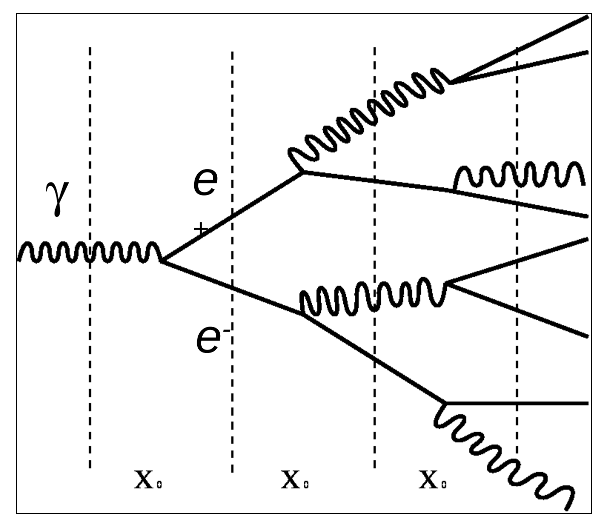

Detecting very high-energy gamma rays

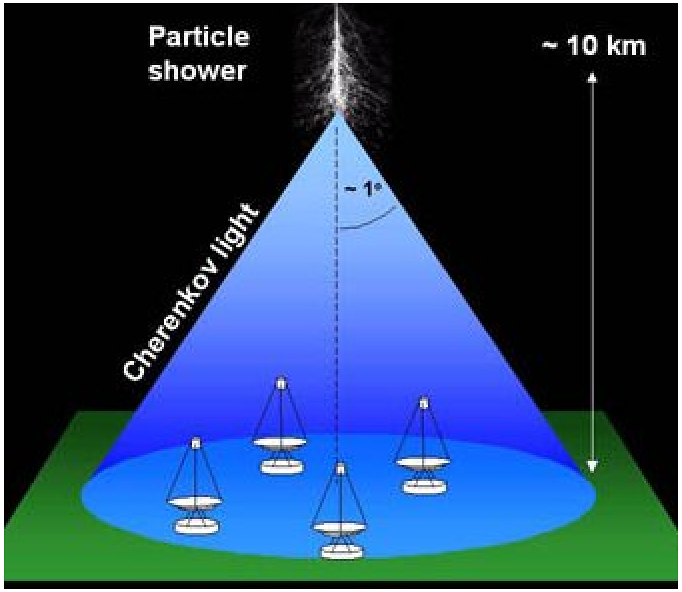

- **Imaging Atmospheric Cherenkov Telescopes** record the Cherenkov light produced by secondary particles in the atmosphere
- **Limited FoV** (~5°) → pointing instruments
- **Low duty cycle** (~10%): observations only during clear and moonless nights
- Cherenkov light pool on ground → very large effective area (~10^5 m^2) can be achieved
- **Excellent gamma / hadron separation and angular resolution** from image analysis

- **Water ponds or tanks** detect charged particles and secondary gamma rays on ground
- **Large FoV** (~1 sr) → source surveys
- **High high duty cycle** (~100%)
- Lower rejection power than IACTs → limited sensitivity
- High altitudes needed for a not-too-high energy threshold (the shower must reach the ground)

Imaging Atmospheric Cherenkov Telescopes

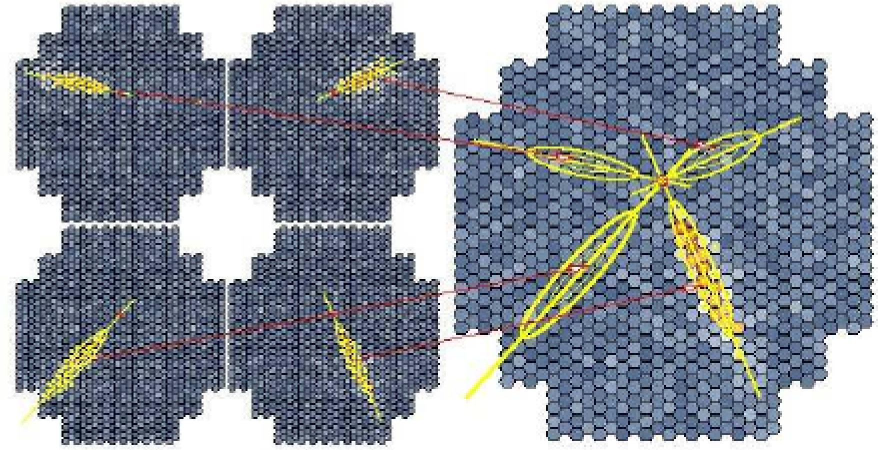

- **The atmosphere is the calorimeter**
- **Cameras with fine pixels**
  - Selection of electromagnetic showers from the form of the images (and direction for point like sources)
- **Stereoscopy**
  - Improves selection and angular resolution (4' to 6')
  - ~15% energy resolution from collected light and reconstructed shower impact parameter

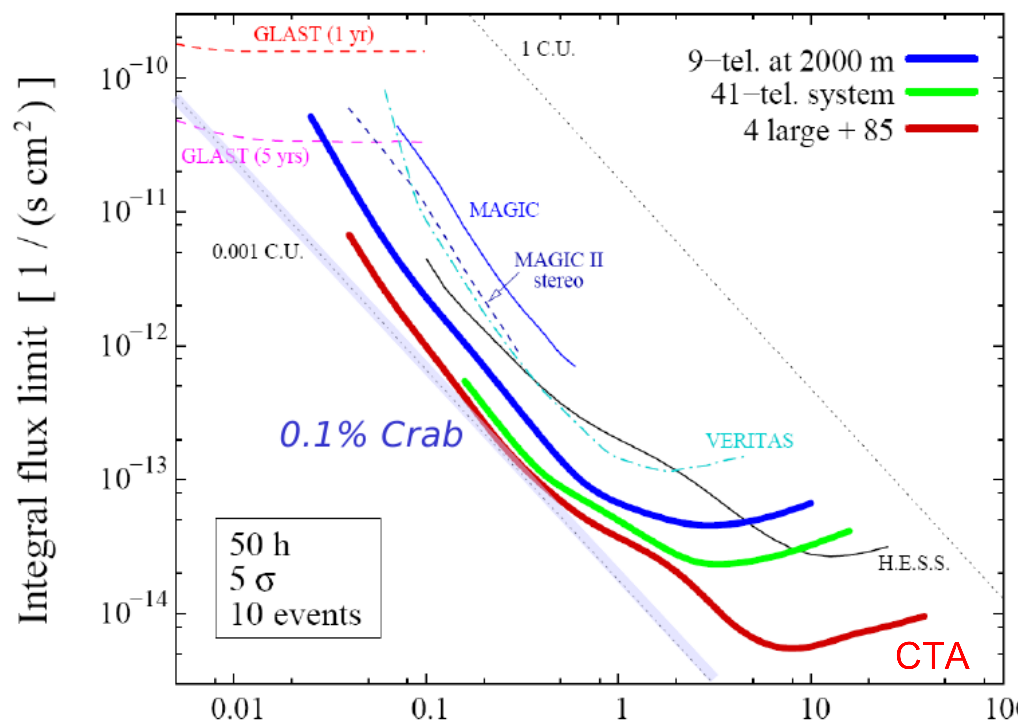

The Cherenkov Telescope Array

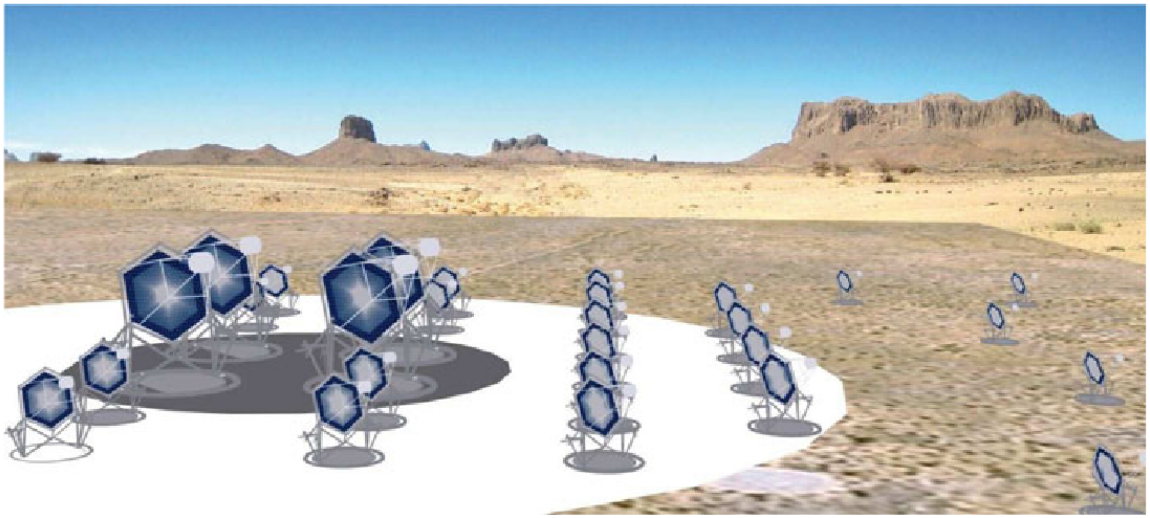

- **Two arrays (North & South) → full sky coverage**

- **Large Size Telescopes (LSTs)**
  - A few 23-m diameter telescopes
  - ~20 GeV to 1 TeV

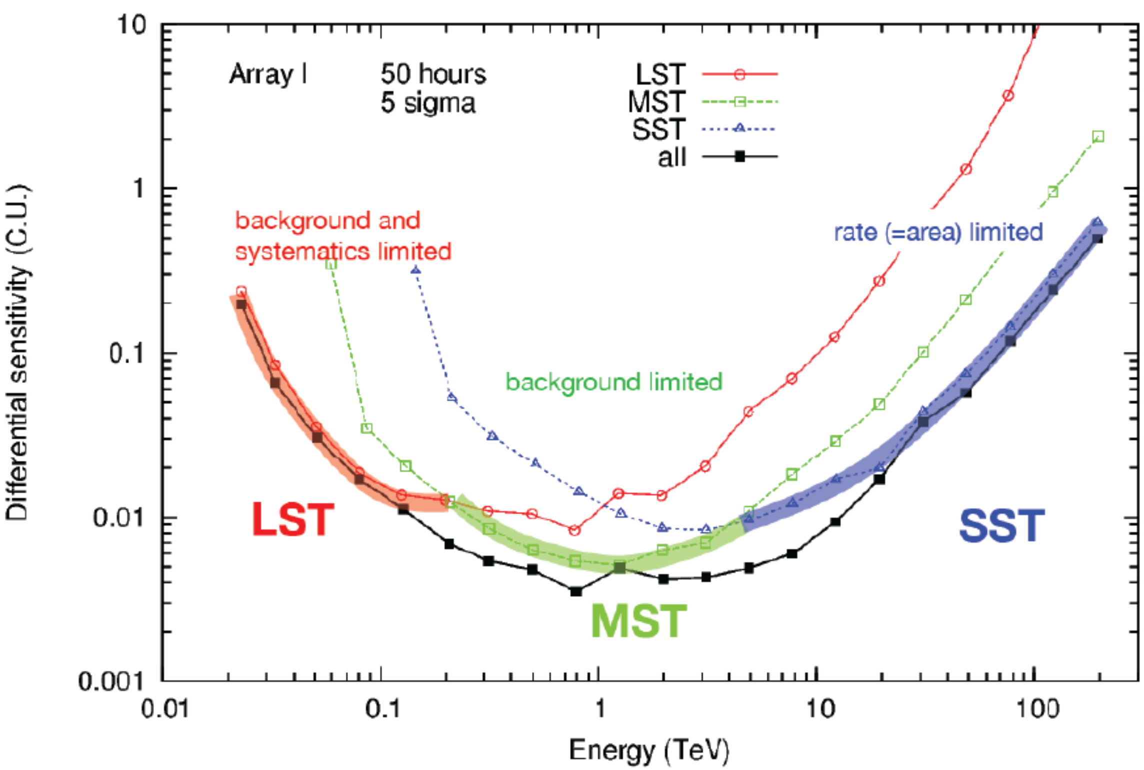

- **Medium Size Telescopes (MSTs)**
  - Core array: ~40 12-m telescopes
  - ~1 km^2 array, 100 GeV to 10 TeV
  - Sensitivity of ~1 mCrab at 1 TeV

- **Small Size Telescopes (SSTs)**
  - ~40 6-m telescopes on a ~10 km^2 area
  - Energies > 10 TeV

CTA response functions and sensitivity

Actis et al. 2011, Exp Astron 32, 193

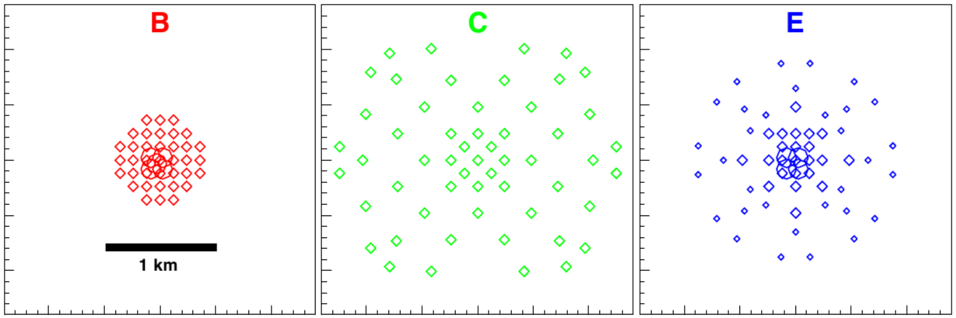

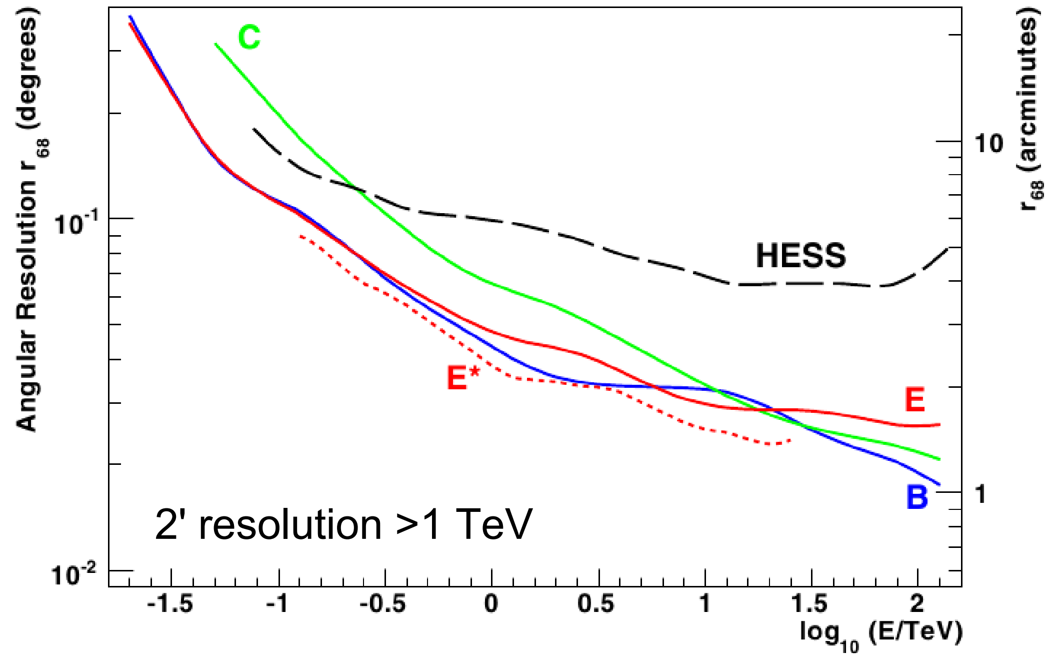

- Possible array configurations

- Integral sensitivity for a point source observed 50 h at zenith angle of 20°

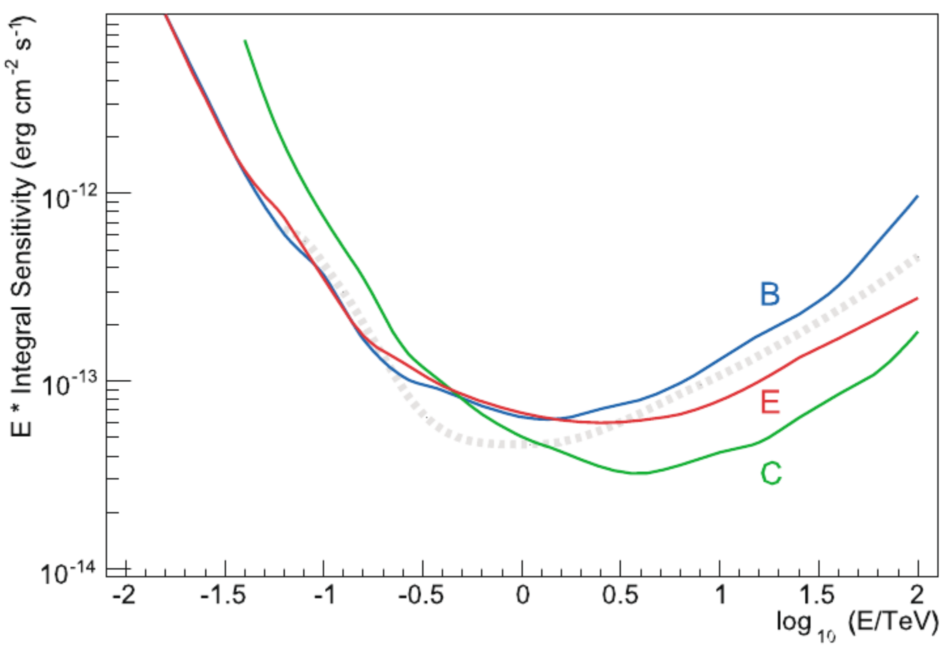

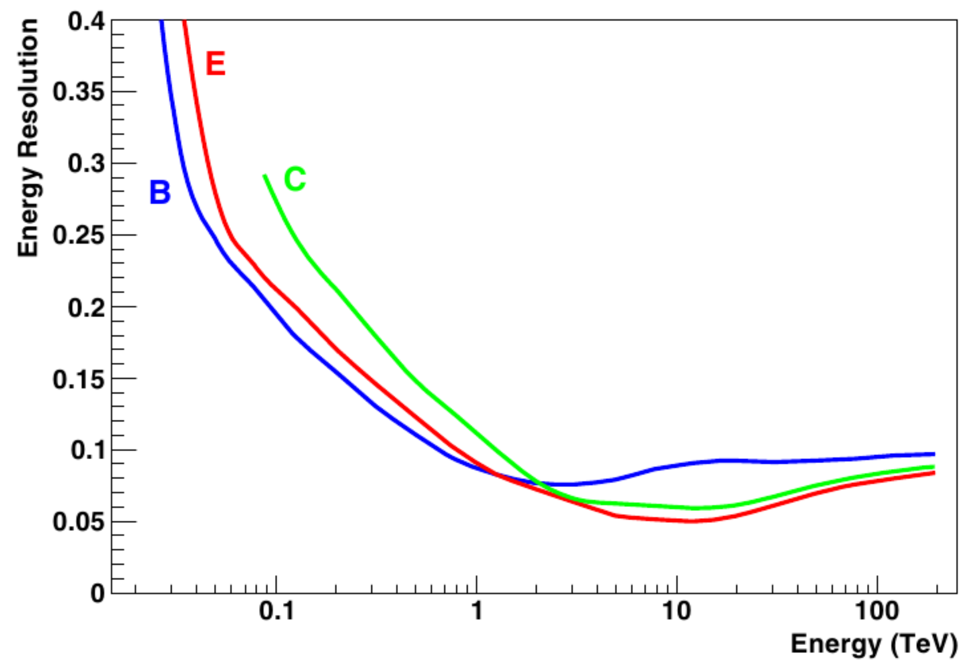

GRB observations with CTA

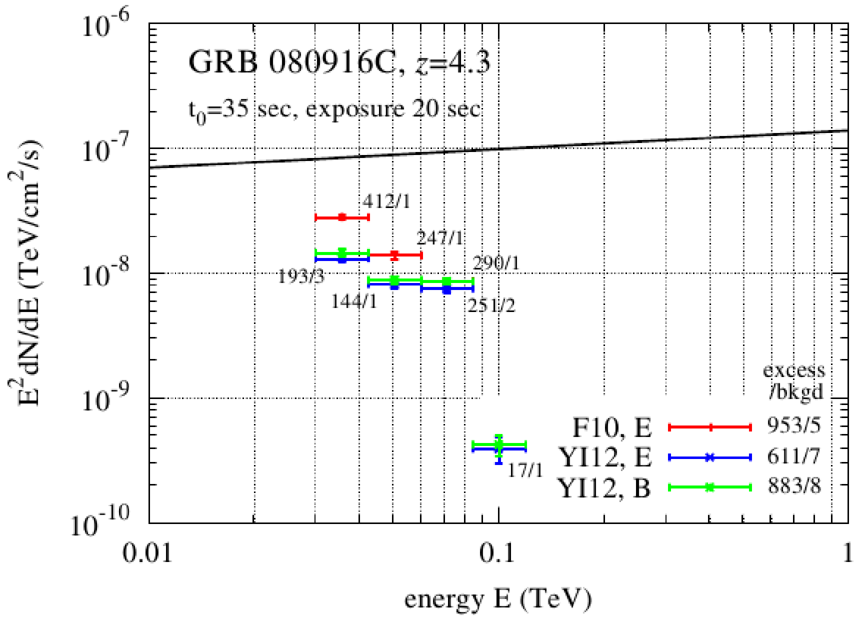

- Intrinsic spectrum extrapolated from *Fermi*/LAT
- Spectrum determination between 50 GeV and 100 GeV (if no spectral break <100 GeV)

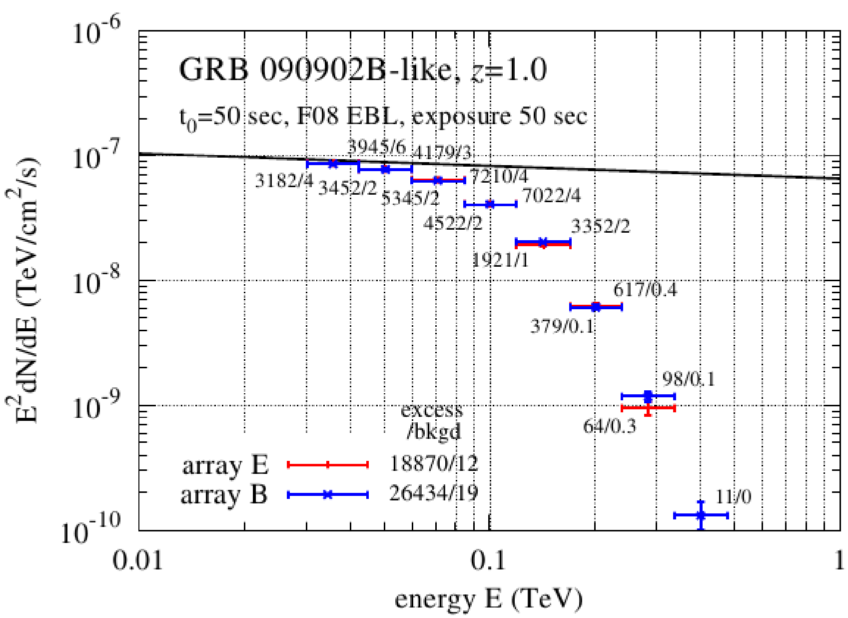

Funk & Hinton 2013, APh 43, 348

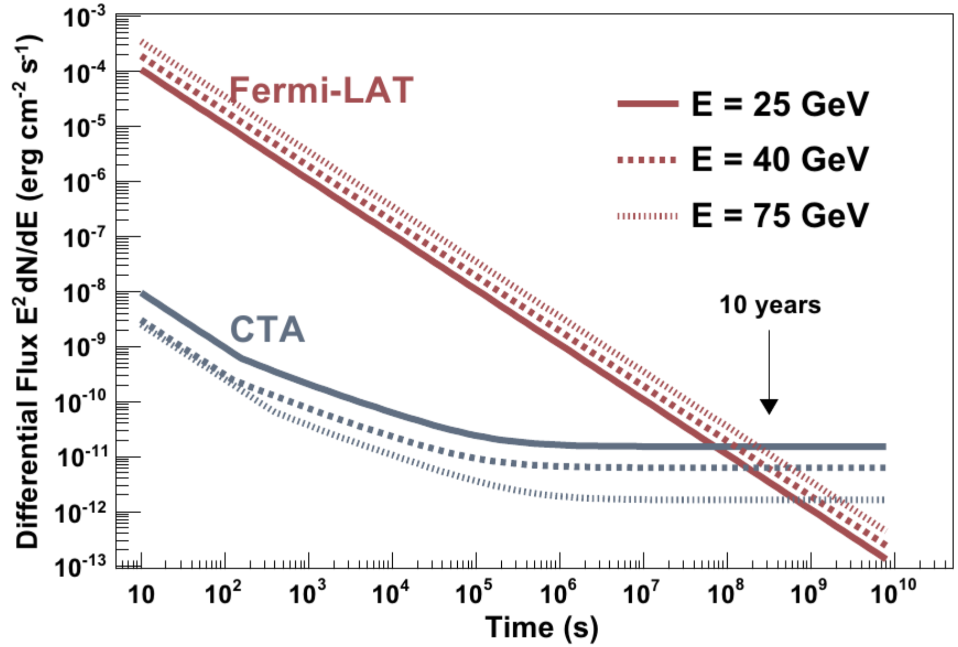

- The *Fermi*/LAT signal is limited above 10 GeV
- **GRB observations at very high energies need**
  - **Low-energy threshold** to fight the EBL → strongly depends on the LST performance (few 10's GeV threshold)
  - **Fast repointing**: 180° in 20 s (LSTs)
    - Scanning mode possible
- **CTA GRB rate: estimates range from 1 GRB every 20-30 months to 1-2 GRBs/yr**

Inoue et al. 2013, APh 43, 252
Gilmore et al. 2013, Exp Astron 35, 413

The HAWC experiment

Abeysekara et al. 2012, APh 35, 641

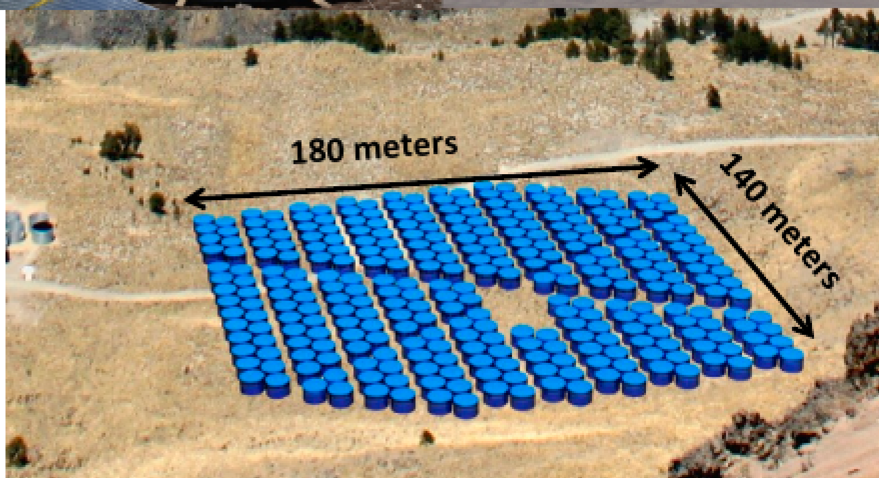

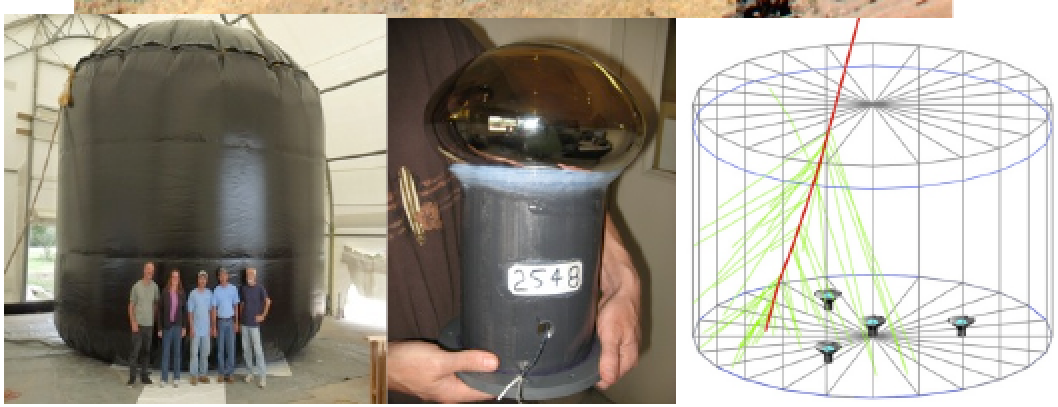

- **High-Altitude Water Cerenkov detector**
  - 4100 m a.s.l., 249 km East of Mexico city
  - Latitude of 19° N
- **Second generation of technique developed for Milagro (2000-2008)**
- **300 water tanks**
  - 7.3 m diameter x 4.5 m deep
  - Covering 22 500 m² area
  - 4 PMTs each
- **Depth and spacing of PMTs optimized for γ-ray sensitivity from 100 GeV to 100 TeV**

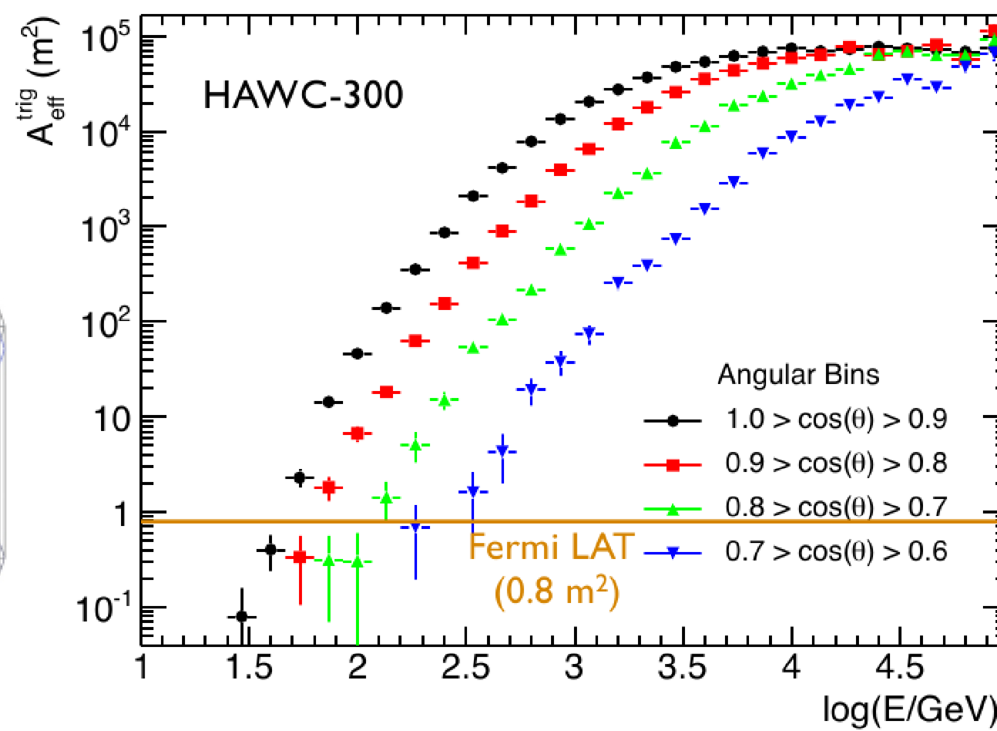

GRB observations with HAWC (1/2)

GRB 090510

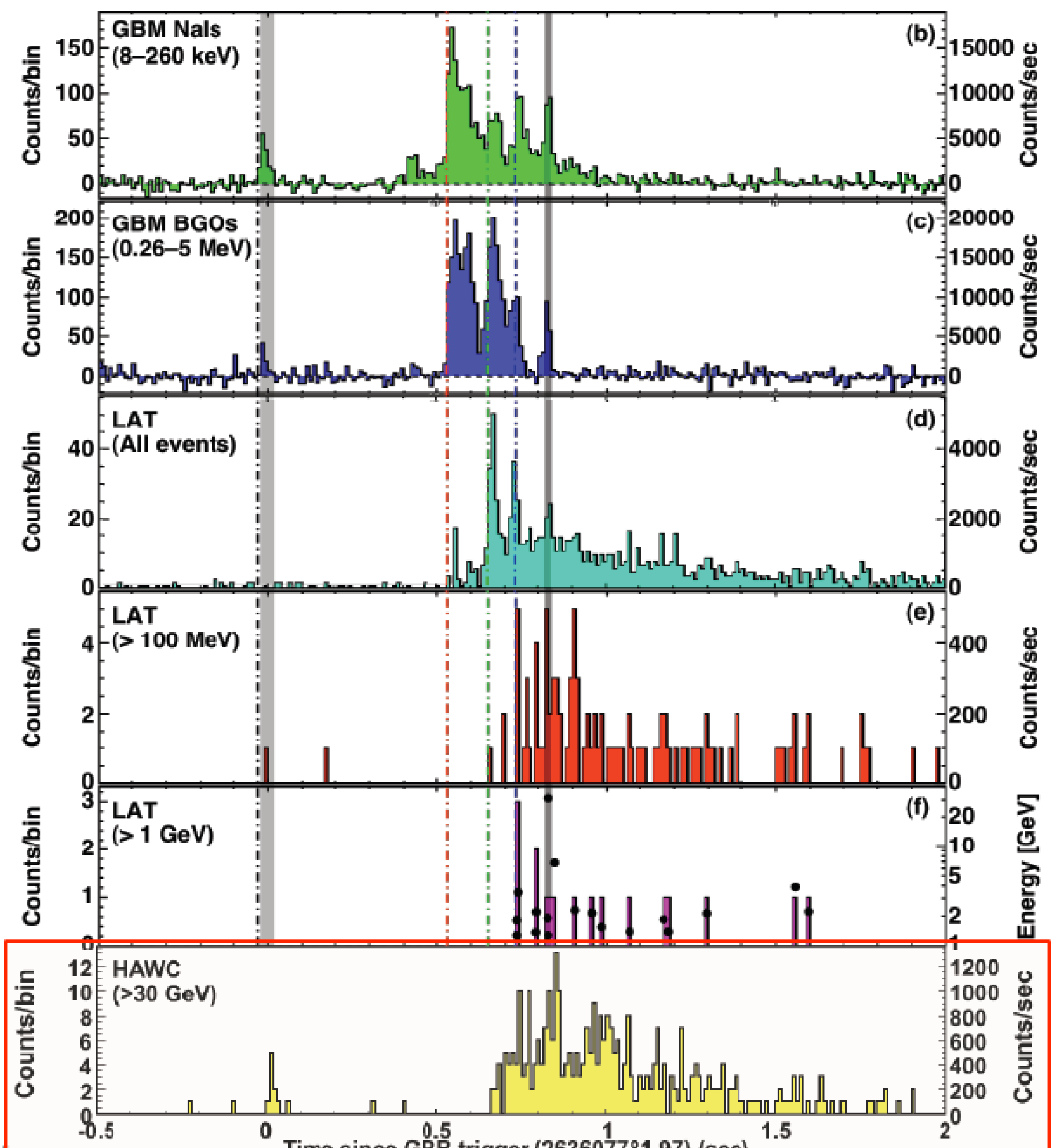

- **Main DAQ**
  - Trigger rate ~8 kHz
  - Gives direction, species, and energy of primary particle
  - Angular resolution of 0.1° can be achieved at E > 5 TeV
  - Rejection of hadronic showers relies on the shower lateral size and high amplitude pulses produced by muons

- **Scalers**
  - Measure PMT counting rates
  - A sudden increase in counting rates may reveal a GRB
  - Energy threshold of a few GeV

GRB observations with HAWC (2/2)

Main DAQ and scalers sensitivity at 20° zenith angle for vasious redshifts, including absorption by Extragalactic Background Light

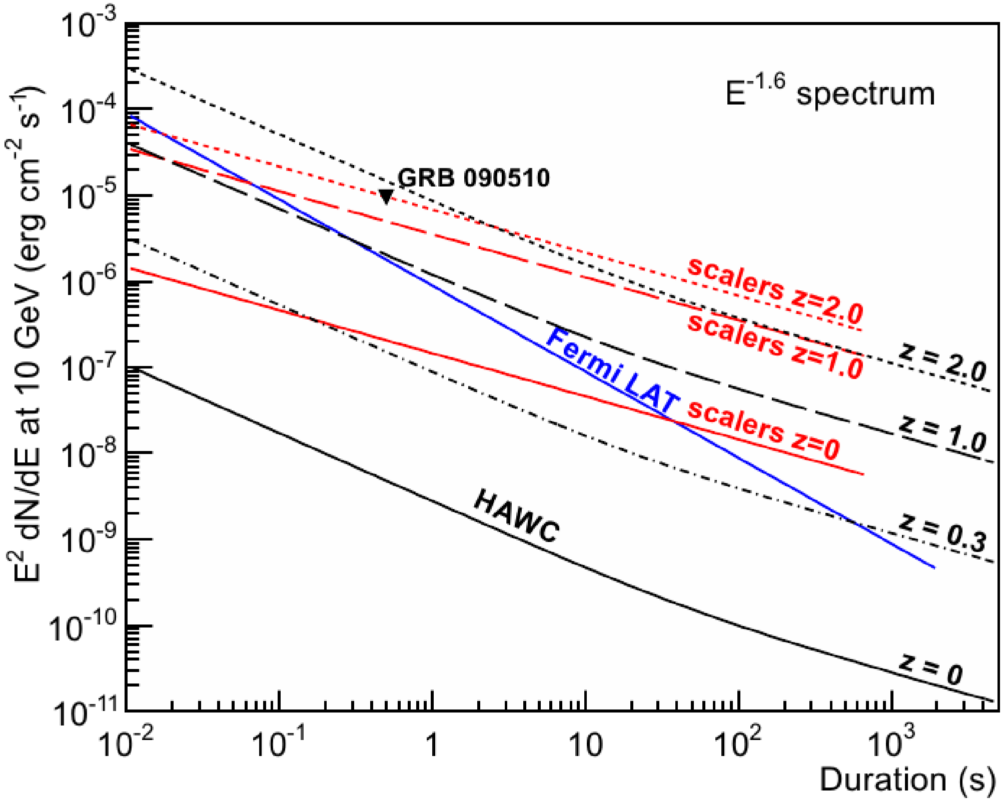

Main DAQ sensitivity at 20° zenith angle (1 s duration) and for various values of a sharp high-energy spectral cutoff

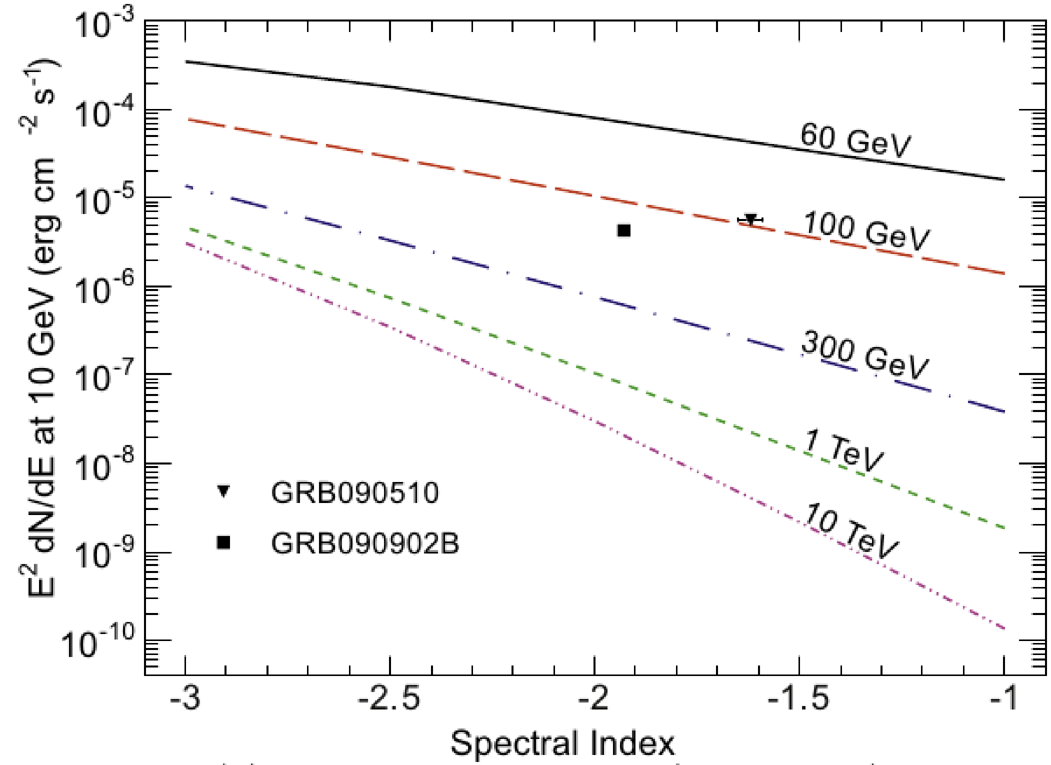

(a) $\approx$ 5 kHz trigger rate ($nHit > 70$)

- **Completing 4 tanks / week**
- 100 tanks operating continuously by August 2013 (5x Milagro sensitivity)
- **300 tanks expected to be complete by August 2014 (15x Milagro sensitivity)**
- **HAWC-300: Crab at 5σ in one day**

The end

More?

- "Gamma-Ray Bursts : the brightest explosions in the Universe", G. Vedrenne & J.-L. Atteia, Springer & Praxis Publishing, 2009
- "Gamma-ray Bursts", Cambridge University Press (Astrophysics Series 51), Edited by C. Kouveliotou, R. Wijers & S. Woosley, 2012
- "Astronomie gamma spatiale", J. Paul & P. Laurent, Gordon and Breach Science Publishers, 1997
- "Observational astrophysics", P. Léna, D. Rouan, F. Lebrun, F. Mignard & D. Pelat, Springer Astronomy and Astrophysics Library, 3rd edition, 2012
- "High-energy Astrophysics", M. S. Longair, Cambridge University Press, 2nd edition volume 1, 1992

- **Lectures of the 2011 School of Astroparticle Physics... on gamma-ray astronomy!**